DISCOVERY AND CHARACTERIZATION OF PH-SENSITIVE, MEMBRANE ACTIVE PEPTIDES

by

Sarah Yeon-Kyoung Kim

A dissertation submitted to Johns Hopkins University in conformity with the requirements for the degree of Doctor of Philosophy

Baltimore, Maryland

October 2019

ABSTRACT

Peptides that self-assemble into pore-like structures in lipid bilayers could have utility in a variety of biotechnological and clinical applications due to their ability to breach the barrier imposed by lipid bilayers. To empower such discoveries, we have used synthetic molecular evolution to select for the pHD peptides, a family of membrane-active, pore-forming peptides that assemble into macromolecular-sized pores at acidic pH. We have also discovered the macrolittins, a related family of peptides that form macromolecular-sized pores at all pH. To understand the mechanism of action of these "pHD peptides", we systematically explored structure-function relationships through measurements of the effect of pH and peptide concentration on membrane binding, peptide structure, and the formation of macromolecular-sized pores in neutral POPC membranes. We find that at low pH, the peptides bind to membranes, fold into alpha helices, and cooperatively assemble into pores. The major role of pH is to regulate the amount of peptide bound per vesicle, with 50% leakage of 40 kDa dextrans occurring at only 75 peptides bound per vesicle. Since cell membranes are complex, composed of lipids with various headgroups and acyl chains, we also sought to determine the effect of anionic headgroups and acyl chain length on the mechanism of action of the pHD peptides We find that pHD15 retains its pH-sensitivity, and is extremely sensitive to the composition of the bilayer. The peptide partitions equally favorably to anionic and neutral membranes, and is equally potent in 1:9 POPG:POPC and POPC membranes, but less potent in 1:9 POPS:POPC membranes. The peptide binds to membranes of various thicknesses in a pH-sensitive manner that is affected by the chain lengths. Leakage is decreased for thicker membranes, which cannot be accounted for by the amount of peptide bound. Overall, we find that the physical chemistry and sequence of the pHD peptides, as well as the lipid composition affects the peptides' potency and pH dependence. The sequence-structure-function

relationships described here can be used for future design and optimization of membrane permeabilizing peptides for specific applications.

Thesis Committee:

Dr. Kalina Hristova (advisor, reader)

Dr. Margaret Johnson (reader)

Dr. Bertrand Garcia-Moreno (chair)

Dr. Jeffrey Gray

Dr. Marc Ostermeier

Dr. Albert Lau (alternate)

ACKNOWLEDGEMENTS

I am incredibly grateful to my advisor, Dr. Kalina Hristova, for her support and guidance through my years at Johns Hopkins. I also grateful to our collaborators Dr. William C. Wimley at Tulane University School of Medicine, Dr. Anna Pittman and Dr. Gavin M. King from the University of Missouri; past and present members of the Hristova lab, especially Gregory Wiedman, Nuala del Piccolo, Fozia Ahmed, Alex Komin, Daniel Wirth, Michael Paul, and Elmer Zapata-Mercado; and to the high school and undergraduate students I mentored, in particular Sijia Li and Dakota He.

A warm thank you to my friends, especially Moustafa Abou Area and Julia Wainger, who gave me a place to stay as I finished my degree, and to the Hopkins Ballroom team who felt like my family away from home. I would also like to thank my family, especially my mom and dad who immigrated with me and my sister to America in hope of a brighter future. I hope seeing a second daughter graduate with a PhD makes all the difficulties and pain our family experienced when we first came to America worth it! And to my twin Stacy who supported me in the ways that only a sister and fellow PhD candidate (now a fully fledged PhD!) can. A special thanks to Hershie and Jemi who made coming home a purr- and affection-filled delight every night no matter how bad my day was. And of course a very big thank you to Subasish Bhowmik, who has made life more rich and fun ever since our undergraduate days at Cornell.

TABLE OF CONTENTS

LIST OF TABLES

LIST OF FIGURES

INTRODUCTION

Membranes as Semipermeable Barriers

Membranes are essential to life, permitting the earliest forms of life to arise[1], the development of eukaryotic life forms with subcellular compartments[2], and the rise of complex neural signaling networks that, at their root, depend on the precise spatial and temporal separation of ions across the neural membrane[3]. Fundamental to all of these functions is the necessity to differentiate inside from outside, a critical role of the membrane.

One essential barrier property of membranes is that they are selective of what they permit across, a characteristic known as semipermeability[3]. Due to their inherent hydrophobicity, membranes permit the passive diffusion of small, relatively hydrophobic molecules such as steroids, and prohibit the passage of hydrophilic and large molecules. The properties that would enable a molecule to passively enter cells has been of interest to drug developers, who wanted to discover rules that would allow a drug to be orally active. Such drugs must cross several membranes, such as the intestinal lining and the vascular epithelium[4]. In 1997, Christopher A. Lipinski proposed several guidelines as the Rule of 5[5]. These rules state that molecules must be smaller than 500 daltons, have a moderate hydrophobicity such that its octanol-water partition coefficient or $\log[P] < 5$, and have less than 5 hydrogen bond donors or 10 hydrogen bond acceptors. Many common orally active, over-the-counter drugs such as ibuprofen, aspirin, acetaminophen, dextromethorphan (a cough suppressant), diphenhydramine (an antihistamine) obey these rules. Although Lipinski's rules are useful for predicting what types of molecules may go across, they emphasize the narrow range of molecules that membranes would allow to passively diffuse into the cell.

Although most molecules are barred from entry, cells require nutrients and metabolites that cannot passively diffuse across the membrane to be brought into the cell. Nature has designed pathways for these molecules to cross the membrane, but they typically require that the molecule has high specificity for the binding sites of membrane transporters or channels, and sometimes the input of energy in the form of ATP[3,6,7]. The result is that healthy cells maintain the composition of molecules that are inside the cell. However, there are circumstances during which destabilizing the membrane to permit the passage of molecules could be useful to disrupt the homeostasis of diseased cells.

For example, the destabilization of the plasma membrane of cancer cells could result in the cells' death as the ions, nutrients, and other molecules diffuse out of the cell[8–11]. Membrane destabilization could also be useful in expanding the number of druggable targets[12]. Many intracellular targets that reside beyond the plasma membrane are largely unreachable by high molecular weight, hydrophilic molecules such as nucleic acids, sugars, and proteins[12,13]. These molecules cannot cross the membrane by passive diffusion, and are excluded from entry by membrane channels and pumps or via endocytosis if they are unable to bind to recognition domains of membrane receptors. Some of these molecules get internalized into cells via endocytosis. However, these molecules remain unable to penetrate the endosomal membrane and therefore remain trapped within endosomes, and eventually degraded as the endosome matures into lysosomes[2,14]. Disrupting the structure of the endosomal membrane would enable the escape of therapeutic molecules to the cytosol.

In either of the above examples, the indiscriminate disruption on any cell membrane would be toxic and limit the therapeutic usefulness of this method. To prevent such a harmful event from occurring, the destabilization of membranes can be triggered to form in response to a signal such as pH – a signature of the cancer microenvironment[15–19] and the endosomal

lumen[2,20,21]. Beyond their use in the clinic, such pH-triggered, membrane-destabilizing agents could be used in biotechnology as biosensors, among other uses[22–25].

Approaches for Designing Membrane Destabilizing Agents

Several approaches have found limited success in disrupting membranes based on pH. Synthetic polymers have been used to burst endosomes via the proton sponge effect[26], and pH-triggered liposomes have been designed to release their contents to the cytosol by fusing with and destabilizing the endosomal membrane[27,28]. However, the endosomal release of cargo remains challenging[14,29].

An additional approach would be to use peptides. Peptides have a number of advantages. They are chemically stable, antigenic[10], straightforward to synthesize, and easy to derivatize to add novel functionalities. Nature has also produced hundreds of peptides which are known to form pores, typically as a first-line of defense against pathogens before the immune system kicks in[30,31]. Consequently, there is a vast number of peptides from which an ideal pore-forming sequence could be identified. Their properties can be modified by swapping a residue with one of 20 amino acids. Furthermore, peptides are small in size, which would permit their entry into tumors[32], which are known to have poorly developed, leaky vasculature.

One challenge in using pore-forming peptides, however, is that the mechanism by which they form pores is not well understood, and even highly controversial. Take for example melittin, the main component of bee venom. Melittin is a 26 amino acid, alpha-helical peptide known to form small pores in membranes that cause the disruption of ion gradients, resulting in the cell's death. The mechanism of action by which melittin forms pores is not well understood in part because its behavior is sensitive to a number of experimental conditions such as pH, lipid composition, ionic strength, temperature, and peptide concentration[33]. Furthermore, the

transmembrane, pore-competent state is short-lived. Oriented circular dichroism indicates that the transmembrane state is a minor component of the total peptide population, with the vast majority of peptide oriented parallel to the surface of the bilayer[34,35]. Furthermore, electrochemical impendence spectroscopy has recorded that pore-formation occurs within seconds after peptide interacts with membranes, and the pores close soon after[36]. Melittin has been proposed to destabilize membranes by forming toroidal pores, carpeting the bilayer, or through a detergent effect.

For designing membrane-active peptides, the absence of detailed information about the sequence-structure relationships of pore-forming peptides poses a design challenge: it is difficult to identify the key residues responsible for forming the pore, or for stabilizing the peptide-lipid and peptide-peptide interactions[37]. Therefore it is difficult to identify the residues to modify to optimize the peptide's function. To overcome this roadblock, membrane-active peptides can be designed by synthetic molecular evolution. This approach has been highly successful in designing membrane-active peptides, including those designed to spontaneously translocate across membranes while attached to cargo[38], beta-sheet pore-forming peptides[39], soluble, potent pore-forming peptides[40], and cell penetrating peptide nucleic acids[41]. The rationale behind this approach is to create hypotheses about the role of the residues, select alternative resides that may bestow novel properties to the peptide, then create a combinatorial library with thousands of members. A high-throughput assay is designed to select outliers that excel at the properties which are desired.

The Road to Discovering the pHD Peptides

The pHD peptides are second-generation derivatives of melittin. Originally, gain-of-function melittin variants were selected through a high-throughput screen in which peptides that formed large, potent, equilibrium pores were selected for[33]. MelP5, like melittin, is a 26 amino

acid peptide, but can allow the escape of 10 kDa dextrans from vesicles at P:L as low as 1:5000[42]. The peptide forms pores in a pH-independent manner. To encode pH-sensitivity, Wiedman et al. attempted to rationally design variants, taking inspiration from the pH-sensitive peptides GALA and pHLIP[23]. GALA, derived from a viral fusion peptide, forms small pores at acidic pH[43]. pHLIP, a peptide derived from bacteriorhodopsin, is not a pore-forming peptide, but inserts into membranes at acidic pH[18]. The rationally designed variants of MelP5, named MelP5_Δ4 and MelP5_Δ6, had 4 or 6 acidic residues. This attempt at rational design was only partially successful. The peptides bound to membranes and folded into alpha helices in a pH-sensitive manner, but lost their ability to form large pores, underscoring that the properties of pore-formation and pH-sensitivity and stable pores are not fully additive[23]. Consequently, we decided to try a high throughput approach to create gain-of-function variants of MelP5 that were large, equilibrium pore-formers that self-assembled into pores only at acidic pH.

Dissertation Objectives

pH-sensitive, pore-forming peptides can be useful for a variety of applications as biosensors, drug delivery agents, and cancer therapeutics. However, due to the technical challenges of probing the interaction of membrane active peptides with the lipid milieu, structure-function relationships between amino acid sequence and pore-forming activity are difficult to characterize. Consequently, the rational design of pore-forming peptides remains challenging.

The primary objective of my thesis research was to discover a novel class of pH-sensitive peptides that form large, stable pores in membranes. In this thesis, I will describe the discovery of the pHD peptides – or the pH-dependent Delivery peptides – through synthetic molecular evolution. In Chapter 2, I will describe the discovery of the pHD peptides from a 18,432 member library of peptides. The peptides were selected with a high-throughput orthogonal screen designed to identify the peptides with exceptional ability to induce no leakage at neutral pH, and abundant leakage of 40 kDa macromolecules at acidic pH. We learn that the peptides share a common motif of 5 or 6 acidic residues that accounts for pH-sensitive macromolecular-sized pore-formation. We also discover the closely related group of peptides, the macrolittins, from the same library of peptides. The macrolittins are potent pH-*insensitive* pore-formers that have three acidic residues which lie along the center of the acidic face of the helix. This may suggest that the central acidic residues are involved in forming potent, macromolecule-sized pores, and the flanking acidic residues of the acidic face of the pHD peptides modulate pH-sensitive activity.

A second objective was to understand the structure-function relationships of the pHD peptides on neutral membranes. In Chapter 3 I describe the characterization of the behavior of the pHD peptides on neutral POPC membranes with circular dichroism, tryptophan fluorescence, and leakage assays. We find that under acidic conditions, the peptides bind to the membrane, fold into alpha helices, and cooperatively assemble into macromolecular-sized pores. Ultimately, the

activity of the peptides depends on the number of peptides bound per vesicle, which can be tuned with pH, peptide to lipid ratios, and peptide sequence. Activity is high under conditions of acidic pH, high peptide to lipid ratios, and 5 rather than 6 acidic residues.

Cell membranes are highly complex environments, composed of proteins, sugars, and many types of lipids with various acyl chains and headgroups. Therefore the final objective of my thesis was to evaluate the effect of anionic headgroups and acyl chain length on the behavior of one pHD peptide, pHD15. In Chapter 4, I describe my findings that the peptide is less active on anionic membranes, despite the same partitioning of peptide on neutral and anionic membranes. This suggests that anionic headgroups interfere with the insertion or association steps of pore-formation. We also find that pHD15 partitions less favorably to and is less active on membranes composed of lipids with longer acyl chains.

The discoveries of the pHD peptides and the macrolittins diversifies the toolbox of peptides that can be used for biotechnological and clinical applications. Furthermore, the principles underlying pHD peptides' pore-formation on membranes will be useful for the future design of membrane active peptides with novel, useful properties.

MATERIALS AND METHODS

Here I collect the materials and methods used throughout the following chapters. Many of these protocols have been published in the following papers:

J. Am. Chem. Soc. (2017) Vol. 13, No. 92, pg. 937-945

J. Am. Chem. Soc. (2018) Vol. 140, No. 20, pg. 6441-6447

J. Am. Chem. Soc. (2019) Vol. 141, No. 16, pg. 6706-6718.

Materials

Peptides of > 95% purity were purchased from BioSynthesis, Inc. The lipids 1-palmitoyl-2-oleoyl-glycero-3-phosphocholine (POPC), 1-palmitoyl-2-(9,10-dibromo) stearoyl-*sn*-glycero-3-phosphocholine (diBrPSPC), 1-palmitoyl-2-oleoyl-sn-glycero-3-phospho-L-serine (POPS), 1-palmitoyl-2-oleoyl-sn-glycero-3-phospho-(1'-rac-glycerol) (POPG), 1,2-dimyristoleoyl-sn-glycero-3-phosphocholine (14:1 (Δ9-Cis) PC), 1,2-dipalmitoleoyl-sn-glycero-3-phosphocholine (16:1 (Δ9-Cis) PC), 1,2-dioleoyl-sn-glycero-3-phosphocholine (18:1 (Δ9-Cis) PC), 1,2-dieicosenoyl-sn-glycero-3-phosphocholine (20:1 Cis PC), and 1,2-dierucoyl-sn-glycero-3-phosphocholine (22:1 Cis PC) were purchased from Avanti Polar Lipids. 8-Aminonaphthalene-1,2,3-trisulfonic acid (ANTS) and p-xylylenebis(pyridinium bromide) (DPX) were purchased from Thermo Fisher Scientific. Chloroform, a mmonium thiocyanate, and other salts and buffer materials were purchased from Fisher Scientific or Sigma-Aldrich. TAMRA-biotin-dextran (TBD) was synthesized as described elsewhere[22,42].

Buffers

Thirteen buffers were prepared with pH from 4 to 7 at 0.25 pH increments. Buffers with a pH between 4 and 5.5 were prepared with 10 mM sodium acetate, and buffers with a pH between

5.75 and 7 were prepared with 10 mM sodium phosphate. Buffers for binding and leakage assays were prepared with 100 mM KCl. Buffers for circular dichroism were prepared without KCl, and their pH was adjusted with phosphatidic acid instead of hydrochloric acid to minimize the CD signal due to the absorption of the chloride ion below 200 nm. All buffers were vacuum filtered through a 0.22 μm pore size membrane to remove dust and bacteria before use.

Peptides

Solutions of ~1 mM peptides were prepared with Millipore water. Concentrations were determined using the absorbance of the single tryptophan on each peptide. The average of three absorbance measurements at 280 nm on a NanoDrop 2000c (Thermo Fisher Scientific) was used to determine the concentration. Peptides were stored frozen until use and were subjected to no more than five freeze-thaws to minimize peptide degradation.

Vesicle Preparation

Three types of 100 nm large unilamellar vesicles (LUV) were prepared with the lipid compositions POPC, 1:9 POPS:POPC, 1:9 POPG:POPS, 14:1 (Δ9-Cis) PC, 16:1 (Δ9-Cis) PC, 18:1 (Δ9-Cis) PC, 20:1 (Δ9-Cis) PC, or 22:1 (Δ9-Cis) PC. For all vesicle types, POPC in chloroform was dried under vacuum overnight, resuspended in buffer, frozen and thawed ten times, and extruded ten times through 100 nm poly carbonate membranes. Vesicles with no probes entrapped were used for binding and circular dichroism. For TBD-encapsulating vesicles, dry lipid films were resuspended in buffer containing 1 mg TBD per 50 μmol lipid. After extrusion, vesicles were incubated on high capacity streptavidin agarose to remove unencapsulated TBD. For ANTS/DPX vesicles, dried lipid films were resuspended in 12.5 mM ANTS and 45 mM DPX. After extrusion, unencapsulated ANTS and DPX were separated from

the vesicles by size exclusion chromatography with Sephadex G-100 resin. Lipid concentration was measured using a modified Stewart Assay[44].

Dextran leakage assays

Leakage of 40 kDa was measured with FRET. Dextran vesicles with entrapped TBD were diluted to 1 mM, and streptavidin-AF488 (the donor fluorophore) was added to a final concentration of 20 nM. In a 96-well plate, peptide and vesicles were mixed, then incubated while shaking at room temperature for 1 hour before measuring FRET by donor fluorescence quenching on a BioTek H4 Synergy Hybrid Microplate Reader with ex/em = 495/519 nm. As a positive control for 100% leakage, 4 µl of 10% Triton X100 was added to three wells, and as a negative control, no peptide was added to three wells. Leakage measurements are the average of at least 3 unique vesicle preparations. Fractional leakage was calculated as:

Fractional leakage was calculated as:

$$f_{leakage} = (F_{no\ peptide}\text{-}F_{sample})/(F_{no\ peptide}\text{-}F_{triton}) \quad (1)$$

The leakage as a function of pH was fit to determine the pH at which leakage is 50% (the midpoint or "pH50"):

$$f_{leakage} = L_{max} + \frac{L_{min}-L_{max}}{1+e^{\frac{pH50-pH}{rate}}} \quad (2)$$

Here, L_{max} and L_{min} are the curve's maximum and minimum values, respectively, and *rate* describes the steepness of the curve.

ANTS/DPX Leakage assays

Small molecule leakage was measured by quenching of ANTS by DPX. ANTS/DPX leakage vesicles were diluted to 1 mM. On a 96-well plate, peptide and vesicles were mixed at P:L

ranging from 1:50 to 1:5000, then incubated with shaking at room temperature for 1 hour before measuring ANTS fluorescence using a microplate reader with ex/em = 360/519 nm. As a positive control for 100% leakage, 4 µl of 10% Triton X100 was added to three wells, and as a negative control, no peptide or Triton was added to three wells. Leakage measurements are the average of at least 3 unique vesicle preparations. Fractional leakage was calculated as:

$$f_{ANTS/DPX\ leakage} = (F_{sample}-F_{no\ peptide})/(F_{triton}-F_{no\ peptide}) \quad (3)$$

The leakage as a function of pH was fit using equation (2) to determine the midpoint of the curve, or the pH50.

Tryptophan Binding

POPC vesicles were prepared at ~30 mM at pH 4.75 and pH 6.25 as described above. Vesicles were diluted to 1 mM with buffers spanning pH 4 to 7, then incubated overnight at 4°C to allow the internal and external pH to equilibrate while minimizing vesicle degradation due to hydrolysis. The next morning, the pH of the solution was verified with MColorpHast pH test strips. Peptide was added with P:L ranging from 1:50 to 1:5000 in 0.5 mL centrifuge tubes. After 1 hour of incubation at room temperature, tryptophan fluorescence spectra were measured on a Horiba Fluorolog 3-22 in a 45 µl cuvette. Samples to correct for lipid scattering, including vesicles, vesicles with tryptophan (at P:L ranging from 1:50 to 1:5000), and tryptophan (at P:L ranging from 1:50 to 1:5000), were also measured at each pH, but without a 1 hour incubation. Scattering correction was made as described previously[45]. The midpoint of the curve, or the pH50, was obtained by fitting using equation (2).

The nmol of peptide bound was calculated as:

$$N_{bound} = f_{bound}N_{total} \quad (4)$$

Where f_{bound} is the fraction of peptide bound, as determined by the normalized tryptophan fluorescence, and N_{total} is the total nmol of peptide in a sample.

Circular Dichroism

Vesicles without KCl were prepared as described above for the tryptophan binding. Scans were collected in a 1 mm pathlength cuvette on a Jasco J-715 spectropolarimeter with a scan rate of 100 nm/min, 3 accumulations, at room temperature. After measurement, the scans were corrected for background using a vesicle sample with no peptides. Relative % helicity was calculated by scaling the average ellipticity at 222 nm. The midpoint of the curve, or the pH50, was obtained by fitting using equation (2).

Oriented Circular Dichroism

Mixtures of peptide and lipid were prepared in methanol at P:L = 1:200 for the macrolittins, or at P:L = 1:50 for pHD15. Aliquots were dried under vacuum onto a quartz disk for at least 1 hour. The disk was sealed in a chamber with a second quartz window. The samples were allowed to hydrate for at least 30 minutes through the vapor phase using MilliQ water in the chamber to form stacked oriented multibilayers. The quartz disk was oriented perpendicular to the beam and CD spectra were collected at eight rotations of the sample holder around the beam axis and averaged. Lipid-only spectra, collected the same way, were subtracted.

To determine the fraction of peptide that had been inserted into the membrane, the hydrated spectra was compared with basis theoretical spectra of fully perpendicular and fully parallel orientations of a helix with respect to the membrane surface. A spectra deconvolution with these basis spectra was performed in Igor Pro.

Tryptophan Quenching

To determine if the pHD peptides can exchange from vesicles to which they are bound into a second population of vesicles added after binding, we measured the change in tryptophan fluorescence upon the addition of a second population of vesicles composed of brominated lipids. Since bromines quench tryptophan fluorescence[46], the exchange of peptides from POPC to brominated vesicles will result in quenching. We prepared vesicles composed of POPC or 16:0-18:0 (9,10 diBr) PC at pH 4.5, and diluted them to 1 mM. To determine the extent of tryptophan quenching by the brominated vesicles, 100 μl of 1 mM diBrPSPC was mixed with peptide added to a final concentration of 20 μM (P:L = 1:50). After 1 hour, the tryptophan fluorescence spectra were measured as described in the binding assay. To measure the kinetics of quenching, the tryptophan fluorescence of pHD15 was measured at 280/334nm. After adding 100 μl of 1 mM POPC to a cuvette, fluorescence was measured for up to 5 minutes, and then peptide was added up to a final concentration of 20 μM. After waiting 30 minutes to ensure maximal binding to the vesicles, diBrPSPC or POPC (as a negative control) was added to final concentrations of 0.2 or 0.33 mM, and fluorescence was measured for 30 more minutes.

High throughput screen for the discovery of the pHD peptides

Library Synthesis

The peptide library was a one-bead-one- peptide library, synthesized using a split-and-recombine approach described in detail previously[33,47,48]. The library members were synthesized on Tentagel Megabead MB NH2 resin beads (Rapp Polymere MB300002), coupled to it by a UV-cleavable photo linker, 4- (4-[1-(9-Fluorenylmethyloxycarbonylamino)ethyl]-2-methoxy-5-nitro-phenoxy) butanoic acid. After synthesis, side chains were deprotected with a mixture of trifluoroacetic acid and scavengers[49]. Beads were then washed extensively and stored dry at −20°C prior to use.

To cleave the photolinker and release the library members, beads were first suspended in methanol and dispersed onto a glass plate. The beads were dried thoroughly and then exposed to UV light at 365 nm for 6 h with illumination from plate top and bottom. One day prior to screening, beads were placed into the wells of a 96-well plate, one bead per well. Water and hexafluoroisopropanol (25 μL each) were added to each well, and the plates were exposed to 365 nm UV light for an additional 3.5 h, releasing and extracting the peptide while also evaporating the solvent. Finally, 25 μL of water was added to each well, and the plates were incubated overnight for peptide solubilization. About 0.5 nmol of peptide was extracted from each bead, as quantified by tryptophan fluorescence.

High-Throughput Screening

In the orthogonal high-throughput screen, we combined the two assays described above and used them in 96-well format as follows.

Step 1. Individual beads were separated into the wells of a plate, and peptides were extracted into a small volume of water as described above. Each bead releases about 0.5 nmol of one peptide sequence from the library.

Step 2. First, 1 mM POPC lipid vesicles in 100 μL of sodium phosphate buffer at pH 7 was added to the peptides in water in the plate from Step 1. These vesicles contained the 350 Da fluorophore ANTS and its quencher DPX, entrapped at mM concentrations. After this step, the nominal peptide concentration was 5 μM, and the peptide-to-lipid ratio was roughly 1:200. Leakage, if it occurs, causes an increase in fluorescence of ANTS. A few wells contained controls: vesicles only, 1 nmol of the peptide MelP5 (P:L = 1:100), 4 nmol of MelP5 (P:L = 1:25), or 0.4% v/v of the detergent Triton X-100. The latter two should completely permeabilize the vesicles.

Step 3. After 60 min of incubation, ANTS fluorescence was measured for each well to quantitate small-molecule release using eq 1.

Step 4. Next, to the same wells, a different preparation of vesicles was added. These vesicles have entrapped 40kD TAMRA-biotin- dextran (TBD) and external Alexafluor488 streptavidin. The TBD vesicles were in sodium acetate buffer at pH 4 so that the final pH in each assay well was 5.0. This second addition of vesicles increased the total volume to 200 μL which decreased peptide to 2.5 μM and decreased ANTS vesicle concentration to 0.5 mM. The new TBD vesicles were present at 1.5 mM so that the total peptide to total lipid ratio was roughly about 1:800.

Step 5. After 60 min, the intensity of the AF488-streptavidin was measured to quantitate macromolecule release, which is calculated with eq 2. This orthogonal and sequential screen gives two measurements that are used to identify peptides with the desired properties: (i) small-molecule release at pH 7 and P:L = 1:200, and (ii) macromolecule release at pH 5 and P:L = 1:800.

High-throughput screen for the discovery of the macrolittins

The library was synthesized as a one bead one sequence library and was screened using a serial, two-assay orthogonal screen. First, ~0.5 nmol of each library member in solution was assayed for induction of leakage of the small molecules ANTS and DPX (21) from POPC vesicles at pH 7 and a peptide to lipid ratio (P:L) = 1:200. Second, additional TBD vesicles were added at 30 minutes to screen for TAMRA-biotin- dextran (40 kDa) leakage at pH 7. The total P:L after the second addition was 1:400. For controls we also tested 4 nmol of MelP5 (final P:L = 1:50) for near complete macromolecule leakage, respectively. We also tested no peptide for a negative control and Triton-X100 detergent for a positive control for complete leakage. After selection of

the positive pore forming library members (see Chapter 1) the peptide remaining on the bead was sequenced by Edman degradation.

CHAPTER 1: PH-TRIGGERED, MACROMOLECULE-SIZED PORATION OF LIPID BILAYERS BY SYNTHETICALLY EVOLVED PEPTIDES

Parts of this chapter were published in the Journal of the American Chemical Society (2017) Vol. 13, No. 92, pg. 937-945.

Gregory Wiedman[1,3], Sarah Y. Kim[2,3], Elmer Zapata-Mercado[2,3], William C. Wimley[4], Kalina Hristova[1,2,3]

[1]Department of Materials Science and Engineering, Johns Hopkins University, Baltimore, Maryland 21218, United States

[2]Graduate Program in Molecular Biophysics, Johns Hopkins University, Baltimore, Maryland 21218, United States

[3]Institute for NanoBioTechnology, Johns Hopkins University, Baltimore, Maryland 21218, United States

[4]Department of Biochemistry and Molecular Biology, Tulane University School of Medicine, New Orleans, Louisiana 70112, United States

Parts of the results and discussion sections appeared in J. Am. Chem. Soc. (2018) Vol. 140, No. 20, pg. 6441-6447 in the article, "Potent Macromolecule-sized poration of lipid bilayers by the macrolittins, a synthetically evolved family of pore-forming peptides".

Sijia Li[1], Sarah Y Kim[1], Anna E Pittman[3], Gavin M King[3,4], William C Wimley[2], Kalina Hristova[1]

[1]Materials Science and Engineering, Johns Hopkins University, Baltimore, MD 21218

[2]Biochemistry and Molecular Biology, Tulane University School of Medicine, New Orleans, LA 70112

[3]Physics and Astronomy, University of Missouri, Columbia, MO, 65201

[4]Biochemistry, University of Missouri, Columbia, MO, 65201

Statement about my role as the second author of these publications

I worked closely with Dr. Gregory Wiedman on the screening, selection, and verification of the pHD peptides. In addition, I characterized the partitioning of the pHD peptides with tryptophan fluorescence, wrote the Python script to identify positive hits, edited the manuscript, and prepared figures. The discovery and characterization of the macrolittins was a project undertaken by a brilliant undergraduate, Sijia Li, who worked under my supervision and mentoring. For this project, I screened many of the peptides, aided in selecting positive hits, took them for sequencing at the Synthesis and Sequencing Facility at JHMI, taught Sijia how to use the fluorimeter, the circular dichroism spectrometer, how to perform leakage assays, and analyze the data, discussed and interpreted the results with her, edited the manuscript, and helped prepare figures.

Introduction

Membrane-permeabilizing peptides could have utility in a variety of biotechnological and clinical applications due to their ability to breach the barrier imposed by lipid bilayers[50–59]. But to enable their practical application, they will first need to be designed to function only in specific environments, or only in response to specific triggers. One potentially useful trigger is pH, which varies in spatially and temporally specific ways in cellular organelles, and also varies locally in tissues under some pathological conditions, including cancer[60–62]. As an example application, pH-sensitive membrane-permeabilizing peptides could be triggered upon endosomal acidification to promote the release of uptaken polar molecules from endosomal compartments into the cell cytosol[50,63–65]. Such an application would eliminate a long-standing barrier to the delivery of generic polar compounds, especially proteins and other macromolecules, to cells[14,63,66]. Indeed, while efficient methods exist to deliver oligonucleotides to cells[65,67], most other types of macromolecules are more difficult to deliver. These macromolecules can be directed to existing cellular uptake mechanisms[68,69], but in the absence of endosome permeabilization or disruption, they often get trapped within the classical pathways that lead to their lysosomal degradation or recycling without significant entry into the cytosol[70,71]. As a second example application, pH-sensitive, membrane-permeabilizing peptides could potentially be used in cancer therapies to selectively permeabilize the plasma membranes of cancer cells. This is possible because the environmental milieu in the vicinity of solid tumors is often acidic due to their high rate of mostly glycolytic metabolism[62]. In support of this application, the locally acidic pH of solid tumors has already been shown in mice to trigger the pH-sensitive insertion of peptides into membranes, although not for peptides that cause permeabilization[60,72].

Some progress has been made in the discovery or design of pH-triggered pore-forming peptides[73,74] including some that we designed rationally[23], and other pH-triggered membrane-

active peptides[65,75]. The state-of-the art in the field has been trial-and-error-based addition of protonatable residues such as aspartate (D), glutamate (E), and histidine (H). Two well-studied examples are pHLIP, which inserts across membranes at pH < 5.5 without permeabilization,11 and GALA, which permeabilizes synthetic membranes at pH < 5.5[76]. However, none of the known pH-sensitive peptides have all of the properties needed for the applications described above. For example, pHLIP does not form pores, although it can deliver small polar molecules that are covalently attached to it by insertion across the membrane[77]. GALA, and others, do form pores in membranes, but only small pores[36,75,76,78,79] with limited utility for cellular delivery, especially for macromolecules.

A uniquely useful combination of properties would be pH-triggered membrane permeabilization that enables the movement of macromolecules across membranes. Until recently, even nontriggered macromolecular poration activity that occurs at low peptide concentration has been rare in pore-forming peptides[80,81]. However, we recently used high-throughput screening of a peptide library to discover a unique peptide, called MelP5, which allows macromolecules through synthetic membranes even at very low concentrations of peptide[33,42]. Thus, with MelP5, there is at least one sequence known that is a non-pH-sensitive macromolecular pore forming peptide. As discussed above, there are also sequences such as GALA and pHLIP and others that have pH-sensitive membrane insertion and permeabilization. However, we are aware of no sequences, other than those discussed below, that have both properties.

There is a lack of detailed molecular understanding of the sequence−structure−function relationships for membrane- active peptides, which hinders their rational design. Here we take a novel high-throughput approach to the discovery of pH- sensitive, macromolecular pore-forming peptides. First, we used the sequence of the macromolecular pore former, MelP5, and sequence

features found in GALA and pHLIP to design a rational combinatorial peptide library. We then developed an orthogonal high-throughput screen to identify sequences from the library that have the following two properties in synthetic bilayers: (i) little membrane permeabilization at physiological pH 7 at high peptide concentration and (ii) efficient formation of macromolecule-sized defects in membranes at acidic pH 5 and low peptide concentration. Such peptides will have no effect on membranes at normal cellular pH, but will be triggered by physiologically reasonable acidic pH to form macromolecule-sized pores. We show below that this approach successfully led to the discovery of a conserved motif for pH-triggered, macromolecule sized poration. We expect these unique sequences to ultimately form the basis for multiple applications that utilize changes in pH as a functional trigger.

Results

Peptide Library Design

The peptide MelP5 is a highly potent, gain-of-function variant of the cytolytic bee venom peptide melittin that was discovered in a high-throughput screen of a library that used melittin as a template.36 While the melittin library was screened only for dramatically increased potency of small-molecule release, we later showed that MelP5, the most potent gain-of-function peptide discovered, also releases macromolecules from vesicles at low peptide concentration[42]. Among the many known membrane-permeabilizing peptides, Melp5 is unique in its ability to induce the passage of dextrans up to a molecular weight of 40,000 through bilayers. MelP5 is unstructured in solution, but folds into an amphipathic α-helix in the presence of membranes, into which it inserts, leading to macromolecule-sized membrane disruption at low peptide-to-lipid ratios, P:L ≤ 1:500.

Previously, we attempted to rationally design pH sensitive, macromolecular pore-forming peptides[23] by encoding pH-sensing motifs, based on the sequences of the pH-sensitive membrane-active peptides GALA[76] and pHLIP[60], into the pH-insensitive, macromolecular pore-forming motif in MelP5[42]. The designed peptides, named MelP5_Δ4 and MelP5_Δ6 (see Table 1), had four or six of the residues along the polar face of the putative amphipathic helix changed to glutamate or aspartate to impart pH sensitivity. Placement and spacing of the acidic residues were based on the helical spacings in GALA and pHLIP. We found that these rationally designed peptides gained pH sensitivity, as they permeabilized membranes only at pH < 5.0. But at the same time, they lost the ability to form macromolecular-sized pores[23], demonstrating that the properties of MelP5, GALA, and pHLIP are only partially additive.

Here, we approached the same goal with combinatorial chemistry and high-throughput screening, instead of rational design. Specifically we designed an iterative 18,432-member library using MelP5 as a template (Figure 1-1), creating a second- generation library that we screened orthogonally for peptides that release macromolecules from lipid vesicles at pH 5, but have little or no membrane-permeabilizing activity at pH 7.

In the library, we varied the amino acids at nine positions (Figure 1-1). Unlike MelP5_Δ4 and MelP5_Δ6, which had a fixed number and pattern of helically spaced acidic residues, the library contained peptides with 0−6 acidic residues distributed in all possible patterns along one face of the MelP5 amphipathic α helix. Our criteria for placement of acidic residues were as follows: (i) maximize the number of i to i+3, i to i+4, and i+ to i+7 α-helical spacings between acidic groups to maximize the electrostatic repulsion between them at neutral pH, and prevent helix formation. For some library members, we expected that such electrostatic repulsion among

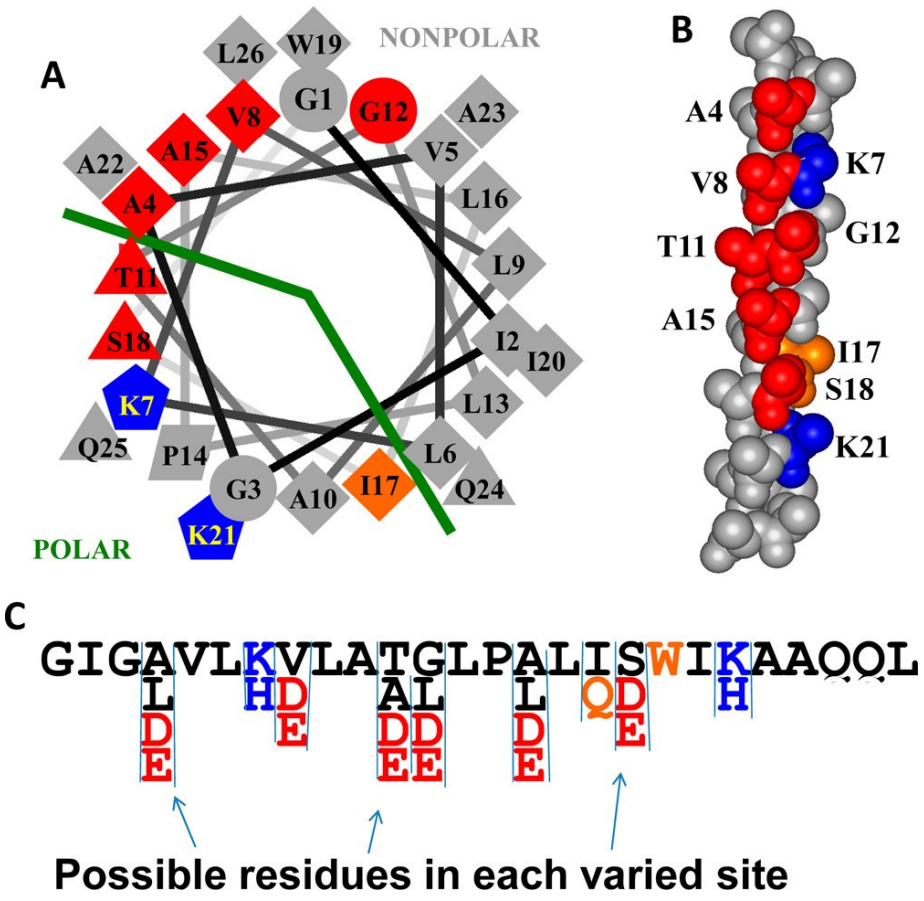

Figure 1-1: Design of an iterative peptide library.

The library is shown in helical wheel and space-filling representations. The library was based on the non pH-sensitive macromolecular pore-former MelP5 which is the sequence shown. Residue shape indicates type in the template sequence of MelP5, with diamonds representing hydrophobic residues and triangles representing polar residues, for example. Colors show residues that were varied in the library. Possible variations present in the library are shown at the bottom. Red positions could be the native residue, or aspartate or glutamate. In some cases, a fourth hydrophobic residue was also possible, as indicated. Blue residues are lysine in MelP5 and could be lysine or histidine in the library members. Position 17 could have the native hydrophobic isoleucine or a polar glutamine. The most important aspect of the library is in the incorporation of six possible protonatable acidic residues, shown in red, that align along one face of the helix, as shown.

the acidic side chains will prevent binding and membrane insertion at pH 7 but allow it at pH 5. This pattern also enables library members to form amphipathic helices in which the protonation state of the acidic residues can make a significant contribution to helical propensity and membrane insertion; (ii) retain basic residues at positions 7 and 21 because we hypothesized that changing them to acidic residues in MelP5_Δ4 and MelP5_Δ6[23] may have altered the peptide function; (iii) retain overlap between the polar face of the MelP5 helix and the positions of the new acidic residues; (iv) reduce hydrophobicity as little as possible to maintain the propensity of the helix to partition into membranes; (v) avoid replacing any residues known to be critical to the activity of MelP5, specifically A10, P14, L16, and A23[33]; (vi) avoid replacing tryptophan 19 because it is useful for concentration determination and as an optical probe of structure. With these criteria in mind, we elected to allow both glutamate and aspartate to appear at six positions: A4, V8, T11, G12, A15, and S18, giving the distribution shown in Figure 1-1. We also allowed the native residue in each of these positions. We allowed hydrophobic leucines to occur at positions A4, G11, and A18 and a somewhat hydrophobic alanine at T11 to modulate hydrophobicity. To potentially compliment the pH sensitivity of the acidic residues, we allowed the native lysines at positions 7 and 21 to also be histidine. Lysine will be cationic at all pH values below 8.5 whereas histidine will be cationic only below its pKa of ~6.5.

Previously, we showed that the presence or absence of polar residues at the boundary of the polar−nonpolar faces is a critical feature of MelP5[33]. Specifically, the native T10 in the first generation library was replaced with alanine, which narrows the polar face substantially (Figure 1-1). In the current library we preserved A10 on the N-terminal half of the peptide and allowed position 17, which defines the cutoff between the polar and nonpolar faces on the C-terminal half of the helix, to vary between hydrophobic isoleucine and polar glutamine.

There are 18,432 unique, 26-residue, MelP5 variants in the library. All library members share at least 17 residues of 26 in common with MelP5 such that the minimum identity is 73%. If we assume that D and E are equivalent, there are 64 different patterns of acidic residues in the library. If D and E are unique, there are 729 different patterns. From the library design in Figure 1-1, we calculate the following abundance values: 2.8% of library members have six acidic residues (1 pattern of 64), 13.8% have five acidic residues (6 patterns), 28.5% have four acidic residues (14 patterns), 30.6% have three acidic residues (20 patterns), 18.1% have two acidic residues (14 patterns), 5.6% have one acidic residue (6 patterns), and 0.7% have zero acidic residues (1 pattern).

The library was synthesized as a one-bead, one-peptide library using a well-established split-and-recombine approach[33,47,48]. Quality control for the synthesis was done using HPLC, MALDI mass spectrometry, and Edman degradation on peptide extracted from multiple individual beads. These methods showed that every bead examined contained predominantly a single pure sequence and that each sequence observed was, in fact, an expected member of the library. Each 0.3 mm polystyrene solid phase peptide synthesis bead releases about 0.5 nmol of one single sequence as described above.

Orthogonal High-Throughput Screen Results for the pHD peptides

The library was screened for peptides that simultaneously (i) cause little or no membrane permeabilization at pH 7, even for small-molecule reporters and high peptide concentrations, and (ii) cause macromolecule passage across bilayers at pH 5, at low peptide concentrations. Two different assays, described above, were used in tandem to achieve these aims. One was an assay for release of ANTS, a small molecule (Figure 1-2A), performed at pH 7. The second was an assay for release of a 40,000 Da TAMRA-biotin-dextran, conducted at pH 5 (Figure 1-2B). These

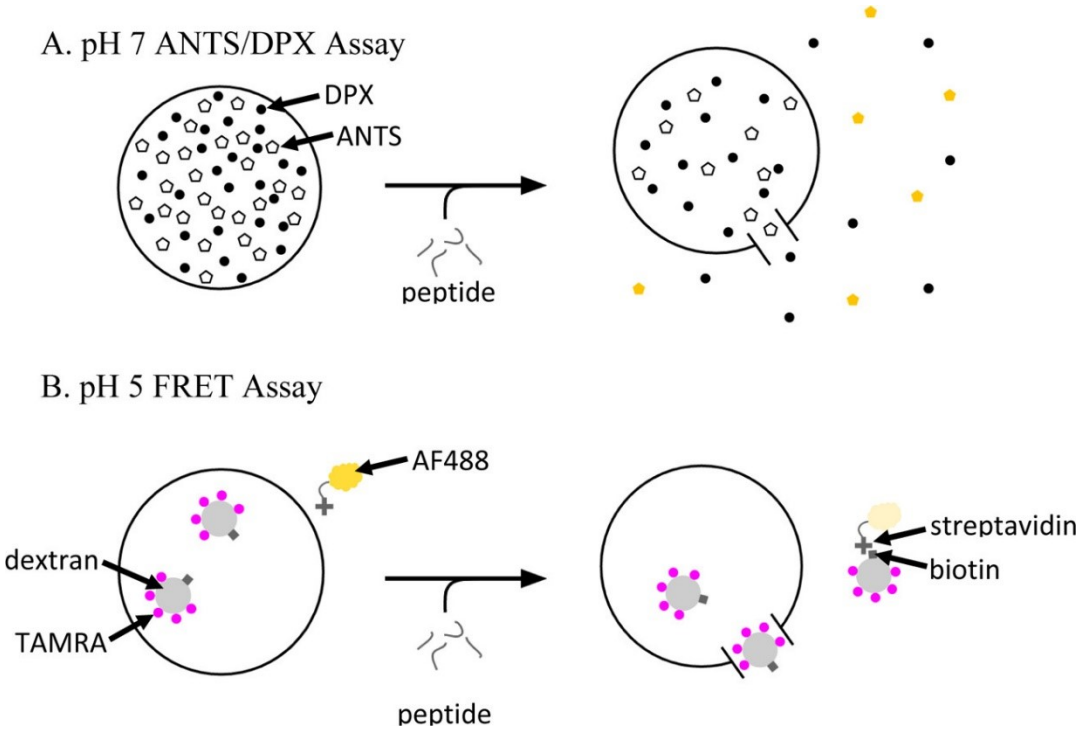

Figure 1-2: Leakage Assays

Two different leakage assays are used to measure the pore-forming activity of the peptides and screen for the desired activities. (A) To evaluate leakage of small molecules we co-encapsulate ANTS, a small-molecule dye, and DPX, its obligate quencher, inside lipid vesicles[82]. Membrane destabilization results in release of ANTS and DPX and recovery of ANTS fluorescence. (B) To evaluate leakage of macromolecules, we used a recently published assay[42] based on FRET detection. In this case, a 40 kDa dextran co-labeled with biotin and the acceptor fluorophore, TAMRA, is encapsulated within vesicles. Streptavidin labeled with the donor fluorophore, AlexaFluor488, is on the outside of the vesicles. Upon macromolecular permeation, the TAMRA-biotin-dextran (TDB) can escape and form a complex with streptavidin, allowing FRET to occur. In our high-throughput screen, we measure leakage of ANTS/DPX at pH 7 and nominal P:L = 1:200 and also leakage of TBD at pH 5 and nominal P:L = 1:800.

two assays can be performed in parallel or in series in the same samples because there is no relevant overlap between ANTS fluorescence (ex/em 350/519 nm) and AF488 fluorescence (ex/em 488/505 nm). In the high-throughput screen described in Materials and Methods, the ANTS/DPX assay was conducted at a nominal peptide to lipid ratio of 1:200 at pH 7, and the dextran leakage assay was performed at nominal P:L = 1:800, at pH 5. Because the peptide release from individual beads varies, P:L could vary between individual wells by a factor of 2 or more.

We screened 15,000 library members using the orthogonal high-throughput screen, covering about 80% of the library's sequence space. In Figure 1-3 we show the ability of each screened peptide to cause small-molecule leakage at pH 7 and macromolecular leakage at pH 5. We present the results in the form of a scatterplot colored according to point density from yellow (highest density) to black (lowest density). Because there were vesicle batch-to-batch variations in the raw intensity values for each assay along the duration of the screen, we have plotted all values in Figure 1-3 as plate-by-plate Z-values; the points plotted are the number of standard deviations from the plate mean, on each axis. The density of points on the Y-axis is centered on zero because the distribution of dextran leakage has a symmetrical Gaussian shape. On the other hand, the distribution of points on the X-axis is offset from zero because ANTS leakage at pH 7 is asymmetric; many library members cause >80% leakage of ANTS at pH 7.

Four points provide useful landmarks. The activities of 1 nmol and 4 nmol of the template MelP5 under the conditions of the screen are indicated in Figure 1-3, to compare with 0.5 nmol of each library peptide. We also show values for blank wells with no peptide and for 0.1% v/v Triton X100, which solubilizes all vesicles. A 1 nmol amount of MelP5 causes high small-molecule permeabilization and partial macromolecule release at all pH values. A 4 nmol amount of MelP5 (P:L = 1:100) and 0.1% v/v of Triton X-100 each cause essentially complete

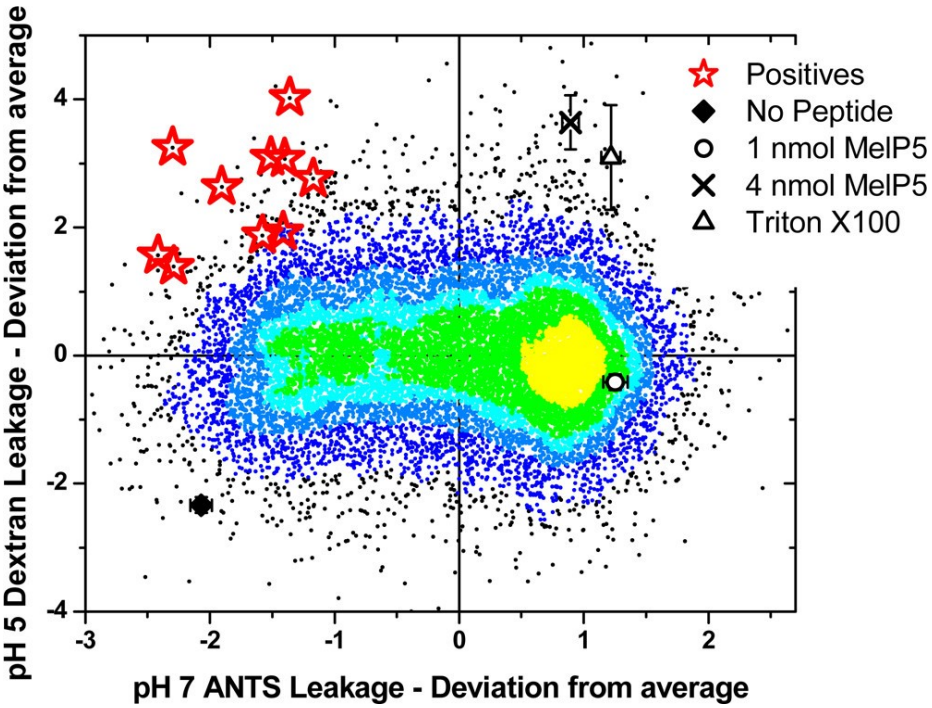

Figure 1-3: Results of the screen.

The serial, two part screen described in Figure 1-2 was used to assay 15,000 randomly selected library members. Vesicles were made from 100% POPC. The two activities for each of the 15 000 library members are shown as points on a temperature scale, where the point color is determined by point density, from yellow (most dense) to black (least dense). The results of each assay are shown as *Z*-values, or the difference of each point from the plate mean expressed as standard deviations. This approach normalizes for batch-to-batch variations in lipid vesicle intensities in the two assays. About 0.5 nmol of each library member was assayed. For comparison, we also show the values for 1 and 4 nmol MelP5, for Triton-X-100 detergent, which solubilizes vesicles, and for buffer only. The center of the yellow area corresponds to ~85% ANTS leakage and ~30% dextran leakage. Most library members are similar to the template MelP5, but there are outliers in all four quadrants. The peptides we seek, with low ANTS leakage at pH 7 and P:L = 1:200 and high TBD release at pH 5 and P:L = 1:800, are found in the upper left corner. Ten positive sequences, highlighted with red stars, were selected and sequenced using Edman degradation. Their sequences are shown in Table 1-1.

release of both types of probes. The activities of most library members are centered on the yellow area in Figure 1-3; on average they have MelP5-like high leakage of ANTS at pH 7 and moderate leakage of dextran at pH 5. The center of the yellow area corresponds to ~85% ANTS leakage and ~30% dextran leakage.

The activity we seek in this work is found in the peptides closest to the upper left corner of Figure 1-3. These peptides have low small-molecule permeabilization at pH 7 (P:L = 1:200) and high macromolecule permeabilization at pH 5 (P:L = 1:800). Ten library members, shown by red stars in Figure 1-3, were selected from within this region, and these peptides were sequenced using Edman degradation. Their sequences are shown in Table 1.1. Below we demonstrate that these selected peptides have exactly the properties we sought in the screen. Thus, our strategy was successful.

Sequence Analysis of Positive pHD Peptides

The positive sequences have many features in common with one another, demonstrating that we have identified a family of closely related sequences with a unique, shared activity. p-values were calculated against null hypotheses determined by the abundance of the particular residue, class, or motif in the library, using exact binomial statistics. Every positive peptide has five or six acidic residues out of six possible ($p < 10{-}5$). Positions 4 and 8 are acidic in all positives ($p = 0.002$ and 0.007, respectively). In the remaining four positions that could have acidic groups, 11, 12, 15, and 18, eight of the ten peptides have three acidic residues and one other nonacidic residue and two have six acidic residues. Of the nine possible i to i+3, i to i+4, and i to i+7 helical spacings of acidic groups available, the positive peptides have an average of 6.5 (range 5−9). The constancy of the acidic residue abundance supports the hypothesis, discussed earlier, that pH-triggered membrane activity is determined mostly by the coupling between electrostatic repulsion and the

Peptide	Sequence	# acidic residues	# helical spacings
Melittin	GIGAVLKVLTTGLPALISWIKRKRQQ	**0**	**0**
MelP5	GIGAVLK**V**L**AT**GL**P**A**L**ISWIK**AAQ**Q**L**	**0**	**0**
MelP5_Δ4	GIGAVLK**E**LA**D**GLPALI**D**WI**E**AAQQL	**4**	**3**
MelP5_Δ6	GIGAVL**EE**LA**DD**LPALI**D**WI**E**AAQQL	**6**	**5**
pHD Peptides			
pHD15-30	GIG**E**VL**H**E**L**A**DD**LP**D**L**Q**E**W**I**H**AAQQL	**6**	**9**
pHD24-52	GIG**D**VL**H**E**L**AA**D**LP**E**L**Q**E**W**I**H**AAQQL	**5**	**6**
pHD34-20	GIG**E**VL**K**E**L**AA**D**LP**E**L**Q**D**W**I**K**AAQQL	**5**	**5**
pHD54-73	GIG**D**VL**K**E**L**A**D**E**L**PA**L**Q**E**W**I**H**AAQQL	**5**	**5**
pHD63-38	GIG**E**VL**K**D**L**AA**E**L**P**E**L**Q**E**W**I**H**AAQQL	**5**	**6**
pHD101-77	GIG**E**VL**K**E**L**A**D**E**L**P**E**L**Q**E**W**I**H**AAQQL	**6**	**9**
pHD108-47	GIG**E**VL**H**E**L**AE**G**L**P**E**L**Q**E**W**I**H**AAQQL	**5**	**6**
pHD118-85	GIG**E**VL**H**E**L**A**DD**L**P**E**L**Q**S**W**I**K**AAQQL	**5**	**7**
pHD145-40	GIG**D**VL**K**E**L**AE**E**L**P**L**L**Q**E**W**I**K**AAQQL	**5**	**5**
pHD187-4	GIG**E**VL**K**D**L**A**D**L**L**P**E**L**Q**E**W**I**H**AAQQL	**5**	**7**

Table 1-1: Sequences of the pHD peptides.

Top panel: Sequences of the natural bee venom pore-former melittin and its synthetically evolved gain-of-function variant, MelP5[42], which enables macromolecules to cross bilayers at low P:L. Using patterns from pH-sensitive membrane-active peptides, we previously designed two variants, MelP5_Δ4 and MelP5_Δ6, which exhibit pH-triggered membrane activity but do not induce macromolecular-sized poration[23]. Bottom panel: All of the positive peptides sequenced (see Figure 1-3). Peptides are named after the plate and well in which the positive bead was identified. For each peptide we list the number of acidic residues, and the number of helical spacings of *i* to *i*+3, *i* to*i*+4, and *i* to *i*+7 between acidic residues.

formation of the amphipathic helix as it relates membrane binding (see measurements of helix content below).

Among the 52 selected acidic residues, there was a strong preference for glutamate with 36 glutamates selected compared to 16 aspartates ($p = 0.007$). The preference for E over D is even more striking in the first two and last two possible positions, where 26 of 33 acidic residues were glutamate ($p = 0.001$). We do not currently know why this preference exists, but speculate that the longer side chain of glutamate enables more conformational flexibility of the side chains by which the electrostatic effects can be modulated, either between acidic groups or in the interactions of acidic residues with basic residues. When an acidic residue was possible but not selected, the selected residues included both native residues and the more hydrophobic residues possible, indicating no strong preference for the native residues at positions 11, 12, 15, and 18. Similarly, 9 lysines and 11 histidines were selected in positions 7 and 21, with no obvious preference or pattern. In fact, all possible patterns (KK, HH, HK, and KH) were observed in the 10 positives. We conclude that the identity of the basic side chains and their charge state at pH 7 are of little consequence to the function of these peptides.

Finally, in position 17, where the native, hydrophobic isoleucine and the polar glutamine were possible, we found that the native residue was replaced with glutamine in 10 of 10 peptides ($p = 0.002$). The current lack of explicit structure− function relationships in these membrane-active peptides makes it difficult to know exactly how this glutamine contributes to activity at this time, but we speculate that its hydrogen bonding capabilities may enable lateral interactions between peptides in the bilayer. We will investigate this and other structural hypotheses in the near future.

It is interesting to compare the positive sequences selected from this library, which have the desired property of macromolecular poration at pH 5.5−5.8, to the rationally designed

sequences MelP5_Δ4 and MelP5_Δ6, which have a lower pKa for permeabilization and do not allow macro- molecules across membranes at any pH. The rational and selected peptides both had 4−6 acidic residues with helical spacings. The acidic residues replacing V8, T11, and S18 are present in both families. The rationally designed peptides have 3 or 5 helical spacings between acidic residues, while the selected peptides have 5−9, but there is overlap. In any case, fewer helical spacings should theoretically lead to a higher pKa whereas the designed peptides actually had a lower pKa than the selected ones. We replaced one or both basic residues in the designed peptides whereas these positions only contained basic residues in the library because we hypothesized that favorable electrostatic interactions with the basic residues could abrogate acidic repulsions in the library-selected peptides. Furthermore, the designed peptides always had isoleucine in position 17, while the selected peptides always had glutamine at position 17. Isoleucine was available at position 17 in the library, but was never selected. While we can list the differences between our screening successes and our design failures, it is currently not possible to explain or predict these behaviors in molecular terms, effectively demonstrating the power of synthetic molecular evolution. We hope that structural and computational scientists will endeavor to explore these mechanistic questions more deeply in the near future.

Verification of Positive pHD Peptides

Since the selected peptides are very similar to each other, we chose to synthesize and purify a subset of them for detailed validation. Tested peptides included four representative sequences with five acidic residues, pHD24, pHD34, pHD108, and pHD118 as well as pHD15, one of the two with six acidic residues. Because we are interested in pH-triggered macromolecule release at low pH, we validated the positive peptides with both the ANTS assay and the macromolecular release assay using 40 kDa dextran and 53 kDa streptavidin, described above.

Dextran leakage was measured as functions of peptide concentration and pH using vesicles made from phosphatidylcholine lipids. The leakage of 40 kDa dextran from lipid vesicles at P:L = 1:200 as a function of pH is shown for these peptides in Figure 1-4A. At this concentration, all of the selected peptides cause 100% dextran release at pH 5 and no leakage at pH 7, as desired. Activity occurs only as pH is decreased into the range of pH 6 to 5.5. The apparent pKa values for the five peptides are similar, ranging from 5.5 to 5.8, with pHD15 having the lowest apparent pKa value, consistent with it having one more acidic residue. Consistent with this result, and with the screen, we also observe <5% ANTS leakage at pH 7 (P:L = 1:200) and ~100% leakage at pH 5 (not shown). We note that the macromolecule leakage activity measured in Figure 1-4 is unique and remarkable, as there are no other peptides known, except for MelP5[42], that have been shown to release macromolecules from lipid vesicles at such low P:L ratios under any conditions. These synthetically evolved peptides have a pH-triggered version of this activity and release macromolecules at pH 5 even better than MelP5 does at any pH.

Dextran release at pH 5 and pH 7 as functions of peptide concentration (expressed as peptide to lipid ratio, P:L) is shown in Figure 1-4B, for pHD 15, pHD 24, and pHD 108. The dashed lines show that there is no activity at pH 7, as desired, even at peptide to lipid ratios as high as 1:50. However, at pH 5 the selected peptides induce substantial macromolecule leakage with 50% leakage activity at peptide to lipid ratios of 1:900 for pHD108 and 1:750 for pHD24. pHD15, which has six acidic, is the least active of the positives tested, with 50% release at P:L = 1:600. While MelP5 has been shown to release a 10 000 Da dextran at similar concentrations,37 it releases the 40,000 Da dextran used in this work at ~P:L = 1:100. Taken together, these results show that we have successfully identified peptides that are significantly more active than the unique MelP5 and are triggered to act only in acidic pH environments.

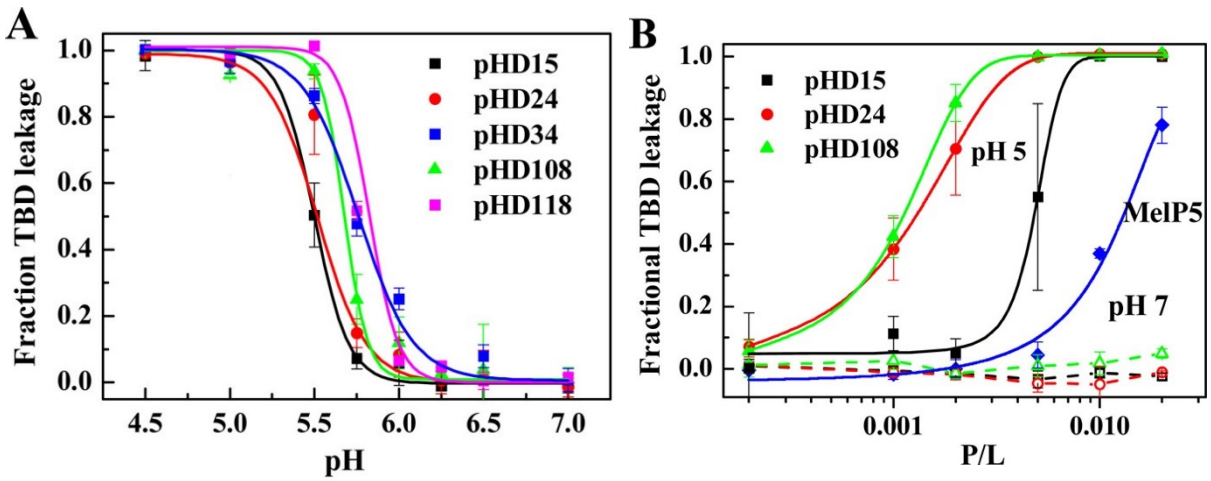

Figure 1-4: Macromolecular Leakage.

(A) Macromolecule leakage versus pH. A representative set of positive peptides from Table 1 were synthesized and assessed for their ability to promote leakage of a 40 000 Da TAMRA-biotin-dextran (Figure 1-2B) at P:L = 1:200 and 1 mM POPC vesicles. Changes in pH lead to sharp transition in macromolecular poration. The apparent pK_a values from the curve midpoints range from 5.5 to 5.8. (B) Macromolecule leakage versus concentration. The peptides assessed for their ability to promote leakage of a 40 000 Da TAMRA-biotin-dextran (Figure 1-2B) at pH 5 and pH 7. The peptides exhibit no activity at pH 7, as desired, even at peptide to lipid ratios as high as 1:50 (dashed lines). At pH 5 all peptides potently cause TBD release with curve midpoints that range from P:L ~1:900 to 1:600.

We also studied the peptide secondary structure in the presence of vesicles as a function of pH by circular dichroism (CD) spectroscopy. Example CD spectra for pHD108 at P:L = 1:200 (Figure 1-5A) show a pH-triggered transition from random coil to α-helical structure with an effective pKa around 5.5. Finally, we measured tryptophan fluorescence as a function of pH at 1:200 which provides a measure of membrane partitioning. Like the CD spectra, example fluorescence spectra for pHD108 (Figure 1-5B) also show a sharp transition from lower intensity emission at 360 nm to higher intensity and 340 nm emission maximum, consistent with a transition from weak to strong membrane partitioning over the expected pH range of 5−6. In Figure 1-6 we directly compare the pH dependence of macromolecule leakage, helicity, and tryptophan fluorescence for three peptides at P:L = 1:200, and show that they are very similar, with pK of 5.5−5.8, consistent with our hypothesis that leakage, helicity, and binding are coupled for macromolecule release.

Macromolecule Leakage Screen for the Macrolittins

The library design, shown in Fig. 1-7C, uses MelP5 as a template and includes six sites in which protonatable aspartate or glutamate residues, as well as the original residue, were possible. In the screen, modified from one described previously[22], two assays were performed in series. First, leakage of the small molecule fluorophore ANTS and its quencher DPX, was measured at pH 7 and at P:L of 1:200. Next, additional vesicles containing entrapped TAMRA-biotin-dextran 40 kDa (TBD) and external AlexaFluor488-streptavidin were added to bring P:L to 1:400, a relatively low P:L value. Leakage of TBD was measured by assessing FRET between TBD and the labelled streptavidin after 1 hour of incubation.

We screened 3200 library members, and the distribution of Z-values (standard deviations from individual plate averages) for the two assays are shown in Fig. 1-7A. Controls included no

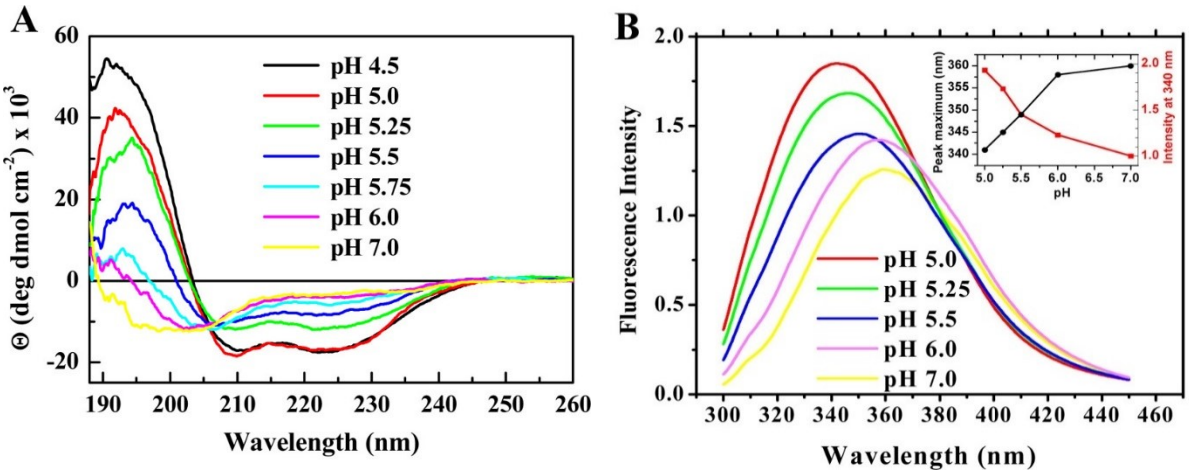

Figure 1-5: Example binding and folding data.

(A) Circular dichroism spectra of pHD108 versus pH at P:L = 1:200 in 1 mM POPC vesicles. Separate samples are made at each pH and equilibrated for 30 min prior to the measurement. The spectra show a structural transition from random coil at pH 7 to classical α-helix at pH 5.75. (B) Tryptophan fluorescence spectra of pHD108 at P:L = 1:200 in 1 mM POPC vesicles. Separate samples are made at each pH and equilibrated for 30 min prior to the measurement. The spectra show a transition from a more polar, water-exposed environment to a less polar, buried environment consistent with peptide that has partitioned into bilayers.

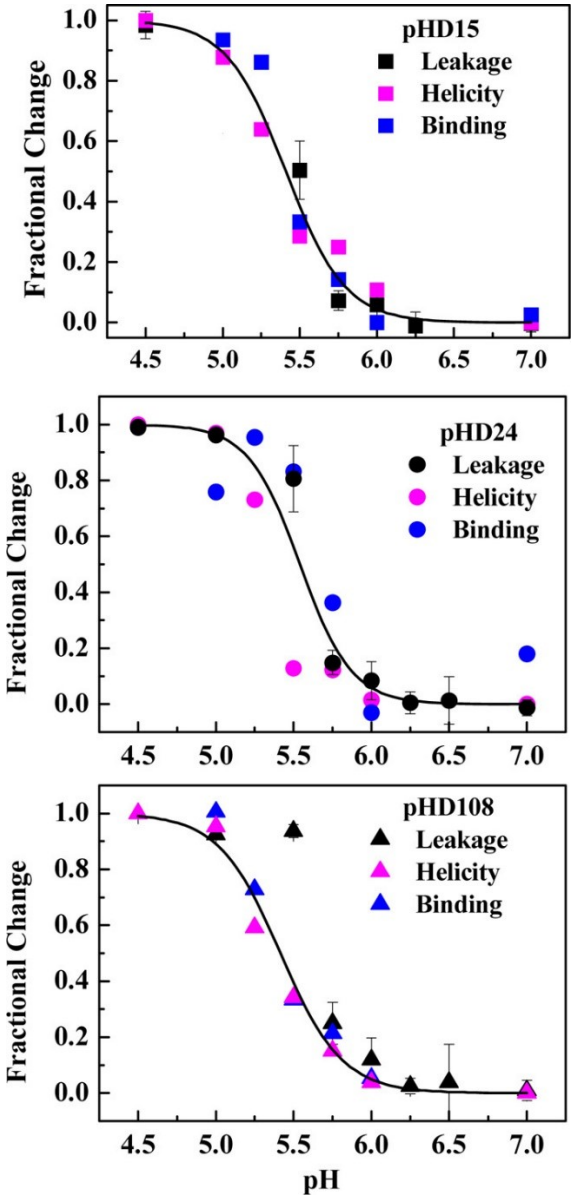

Figure 1-6: Coupling of binding, structure, and activity.

For three pHD peptides we plot changes in TBD leakage, changes in α-helicity from CD, and changes in tryptophan fluorescence as pH is varied. All measurements are at P:L = 1:200. Curves represent the global fit for each peptide of a cooperative transition using all three data sets. There is little or no detectable difference between the pKa values for leakage, structure, and binding, consistent with our hypothesis that they are coupled.

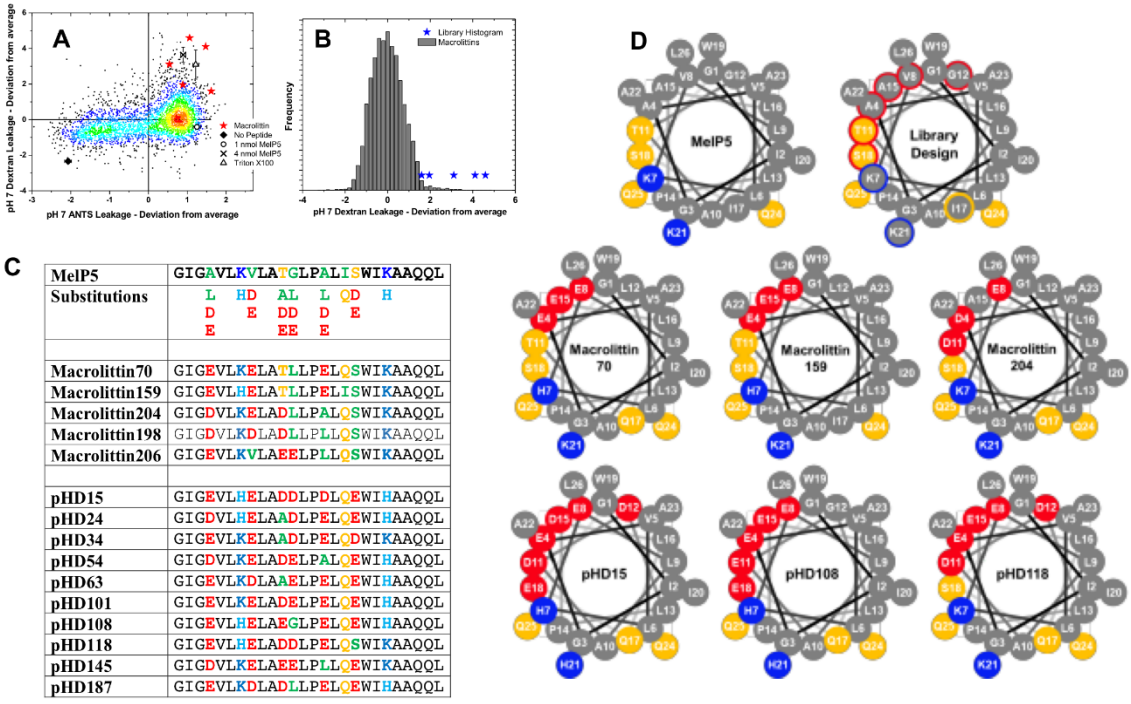

C	
MelP5	GIGAVLKVLATGLPALISWIKAAQQL
Substitutions	L HD AL L QD H D E DD D E E EE E
Macrolittin70	GIGEVLKELATLLPELQSWIKAAQQL
Macrolittin159	GIGEVLHELATLLPELISWIKAAQQL
Macrolittin204	GIGDVLKELADLLPALQSWIKAAQQL
Macrolittin198	GIGDVLKDLADLLPLLQSWIKAAQQL
Macrolittin206	GIGEVLKVLAEELPLLQSWIKAAQQL
pHD15	GIGEVLHELADDLPDLQEWIHAAQQL
pHD24	GIGDVLHELAADLPELQEWIHAAQQL
pHD34	GIGEVLKELAADLPELQDWIKAAQQL
pHD54	GIGDVLKELADELPALQEWIHAAQQL
pHD63	GIGEVLKDLAAELPELQEWIHAAQQL
pHD101	GIGEVLKELADELPELQEWIHAAQQL
pHD108	GIGEVLHELAEGLPELQEWIHAAQQL
pHD118	GIGEVLHELADDLPELQSWIKAAQQL
pHD145	GIGDVLKELAEELPLLQEWIKAAQQL
pHD187	GIGEVLKDLADLLPELQEWIHAAQQL

Figure 1-7: Selection of macrolittins by synthetic molecular evolution.

(A) The results of the screen. Z-values (library member – plate mean)/ (plate standard deviation) for each library member are shown for the small molecule screen at pH 7 and for the macromolecule screen at pH 7. The macrolittins, red stars, were selected for simultaneous potent pore-forming activity in both screens. (B) Histogram of macromolecule leakage values for the library members screened at P:L = 1:400 and pH 7. The macrolittins are in the most active 2% of the peptides screened. (C) Table of peptide sequences. The sequence of the parent MelP5 and the MelP5-derived library is shown. The macrolittin sequences and pHD peptide sequences selected during the screens are also shown. Bold residues were varied. Acidic residues are red, basic residues are blue, hydrophobic residues are green, and polar residues are orange. (D) Helical Wheel projections of the peptides discussed in this work. Acidic (red), basic (blue), and polar (yellow) residues are shown to highlight amphipathicity. Varied residues in the library are indicated by colored outlines, where red signifies acidic residues were included and blue signifies lysine and histidine were possible.

peptide, Triton-X100 detergent for 100% release, and 4 nmol which causes near total macromolecule release. For comparison, there was about 0.5 nmol of each library member present in the screen. The MelP5 controls correspond to P:L of 1:25 in the small molecule and P:L of 1:50 in the macromolecule screen. This amount of MelP5 releases nearly 100% of the small molecules ANTS and DPX and the dextran.

The majority of library members screened cause significant small molecule leakage, and some macromolecule leakage. Here, we are interested in the outliers that cause significant macromolecule release. Therefore, positive peptides were selected from the area around the upper right hand quadrant of the plot. This quadrant represents simultaneous high small molecule leakage at pH 7 and high macromolecule leakage at pH 7. The sequenced library members are shown as red stars. They are found in the upper 2 percentile of the screened sequences on the macromolecular leakage axis (Fig. 1-7B). Thus, these peptides are gain-of-function daughter sequences of MelP5; they form macromolecule size pores in PC bilayers at pH 7 and at low peptide concentration. The screen suggested that the selected positives are much more potent than the parent peptide MelP5 at macromolecular poration, because ~0.5 nmol of these library members (P:L = 1:400) and as much as the 4 nmol MelP5 control (P:L 1:50).

Sequence Analysis of the Macrolittins

The sequences of five selected peptides, which we named “macrolittins” are shown in Fig. 1-7C along with the sequences of MelP5, the MelP5-based library, and the pHD peptides, for comparison. In Fig. 1-7D we show helical wheel representations of the idealized helical surfaces of the parent MelP5, and representative members of the sequence families. The macrolittins have a sequence motif that always contains three acidic residues, either glutamic or aspartic acid out of six possible acidic residues in the library. The probability of this occurring by chance five times (p) is 0.013. The acidic residues at the fourth and eighth positions are highly conserved (9/10 in

total) in the five macrolittins. They are also conserved in the ten pHD peptides (20/20 total). The macrolittins sometimes have acidic residues in position 11 (3/5 peptides), position 15 (2/5), infrequently in position 12 (1/5) and position 18 (0/5), averaging about 1.0 acidic residues per peptide in those four positions. In comparison, each pHD peptide has either 3 or 4 acidic residues in those four positions, averaging 3.2 acidic residues per sequence in those four positions. More specifically, while positions 12 and 18 are acidic in the pHD peptides in 17 out of 20 chances, they are rarely acidic in the macrolittins (1/10) giving a probability of < 0.0001 for this to have arisen by chance.

For the basic residues in positions 8 and 21 of the macrolittins, lysine was selected over histidine, 9 times in 10 chances ($p=0.01$). This demonstrates a strong preference for lysine in the macrolittins that does not exist in the pHD peptides. Slightly more than half (11/20) of the possible basic residues in the pHD peptides were histidine instead of lysine, indicating that there is no preference. We note that both histidine and lysine are charged at $pH < 5.5$ where the pHD peptides are active, while only lysine is charged at pH 7 where the macrolittins are active.

Macromolecule Leakage of the macrolittins

To fully characterize the sequences identified in the screen, we synthesized three representative macrolittins, 70, 159 and 204 (Fig. 1-7) and measured their ability to permeabilize lipid vesicles made from POPC to a 40 kDa dextran as a function of peptide concentration. The leakage activity curves at pH 7 are shown in Fig. 1-8A. Macrolittins release TAMRA-biotin dextran (40 kDa) with a leakage inducing concentration of 50% effect (LIC_{50}) of $P:L \leq 1:800$. This is remarkably potent activity for macromolecule release, matched only by the pHD peptides at pH 5 (Fig. 1-8B). While MelP5 releases a 10 kDa dextran at similar LIC_{50},[42] its ability to release a 40 kDa is much lower, with LIC_{50} at P:L = 1:50 (Fig. 1-8A). For comparison, the most

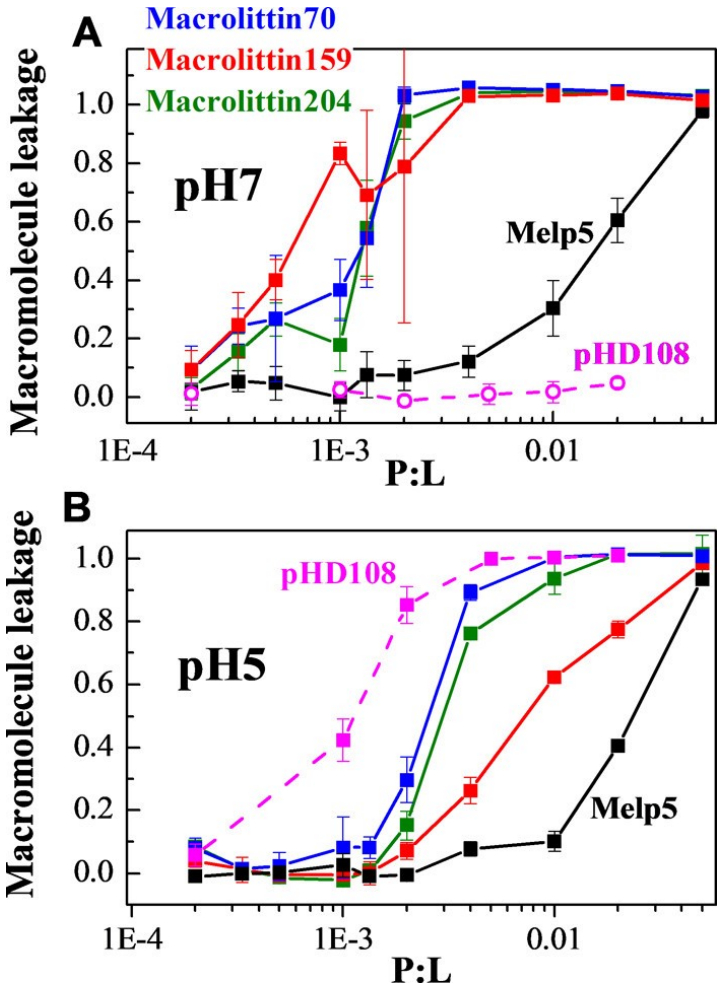

Figure 1-8: Macrolittin-induced leakage of a 40 kDa dextran from POPC vesicles. Vesicles with entrapped TAMRA-biotin-dextran 40 kDa (TBD) were incubated with serial dilutions of peptide in the presence of Alexafluor488-streptavidin (AF488-SA) for 1 h. FRET between TBD and AF488-SA was measured, followed by disruption with Triton-X100 to determine the FRET for complete leakage. (A) Experiments at pH 7, where the pHD peptide pHD108 is inactive. (B) Experiments at pH 5, where pHD108 is active.

active pHD peptides, at pH 5, release 40 kDa dextran with LIC_{50} values of P:L=1:800[22], similar to the macrolittins at pH 7.

We also measured macrolittin-induced dextran leakage at pH 5 (Fig. 1-8B) to directly compare the macrolittins to the pHD peptides under identical conditions. Surprisingly, the two families have opposite pH dependences. Unlike the pHD peptides which gain activity at pH 5, the macrolittins are somewhat less potent at pH 7 than they are at pH 7, with LIC_{50} values between 1:150 and 1:400. However, even at pH 5, the macrolittins are more potent than MelP5. The activity of MelP5 is similar at both pH values as reported previously[22].

Circular Dichroism and Tryptophan Fluorescence for the Macrolittins

To assess the secondary structure of the macrolittins, we measured their circular dichroism spectra, at pH 7 and pH 5, in buffer with and without lipid vesicles. The control peptide MelP5 is random coil in buffer and becomes highly helical only upon membrane binding (Fig. 1-9). Surprisingly, the macrolittins are highly helical in buffer at pH 7 (Fig. 1-9A), and also at pH 5 (Fig, 1-9B), even in the absence of lipid vesicles. This unexpected finding suggests that they readily self-assemble into stable helical multimers in buffer perhaps like the melittin tetramers that form under some conditions[83]. In the presence of POPC vesicles, the macrolittins retain their well-organized alpha helical secondary structure, while the control peptide MelP5 shows a sharp transition to alpha helix only upon binding to vesicles.

We used the fluorescence of the single tryptophan at position 19 of the peptides, to further assess their structure in buffer and in membranes. The tryptophan in MelP5, which is random coil and monomeric in buffer, has an emission maximum of 349 nm at pH 7 and at pH 5 as expected for a water-exposed tryptophan in a monomeric peptide (Fig. 1-10). On the other hand, the macrolittins in buffer have tryptophan emission maxima from 319-333 nm, significantly blue-shifted from those expected for water-exposed tryptophan. This observation is consistent

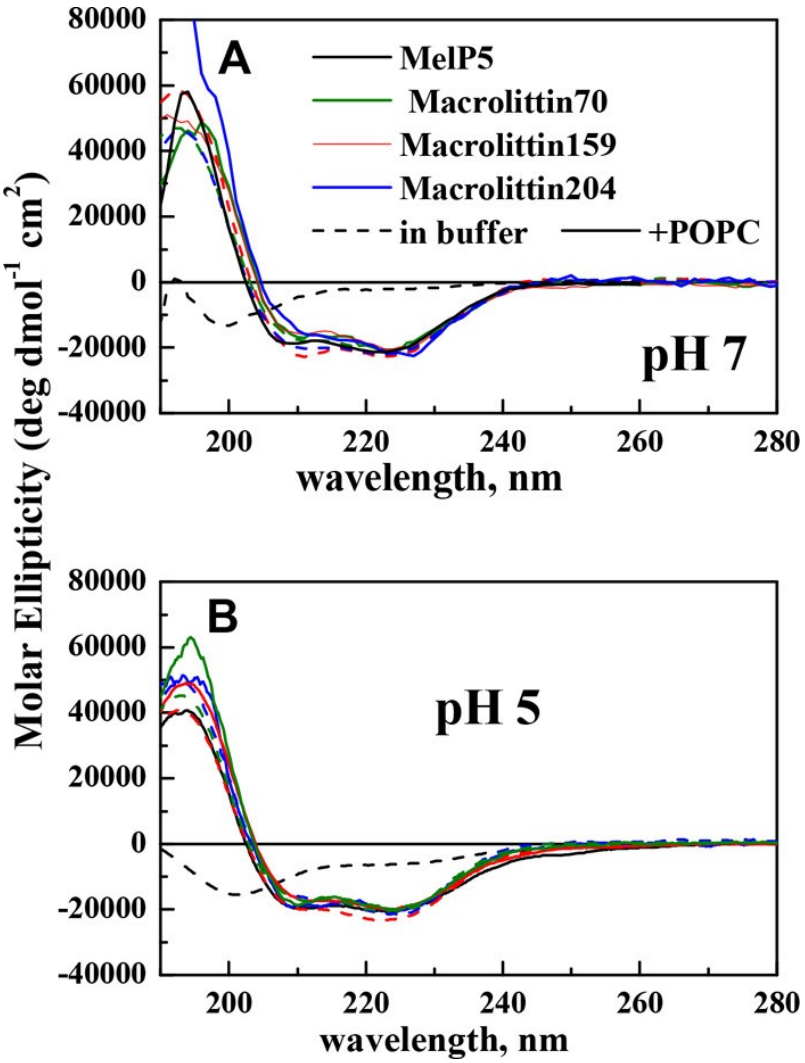

Figure 1-9: Solution circular dichroism spectra of macrolittins and MelP5 at 25 uM. Measurements were made before addition (dashed lines) and after addition (solid lines) of 1 mM POPC vesicles. (A) Measurements made at pH 7. (B) Measurements made at pH 5.

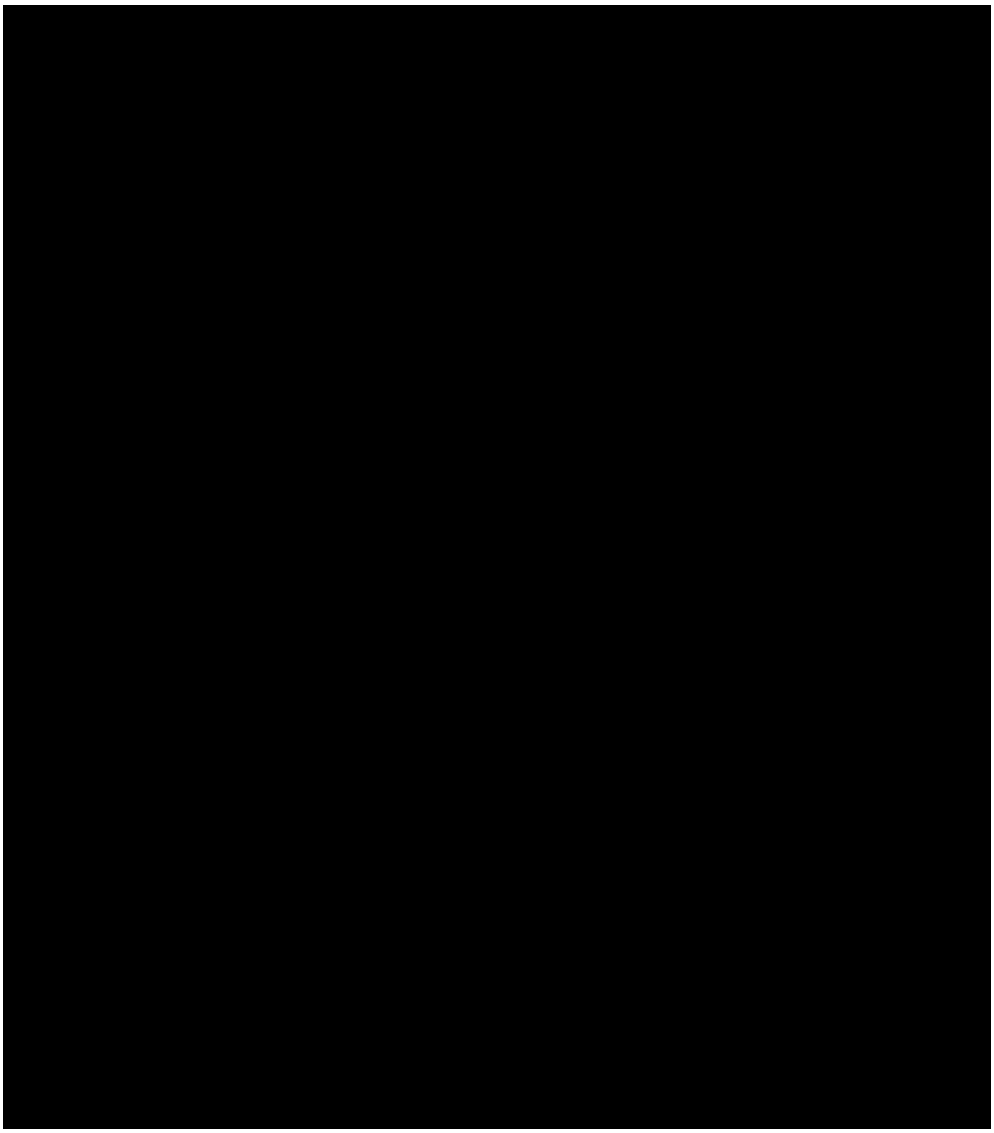

Figure 1-10: Tryptophan fluorescence spectra of the macrolittins and MelP5. Spectra were measured for 5 M peptide before addition (dashed lines) and after addition (solid lines) of 1 mM POPC vesicles. Excitation was at 280 nm. Emission spectra are normalized to the maximum intensity in buffer.

with our conclusion that the macrolittins form helical multimers in buffer, as multimer formation would bury the Trp residue in a less polar environment. In the presence of POPC vesicles, MelP5 and the macrolittins have very similar tryptophan emission maxima of 320-330 nm, signifying a similar environment in the membrane. These emission maxima are in the expected range for a tryptophan that is membrane inserted[45] as we have reported for MelP5[33] and the pHD peptides at pH 5 in bilayers[22].

Oriented circular dichroism spectroscopy of the Macrolittins

To determine the orientation of the macrolittin helices in bilayers, we used macrolittin159 as a representative of the family, and subjected it to oriented circular dichroism (OCD). Samples for OCD were hydrated stacked multilayers containing 5 mol% peptide. The experimental OCD spectra are shown in Fig. 1-11, and can be compared to the theoretical OCD spectra shown as a function of fraction of peptide inserted in a membrane spanning orientation[84]. Comparison of the positions and ratios of the experimental macrolittin159 OCD spectral peaks to the theoretical peaks suggested that macrolittin159 is a membrane-spanning helix at pH 7. We estimate an inserted fraction of at least 80%. Previously, we showed that MelP5 is also a membrane-spanning helix under these conditions[33].

Discussion

Several thousand membrane destabilizing peptides, including antimicrobial peptides and other classes of pore-forming peptides, have been described and investigated over the past decades[81,85–88]. Many of these peptides are cationic and destabilize anionic bilayers in a manner driven by strong electrostatic interactions. Efficient permeabilization of zwitterionic phosphatidylcholine (PC) bilayers at low P:L (≤1:100) is uncommon, and efficient release of macromolecules from PC vesicles at low P:L ratios was essentially unknown until we reported the discovery of a novel peptide, MelP5[33]. This peptide is unique in its ability to allow the efficient passage of

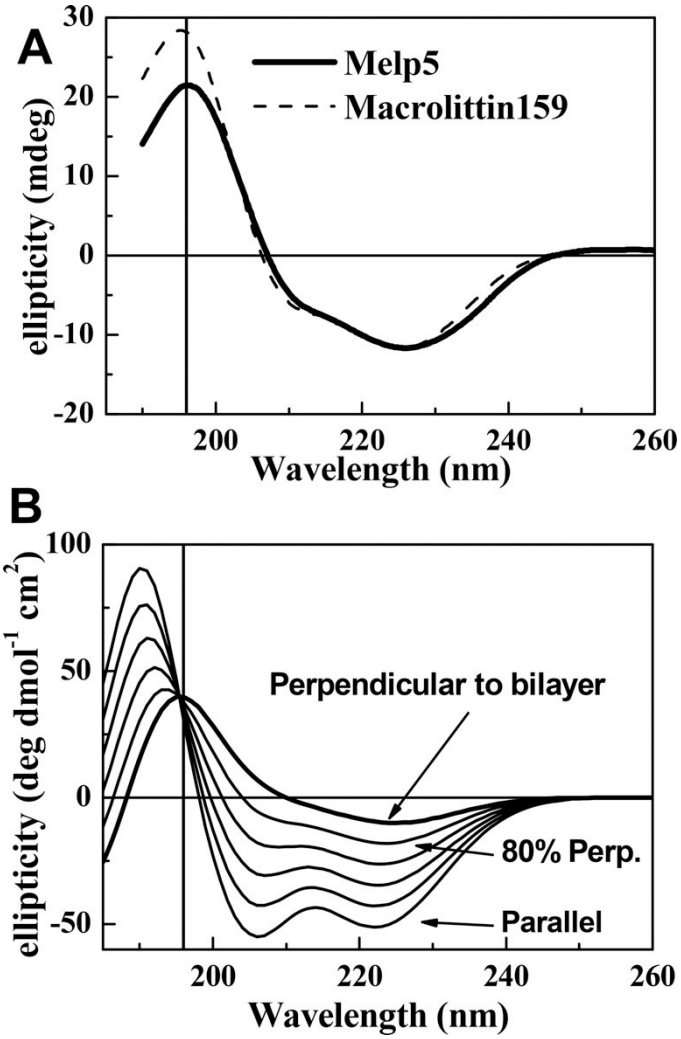

Figure 1-11: Oriented Circular Dichroism.

(A) OCD spectra are shown for macrolittin159 and for MelP5 in comparison in stacked, oriented POPC multibilayers on a quartz substrate hydrated with water through the vapor phase. Spectra are the average of eight individual spectra collected at rotations around the beam axis. The lipid only spectra have been subtracted. (B) Basis theoretical OCD spectra, (top and bottom curve) and linear combinations for parallel and perpendicular helices calculated as described previously[84]. The four intermediate curves are for increments of perpendicular helix increasing by 20% per step.

macromolecules through membranes, even at very low peptide-to-lipid ratios (P:L ≤ 1:500 when using 10,000 Da dextran as a probe) where detergent-like vesicle solubilization is unlikely[36,42]. Here, we used MelP5 as a template for an iterative peptide library that we designed and screened to select peptides that cause macromolecular permeabilization of a 40000 Da dextran at low P:L, like MelP5, but in a pH-dependent manner. The peptides that were identified are remarkably potent, macromolecular sized pore-formers at pH 5, while having little or no membrane activity at all at pH 7. Thus, we succeeded in "evolving" MelP5 for gain of function. All of the selected peptides possess exquisite pH sensitivities, with activities transitioning from ~0 to ~100% over one pH unit, centered on apparent pKa values of 5.5 to 5.8. This success in achieving a goal that we previously failed to achieve using a completely rational design approach[23] highlights the power of synthetic molecular evolution.

Mechanism of Action of the pHD peptides

All 10 of the positive peptides identified in the library have five or six acidic residues out of the six possible, despite the fact that only 17% of library members have five or six acidic residues. The peptide with six charges that we tested is somewhat less potent and has a lower pKa than the peptides with five charges (Figure 1-4B), suggesting that five negative charges arranged with helical spacing on an amphipathic helix are optimal for the observed pH-triggered activity. The fact that we observed various patterns of five acidic residues in the selected positives indicates that the pH sensitivity is due to the physical chemistry of folding and membrane binding. Yet, the specific preference of glutamate compared to aspartate, the overabundance of acidic residues is several positions, and the 100% conservation of glutamine at position 17 suggests that sequence-specific interaction may also play a role in this activity.

According to the Henderson−Hasselbalch equation, an equilibrium that simply reflects protonation of glutamate or aspartate should transition from 10% to 90% complete over two pH

units and 1% to 99% over four pH units. However, we observe transitions in dextran leakage, secondary structure and binding by the pHD peptides from near 0% to near 100% over one pH unit (Figure 1-6), indicative of highly cooperative behavior. Furthermore, the apparent pKa values that we measure for the selected peptides range from 5.5 to 5.8, much higher than the pKa of ~3.5 to 4.0 expected for the free side chains for Glu or Asp. We hypothesize that the tight coupling between membrane partitioning, α-helix formation, and electrostatic repulsion between acidic side chains drives both the upward shift in pKa, relative to that of the free side chains, and the unexpectedly sharp transition. Potentially favorable electrostatic interactions between the basic lysine and histidine residues, and some of the acidic side chains may also contribute to the pH sensitivity.

To estimate the protonation state of the peptide, we used the Membrane Protein Explorer (MPEx)[89] to predict free energies of membrane partitioning of the pHD peptides compared to MelP5. Assuming that bound peptides are 75% α-helix[33] (Figure 1-5A), protonation of at least four or five of the acidic side chains in the pHD peptides would be required for strong membrane partitioning that we observed at pH 5. Thus, we hypothesize that most of the acidic side chains in the pHD peptides are cooperatively protonated with an apparent pKa of 5.5−5.8.

Implications for Peptide Design and Applications

In previous work, we attempted to engineer pH sensitivity into the unique macromolecular poration activity of MelP5, but failed. Here we achieved the goal of pH-triggered macromolecular poration using a fundamentally different approach: synthetic molecular evolution, which is accomplished with orthogonal screening of a rationally designed, iterative, combinatorial peptide library. Despite being able to list similarities and differences between the rationally designed and molecularly evolved peptides, we are not able to identify obvious logical flaws in the rational design approach based on any molecular principle. Specific design principles are not yet apparent

from sequence comparison alone. Given the lack of complete understanding of structure−function relations for membrane-active peptides in general, our work shows that synthetic molecular evolution is a powerful, and necessary, method to drive the discovery of novel peptides with specific membrane activities.

The peptides we have selected cause pH-triggered macromolecular poration, a property that could potentially be exploited in multiple ways. For example, there are applications in medicine where acidic environmental pH could be used to trigger the activity of the new peptides. One example is the acidic environment around solid tumors[62] where tumor selective cytolytic activity could be triggered. A second example are acidified organelles, such as endosomes and lysosomes[14,90,91],17,49−51 where selective cargo delivery into the cytosol could be enabled by pH-induced macromolecular poration. The work described here opens new doors to exploring such applications using peptides with activities that are triggered by a physiologically relevant decrease in pH.

Macrolittin Discussion

Here we have also described the macrolittins, a family of peptides that release macromolecules from lipid bilayers made from zwitterionic PC lipids at very low peptide concentration and at neutral pH. Macrolittins readily enable the passage of a 40,000 Da dextran, a macromolecule with 4.5 nm hydrodynamic radius through lipid bilayers. Macromolecule release from liposomes is measurable at P:L as low as 1:5000 (20 peptides per vesicle) and reaches 50% at P:L as low as 1:1000, or 100 peptides per vesicle. Except for the pHD peptides at low pH (Fig. 1-8B), such potent macromolecular poration by peptides in PC bilayers is unprecedented in the literature.

In the MelP5-based library from which both the macrolittins and the pHD peptides were selected, six positions had the possibility of containing an acidic aspartate or glutamate residue, or

the native residue or, in some cases, another nonpolar residue (Fig. 1-7). The selected macrolittins share a common, variable motif, always with three acidic amino acids per peptide, compared to five or six in all pHD peptides. In Fig. 1-7D, we show the helical wheels of MelP5, the library, representative macrolittins, and representative pHD peptides. We note that these helical wheels may not be precisely correct because the Gly-Leu-Pro segment at residues 12-14 may be poorly structured and may lead to N- and C-terminal helices that are somewhat independent of each other. Nonetheless, the helical wheels show that the library template sequence of MelP5 is highly amphipathic with a narrow polar face width. The library contains protonatable residues spread across a face that is much wider than the polar face of MelP5 and could potentially increase the polar face angle to almost 180°. While the polar face of the pHD peptides encompasses the largest widths that are encoded in the library, some of the acidic residues may be protonated at pH 5 where the peptides are active. The macrolittins show a narrower polar face with acidic residues mostly in positions 4,8 and 11 or 15, which comprise the center or the polar face. Residues 12 or 18, which are the outside-most two residues on the acidic face, are rarely found to be acidic in the macrolittins (1/10), while they are acidic most of the time (17/20) in the pHD peptides.

The fact that two acidic residues at positions 4 and 8 are nearly 100% conserved in the five macrolittins (and also in the ten pHD peptides) may indicate that they are critical for the function that we observe for both families of peptides. The core of the polar face may be important for the structure that enables macromolecular poration. If so, the outermost residues of the wide polar face of the pHD peptides may be important for pH sensitivity. The conserved anionic residues at residues 4 and 8 are found on the same face of the N-terminal half of the helix. They are at about a 90° angle on the helical wheel from either of the two positive residues, residues 7 and 21. The fact that we found lysine over histidine in these positions in 9/10 chances indicates that having a positive charge at pH 7 is important for macrolittin function. We speculate

that parallel macrolittin helices have lateral electrostatic interactions between the conserved acidic groups and the basic amino acid at position 7. Such a stabilized structure would create an amphipathic surface that could participate in a large pore. Antiparallel helices that are electrostatically stabilized by interactions between the N-terminal acidic residues and the basic residue at position 21 are also possible, however the surface formed would be less amphipathic and thus seems less likely.

The ability to fold into an amphipathic -helix in membranes is a common property for all of the generations of peptides discussed here, and for many other membrane permeabilizing peptides[92]. The original natural parent peptide, melittin, forms an amphipathic helix in membranes that lies mostly parallel to the membrane surface and creates transient pores at moderate concentrations[36,93–95]. The synthetically evolved daughter sequence MelP5 has a more ideally amphipathic structure than melittin. It exists in a stable transmembrane configuration in PC bilayers and forms equilibrium pores[33] that release macromolecules[42]. This behavior is consistent with the observation reported here that the macrolittins also have a transmembrane orientation. Transmembrane orientation is likely a critical structural requirement for macromolecular poration[33].

We do not yet know the pore structure, but we can narrow the possibilities by considering minimal possible geometries. An extruded unilamellar vesicle is nominally 50 nm in radius, has about 100,000 lipids and has a surface area of ~ 3x104 nm^2. A dextran of 40 kDa has a hydrodynamic radius of ~4.5 nm meaning that a “pore” of at least 80 nm^2 (5 nm radius, 1/300 of the vesicle surface area) would be minimally required to pass it. If we consider a classical barrel-stave pore, in which the peptides are laterally close-packed, the pore would have a circumference of at least 30 nm, which would require ≥ 30 peptides to line it. Thus, a lipid vesicle can have only a few pores at P:L ~ 1:1000 (100 peptides per vesicle), where activity is high.

With such large pathways across the bilayer, it may be more fruitful to consider a structural model in which these amphipathic peptides drive bilayer thinning and stabilize exposed bilayer edges by reducing line tension at low concentration as other amphipathic peptides, proteins, polymers and detergents do at higher concentration[96–99]. In this scenario, individual peptides are not in direct contact with each other, but instead cooperatively alter lipid thickness and curvature to stabilize an exposed bilayer edge in a so-called toroidal pore geometry[100–102]. In this architecture, electrostatic stabilization remains possible because such interactions have a long range. Fewer peptides could be needed to stabilize such a toroidal "pore". The critical interactions, in this case, would be curvature-dependent interactions between peptides and the bilayers that may work synergistically with electrostatic interactions between peptides.

CHAPTER 2: MECHANISM OF ACTION OF PEPTIDES THAT CAUSE THE PH-TRIGGERED MACROMOLECULAR PORATION OF LIPID BILAYERS

A version of this chapter is published in the Journal of the American Chemical Society (2019) Vol. 141, No. 16, pg. 6706-6718.

Sarah Y. Kim[1], Anna E. Pittman[2], Elmer Zapata-Mercado[1], Gavin M. King[2,3], William C. Wimley[4], and Kalina Hristova[1]

[1]Department of Materials Science and Engineering, Institute for NanoBioTechnology, and Program in Molecular Biophysics, Johns Hopkins University, Baltimore, MD 21218

[2]Department Physics and Astronomy, University of Missouri, Columbia, MO, 65211

[3]Department of Biochemistry, University of Missouri, Columbia, MO, 65211

[4]Department of Biochemistry and Molecular Biology, Tulane University School of Medicine, New Orleans, LA 70112

Abstract

Using synthetic molecular evolution, we previously discovered a family of peptides that cause macromolecular poration in synthetic membranes at low peptide concentration, in a way that is triggered by acidic pH. To understand the mechanism of action of these "pHD peptides", here we systematically explored structure-function relationships through measurements of the effect of pH and peptide concentration on membrane binding, peptide structure, and the formation of

macromolecular-sized pores in membranes. Functional assays demonstrate the peptide-induced appearance of large pores in bilayers. Pore formation has a very steep pH dependence, and is also dependent on peptide concentration. In vesicles, 50% leakage of 40 kDa dextrans occurs at 1 bound peptide per 1,300 lipids, or only 75 peptides per vesicle, an observation that holds true across a wide range of acidic pH values. The major role of pH is to regulate the amount of peptide bound per vesicle. The physical chemistry and sequence of the pHD peptides affects their potency and pH dependence, and therefore the sequence-structure-function relationships described here can be used for future design and optimization of membrane permeabilizing peptides for specific applications.

Introduction

Membrane active, pH-sensitive peptides can be utilized for delivering cargo to cells through endosomes[78,103,104], or for new therapies that target cancer cells[60,72,77], among other applications. Although the mechanism of action of several such pH-sensitive peptides have been studied, the peptides previously investigated either insert as monomers without pore formation (i.e. pHLIP), or form only small pores in membranes (e.g. GALA)[75,76]. Large pores are needed for most applications. The mechanism of action of pH-sensitive peptides that form large, macromolecule-sized pores will likely involve additional factors such as cooperativity and peptide-peptide interactions. By rationally designing an iterative peptide library based on a pH-insensitive pore-forming peptide, MelP5[23,42], and using a high-throughput functional screen, we have previously discovered a family of peptides that cause macromolecular poration in synthetic membranes at low concentration, in a way that is triggered by acidic pH[22]. These peptides, which we named the pH-dependent Delivery (pHD) peptides, are unprecedented in their ability to cause highly efficient, pH-triggered leakage of large molecules through synthetic membranes. At pH 7 or above, the members of this synthetically evolved family of sequences are essentially inactive;

they induce little release of small or large molecules from lipid bilayer vesicles. Yet, at pH ≤ 6, they bind to membranes, fold into α-helices, and enable efficient release of macromolecules at very low peptide concentration.

To understand the mechanism of action of the pHD peptides, here we asked how peptide density on membrane surfaces and cooperativity between peptides promote macromolecule-sized pore-formation. Furthermore, we asked how pH regulates these processes. To answer these questions, we examined the structure of the pores formed, and we systematically explored structure-function relationships through measurements of the effect of pH and peptide concentration on membrane binding, peptide structure, and the formation of large pores by the pHD peptides in fluid phase phosphatidylcholine (PC) membranes.

Results

Peptides Selected for Study

Here, we selected three pHD peptides for detailed characterization. The peptides pHD24 (GIGDVLHELAADLPELQEWIHAAQQL) and pHD108 (GIGEVLHELAEGLPELQEWIHAAQQL) were selected because they are canonical sequences, with 5 acidic residues like most of the active sequences identified. These two peptides had similarly potent activity, and similar pH50 values in our preliminary studies[22]. pHD24 has 3 aspartate residues and two glutamates, the more common acidic residue found across the family, while pHD108 has 5 glutamates. The peptide pHD15 (GIGEVLHELADDLPDLQEWIHAAQQL) is an outlier which has 6 acidic residues. Its potency is somewhat lower, and it becomes active at a somewhat lower pH than the others. We include it here to enable characterization across a range of potencies and pH dependences.

Macromolecular poration by the pHD peptides

Using the same fluorescence-based assay we developed for the screen in which we discovered the pHD peptides[22], we characterized the ability of pHD15, pHD24, and pHD108 to form large pores in vesicles as a function of both pH and peptide concentration. Results from these assays are shown in Figure 2-1. Figure 2-1A shows a schematic of the assay. The entrapped probe used to detect macromolecule leakage was a 40,000 Da dextran labelled with the dye TAMRA (fluorescence acceptor) and with biotin (called "TBD" for TAMRA-biotin-dextran). The external solution contained streptavidin labelled with Alexafluor488 (fluorescence donor). In this assay, leakage of encapsulated TBD leads to streptavidin-TBD complex formation and quenching of Alexafluor488 due to FRET[23,42]. The hydrodynamic radius of dextran is about 4.5 nm[105], and therefore a pore with a radius of at least 45 Å is required to form in the bilayer, for dextran leakage to occur. In Figure 2-1B, we show the kinetics of TBD leakage. Upon addition of peptide to solution of vesicles at pH 5, the donor fluorescence drops steeply and reaches a plateau. Leakage is rapid, with greater than 90% leakage occurring over 10 minutes. In Figure 2-1C we show the fractional leakage of TBD, measured at 60 minutes, as a function of peptide-to-lipid ratio (P:L) at pH 5. pHD24 and pHD108 are very potent at pH 5, with substantial activity observed at concentrations as low as 1 peptide per 1000 lipids, and ≥95% activity at P:L = 1:200. pHD15 is less active, with ≥95% activity occurring at about P:L = 1:100. MelP5, the parent peptide used for library design, is less active than pHD15 with ≥ 95% activity at P:L > 1:50. No leakage is observed at pH 7 for any of the pHD peptides, even at the highest concentrations measured. In Figures 2-1D-F, we show the leakage as a function of pH for pHD15, pHD24, and pHD108. At the lowest concentrations, little or no leakage is observed at any pH. At the highest concentrations, leakage sharply transitions to 100% with decreasing pH. Under these conditions, the transition as a function of pH is steep, occurring over 1 pH unit. Such steepness likely

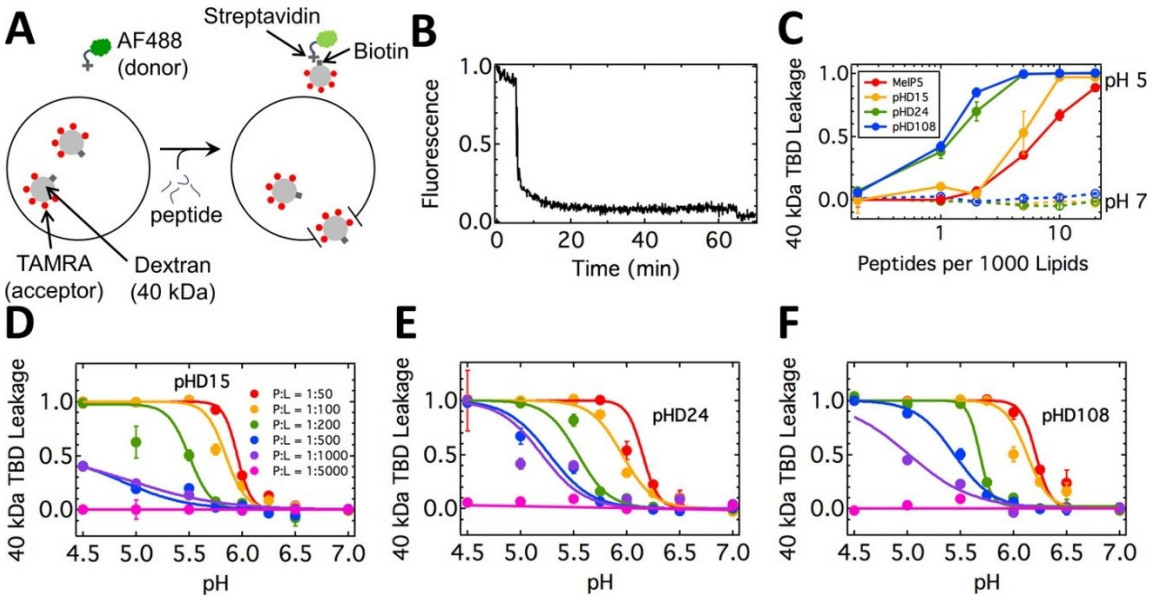

Figure 2-1: Macromolecular leakage assay.

(A) Schematic of the assay. Peptides were incubated with streptavidin-AlexaFluor488 and POPC vesicles containing TAMRA-biotin-dextran (TBD) for 1 h. Upon peptide-mediated macromolecular poration, the 40 kDa dextran can leak out of the vesicles and form a complex with streptavidin, leading to FRET. (B) Time course of streptavidin-AlexaFluor488 (donor) intensity upon TBD vesicle permeabilization. At about t = 5 min, pHD108 (P:L = 1:100) was added to a solution of 1 mM POPC at pH 6. After 1 h, Triton X100 was added for the 100% leakage fluorescence value. (C) Extent of dextran leakage as a function of concentration at pH 5 and 7. At pH 5, the pHD peptides are more potent than MelP5. At pH 7, the pHD peptides are not active, even at the highest concentrations measured. (D–F) Dextran leakage as a function of pH and P:L for pHD15 (D), pHD24 (E), and pHD108 (F).

indicates that the acidic residues protonate and deprotonate cooperatively[106]. Interestingly, we observe a large increase in pH50 as peptide concentration is increased. Peptides pHD24 and pHD108 experience a shift of about one pH unit when the peptide concentration is increased from P:L of 1:500 to 1:50. For pHD15, the shift is somewhat smaller at P:L where it can be compared.

Small molecule release in response to the pHD peptides

To determine if the pHD peptides form small pores at low peptide concentrations, we measured pore formation with an ANTS/DPX leakage assay, which detects the leakage of ~0.4 kDa ANTS[107]. Results from these assays are shown in Figure 2-2. Vesicles containing co-encapsulated fluorophore (ANTS) and quencher (DPX) were incubated with peptide for 1 hour. Figure 2-2A shows a schematic of the leakage assay. Crowding of ANTS and DPX within the vesicles quenches ANTS fluorescence. Pore-formation results in ANTS/DPX release and a concomitant increase in ANTS fluorescence. In Figure 2-2B, we show the kinetics of leakage. Upon addition of peptide, ANTS fluorescence increases sharply, then reaches a plateau. Release of ANTS and DPX is rapid, and very similar to TBD leakage, with greater than 90% leakage occurring over 10 minutes. In Figure 2-2C we show fractional leakage of ANTS and DPX, measured at 60 minutes, as a function of peptide-to-lipid ratio. The peptides are very potent at pH 5, with substantial activity observed at concentrations as low as P:L = 1:1000 , and ≥95% activity at P:L = 1:200. Small molecule release is more potent than macromolecule release (Figure 2-1). In small molecule leakage, as with macromolecule leakage, pHD15 is less active than pHD24 and pHD108, and MelP5 is less active than pHD15, but the differences are smaller than for macromolecule release.

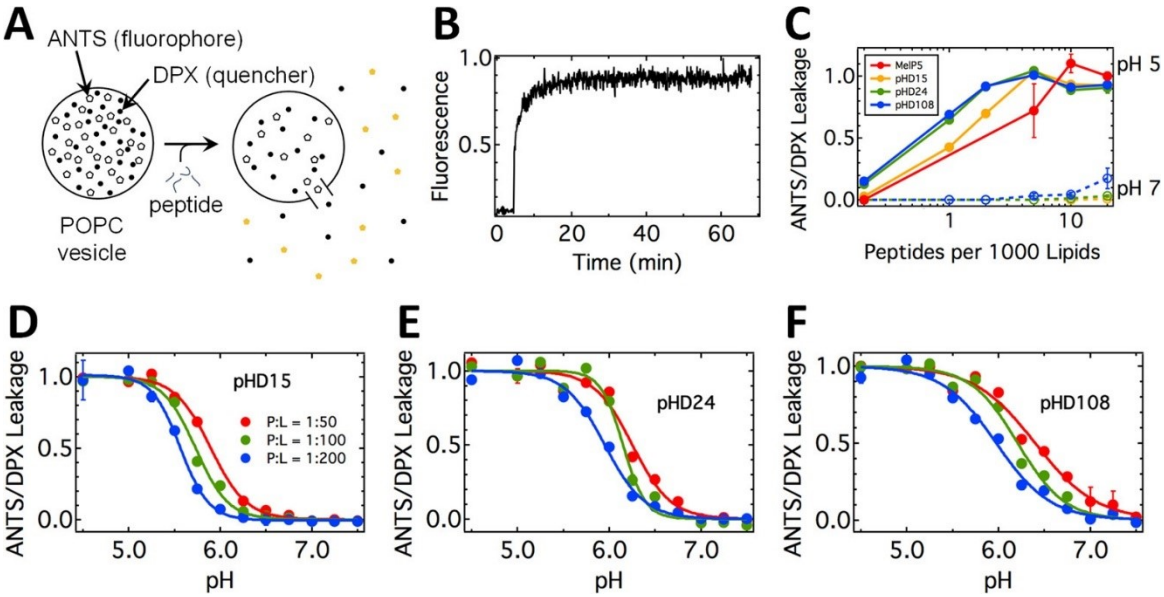

Figure 2-2: ANTS/DPX leakage assay.

(A) Schematic of the assay. Peptides were incubated with POPC vesicles with encapsulated ANTS (fluorophore) and DPX (quencher) for 1 h. Upon pore formation, the dilution of ANTS and DPX results in an increase in ANTS fluorescence. (B) Time course of ANTS leakage by pHD108 at pH 5. ANTS fluorescence was monitored on a fluorimeter (ex/em = 350/519 nm). At about t = 3 min, peptide was added to a cuvette with 1 mM POPC vesicles for a final P:L of 1:100. After 1 h, Triton X100 was added to obtain the 100% leakage fluorescence value. (C) Leakage as a function of P:L. At pH 5, the pHD peptides are more potent than MelP5. At pH 7, (dashed lines) the peptides do not cause much leakage, even at the highest concentrations measured. (D–F) Leakage as a function of pH for pHD15 (D), pHD24 (E), and pHD108 (F).

Little or no ANTS leakage is observed at pH 7 for the pHD peptides, even at the highest concentrations measured. In Figures 2-2D-F, we show the leakage as a function of pH for pHD15, pHD24, and pHD108. At the concentrations shown, leakage sharply transitions to 100% with decreasing pH. The transition as a function of pH is steep. Again, pH50 increases as peptide concentration is increased, with a shift of about 0.3 pH units when the peptide concentration is increased from P:L = 1:200 to 1:50. For pHD24 and pHD108, the pH50 increases from 6.0 to ~6.4. For pHD15, the pH50 is lower; it increases from 5.6 to 5.9 as peptide concentration is increased from 1:200 to 1:50.

Binding of the pHD peptides to membranes

We characterized the binding of the peptides as a function of pH and peptide concentration with tryptophan fluorescence titration[45]. As shown in Figure 2-3A, the fluorescence emission maximum shifts from ~350 nm at neutral pH to 330 nm at acidic pH, indicative of a transition from aqueous, exposed tryptophan to membrane-inserted tryptophan[45]. In Figure 2-3B, we show a kinetic trace of binding at pH 4.5, under conditions at which the peptide is active. Upon addition of peptide to a 1 mM vesicle solution at t = 8 minutes, binding occurs rapidly, and is essentially complete in 1 minute. In Figure 2-3C-E, we show the scaled fluorescence intensities at 335 nm as a function of pH for different peptide concentrations for pHD15, pHD24, and pHD108. In all cases, binding is dependent on pH with a sharp transition occurring over about 1 pH unit, which is indicative of cooperativity. Peptides pHD108 and pHD24 show a small increase in pH50 and a sharper slope as peptide concentration is increased. The pH50 increases from 5.1 to 5.6 for pHD108, and from 5.0 to 5.5 for pHD24 as P:L increases from P:L of 1:5000 to 1:50.

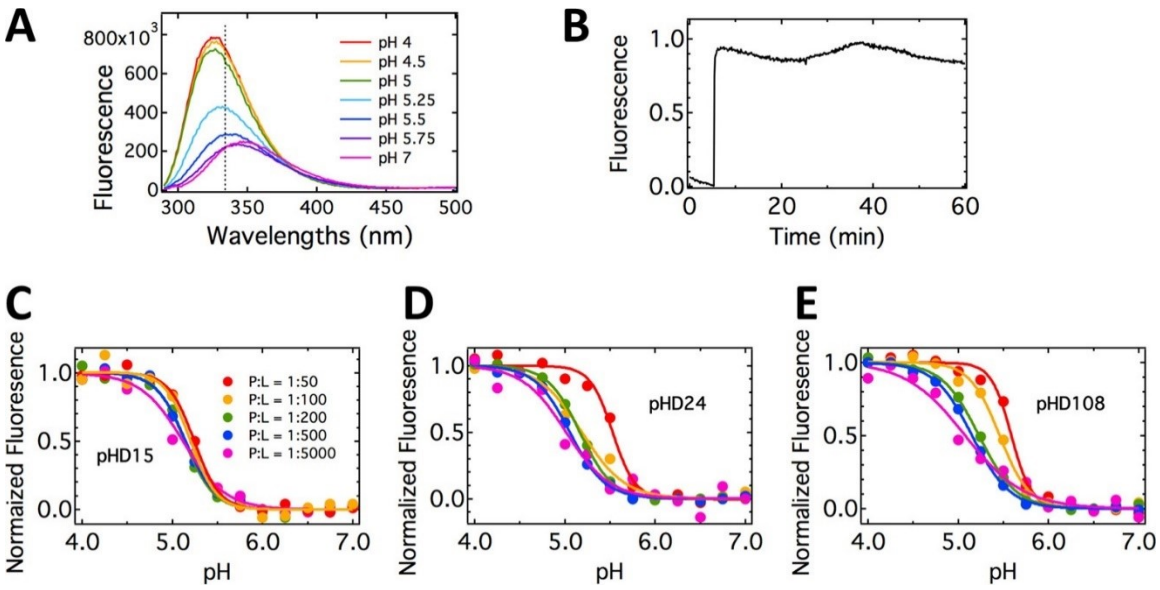

Figure 2-3: pHD peptide binding to lipid bilayers, as followed by tryptophan fluorescence.

Each pHD peptide has one tryptophan, and its fluorescence is sensitive to the polarity of its environment. (A) Fluorescence spectra of pHD15 as a function of pH ranging from 4 to 7. Samples with 10 μM pHD15 and 1 mM POPC (P:L = 1:100) were incubated for 1 h before spectra were recorded. The dotted line is at 334 nm. (B) Time course of pHD108 tryptophan fluorescence. Upon addition of vesicles at about t = 5 min, binding is rapid. (C–E) Normalized fluorescence as a function of pH for pHD15 (C), pHD24 (D), and pHD108 (E).

Acquisition of secondary structure upon membrane binding

To determine the secondary structure of the peptides, we used circular dichroism (CD) spectroscopy. We could only study peptides at the highest three peptide concentrations because the technique lacks high sensitivity. As shown in Figure 2-4A, the CD spectra of the pHD peptides transition from a spectrum typical of a random coil with one minimum at 200 nm at pH 7 to a spectrum characteristic of an α-helix with two minima at 208 and 220 nm at pH 4.5. The spectra indicate that the pHD peptides undergo transitions from random coil to α-helix as pH is decreased from 7 to 4.5. In Figure 2-4B-D, we show the relative % helicity as a function of pH and P:L for pHD15, pHD24, and pHD108. Folding, like binding and leakage, is dependent on pH and exhibits a cooperative transition occurring over 1 pH unit. All peptides show little to no change in pH50 as peptide concentration is increased over the available range. The pH50 for pHD15 is 5.3 ± 0.1 for all P:L. For pHD24, the pH50 increases from 5.3 to 5.5, and for pHD108 the pH50 increases from 5.4 to 5.5 as P:L increases from 1:200 to 1:50.

Comparison of pH50 values for binding, folding, and leakage of vesicle contents

In Figure 2-5, we compare the pH dependence of binding, folding, small molecule leakage and macromolecular leakage for the three highest peptide concentrations, for pHD15, pHD24, and pHD108. Several features are common for all peptides, at all P:L ratios. First, the differences in pH50 values for binding and helicity are not statistically significant, which is expected, given the binding-folding coupling that is typical of membrane active peptides[108]. pH50 for binding and structure also do not depend strongly on peptide concentration (discussed below). Second, the differences in pH50 for dextran and ANTS/DPX leakage are not statistically significant, with one exception. Third, and most interesting, the pH50 values for binding and helicity are always

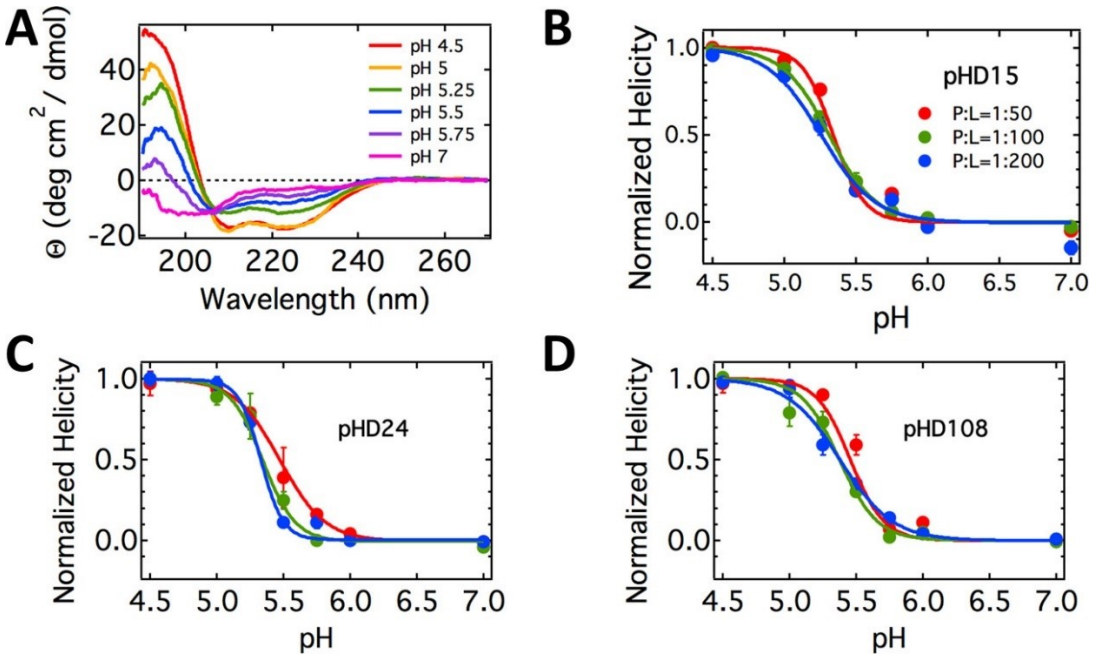

Figure 2-4: Secondary structure of the pHD peptides as a function of pH.

(A) Circular dichroism spectra of pHD108 at P:L = 1:200, measured after 1 h of incubation with 1 mM POPC vesicles. Separate samples were made for each pH. (B–D) The % helicity, measured as a function of pH, was calculated from the absorbance at 222 nm and scaled from 0 and 1 for pHD15 (B), pHD24 (C), and pHD108 (D).

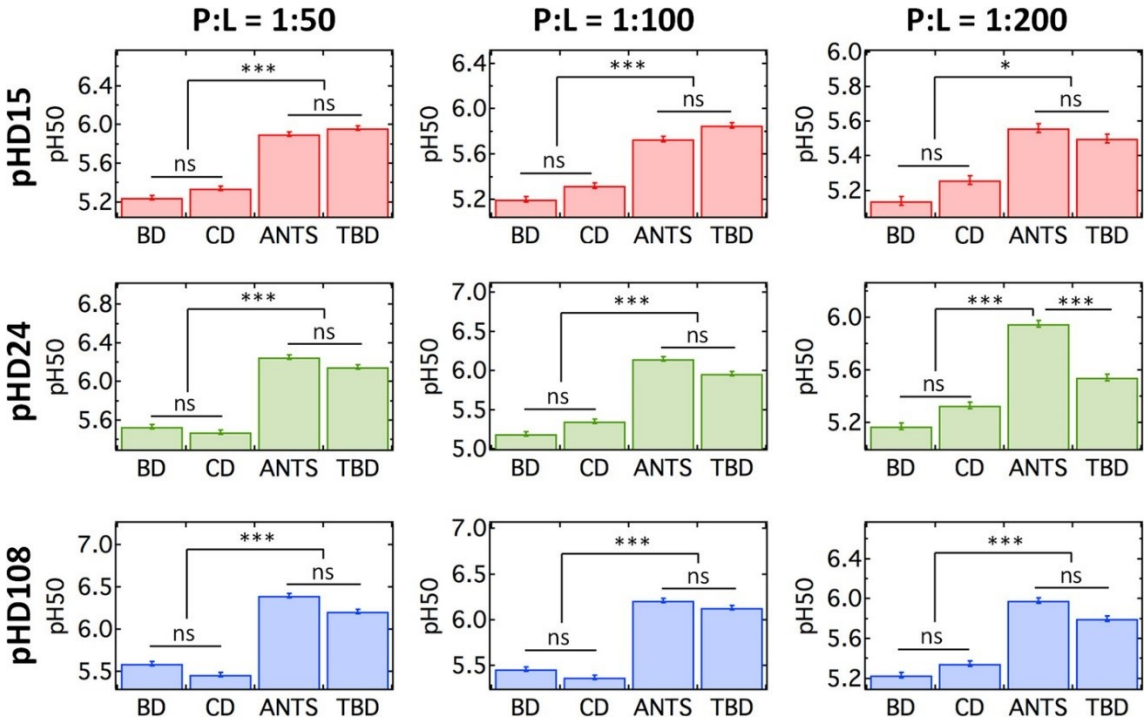

Figure 2-5: Comparison of pH50s

for binding (BD), folding (CD), ANTS/DPX leakage (ANTS), and TAMRA-biotin-dextran leakage (TBD) pKa's. Significance was calculated by ANOVA and a Tukey test for multiple comparisons, where **** indicates P< 0.0001, *** indicates P = 0.0001 to 0.001, ** indicates P = 0.001 to 0.01, * indicates P = 0.01 to 0.05, and ns indicates P ≥ 0.05.

significantly lower than pH50 for leakage. This effect is most pronounced at high peptide concentrations, a consequence of the observation in Figure 2-1 and 2-2 that the pH50 values for leakage increase with increasing peptide concentration.

Comparison of binding and dextran leakage pH50s

An intriguing consequence of the higher pH50 of leakage than of binding and folding is that at high overall peptide-to-lipid ratio, leakage is high despite the fact that binding and helicity appear to be negligible. In Figure 2-6, we compare the binding and dextran leakage curves for pHD15, pHD24, and pHD108 as a function of pH and peptide-to-lipid ratio. At P:L = 1:50 (top row), the binding and leakage curves are offset such that the pH50 for binding is lower than that for leakage. At high P:L, the greatest discrepancies in the fraction bound and fraction leakage occur at intermediate pHs. For example, at pH 5.75, pHD15 induces 96% TBD leakage when only 3% of the peptide is bound. At low P:L, the converse is true: leakage is close to zero despite the fact that the fraction bound is high. At P:L = 1:5000, the pH50 for binding for pHD15 is 5.12 ± 0.05. The pH50 for leakage cannot be calculated since no leakage is observed at any pH. The large discrepancies between fraction bound and fraction leakage indicate that the fractional leakage is not dependent on the fraction of peptide bound or folded.

Leakage is dependent on the number of peptides bound per vesicle

We sought to explain the discrepancies between fractional leakage and fraction bound by accounting for the actual amount of peptide that is bound to membranes under the different conditions. Since only bound peptides can induce pore formation, we calculated the number of peptides that are bound per lipid, under each condition, to determine if leakage scales with this variable. In Figure 2-7A, we show leakage as a function of bound peptide per lipid for pHD15

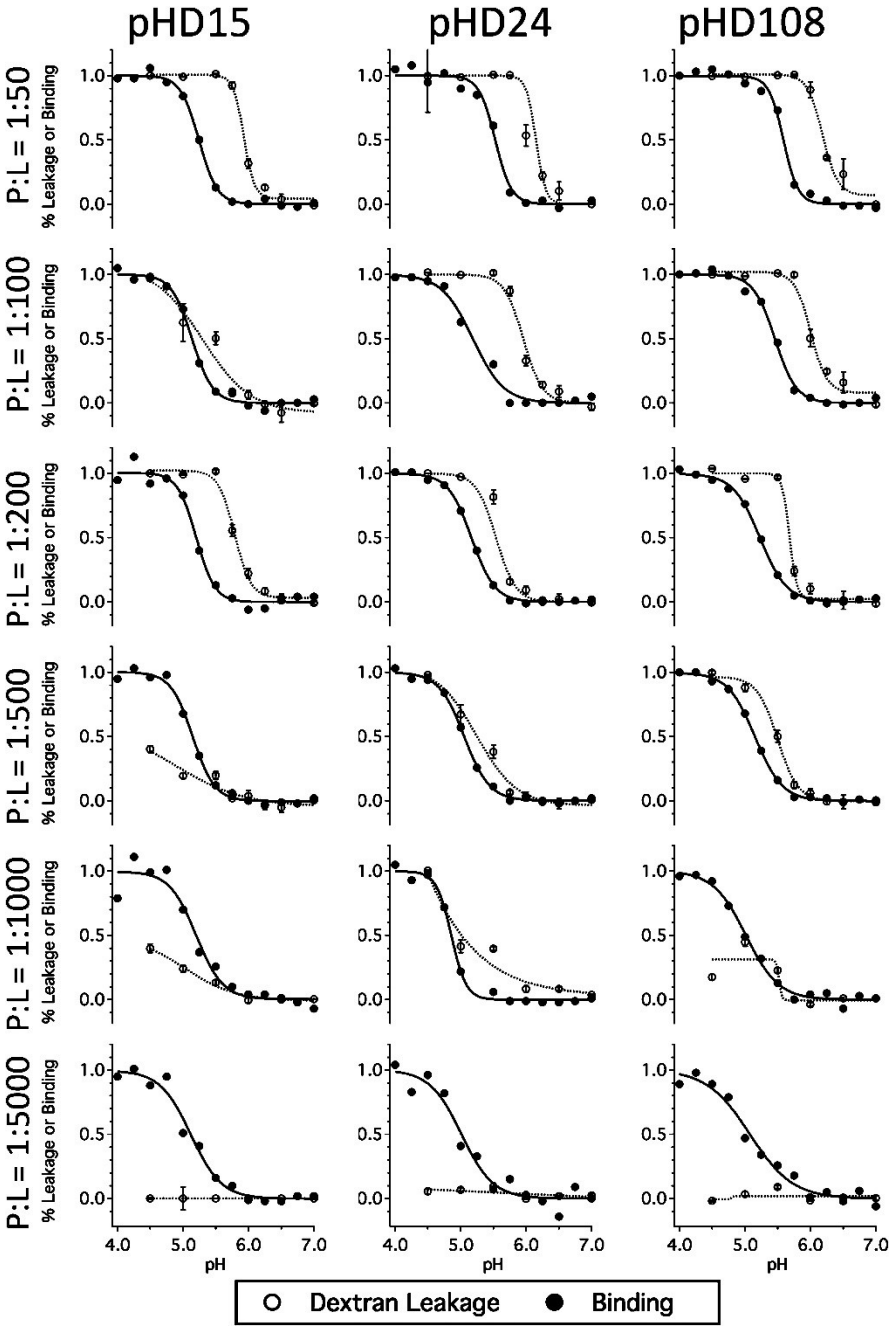

Figure 2-6: Comparison of binding and dextran leakage activity curves as a function of pH and P:L.

At the highest P:L, 100% leakage is possible when only a small fraction of peptide is bound, and at the lowest P:L, no leakage occurs even when all peptide is bound.

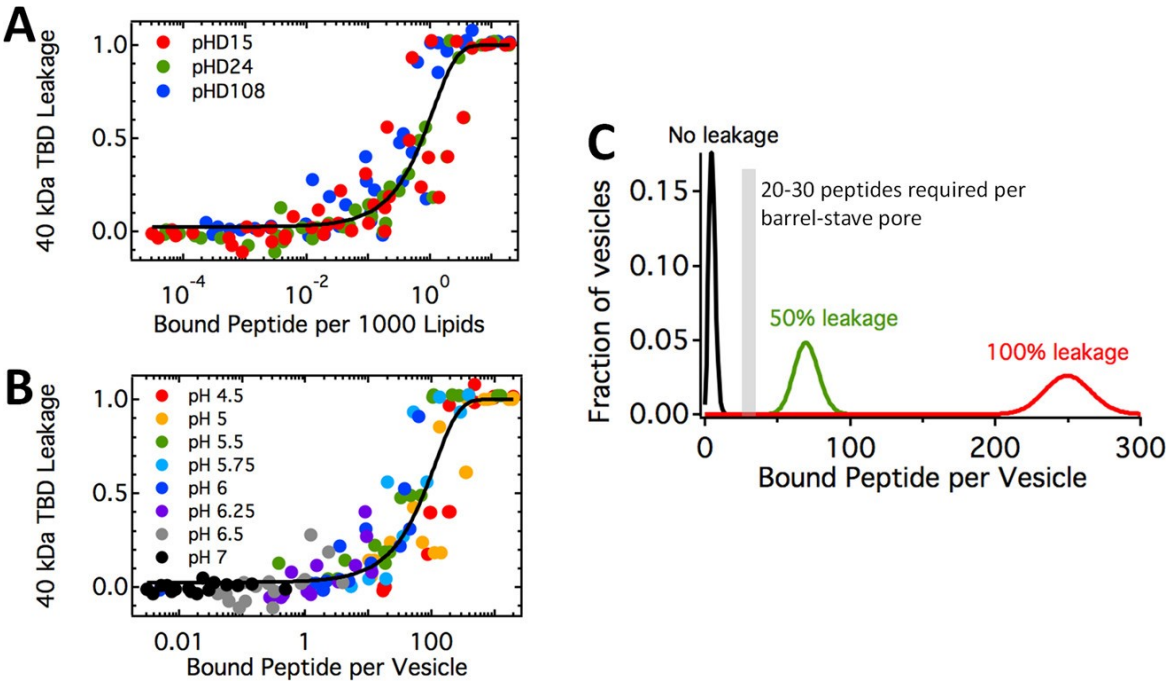

Figure 2-7: Activity of the pHD peptides depends on the number of bound peptides per vesicle.

(A) Dextran leakage as a function of bound peptide per lipid for the three peptides: red, pHD15; green, pHD24; and blue, pHD108. Leakage (50%) occurs when roughly 1 peptide is bound per 1300 lipids. (B) The same as in panel A but replotted as a function of bound peptides per vesicle, assuming that each vesicle has ~90 000 lipids. The different colors indicate the different pH values used in the experiment. Leakage (50%) occurs when on average 75 peptides are bound per vesicle. (C) Poisson distribution of peptides per vesicle, when averages are 10, 75, and 250 peptides per vesicle. The data in panel B show that in these three cases we observe no leakage, 50% leakage, and 100% leakage, respectively. This result can be rationalized, as we calculate that 20–30 peptides are needed to form a barrel-stave pore of ~4.5 nm diameter to allow for the passage of 40 kDa dextran. Thus, no leakage is expected when fewer than 20 peptides are bound per vesicle. Only partial leakage is expected when ~75 peptides are bound. Leakage (100%) is expected when more than 200 peptides are bound per vesicle.

(red), pHD24 (green), and pHD108 (blue). Plotted in this way, all of the data for all three pHD peptides can be fitted by a single curve (solid black line), indicating that the pHD peptide function depends solely on the amount of bound peptide. Leakage of 50% occurs when 1 peptide is bound per 1,300 lipids, a manifestation of the exquisite potency of the pHD peptides as we know of no other peptide, except the closely related macrolittins[24], that approach this potency for macromolecular poration.

Assuming an area per lipid of 70 Å^2,[109] it can be estimated that there are about 100,000 lipids per vesicle[81]. In Figure 2-7B, we rescale the data in Figure 2-7A, now plotting the leakage as a function of bound peptides per vesicle. The different colors in Figure 2-7B indicate the different pHs, and provide an illustration of the fact that the pH controls function entirely by controlling the amount of bound peptide. In Figure 2-7B we further see that 50% leakage occurs when only 75 peptides are bound per vesicle.

To rationalize these data, in Figure 2-7C we plot the Poisson distribution of peptides per vesicle, when averages are 10, 75, and 250 peptides per vesicle, corresponding to the cases of no leakage, 50% leakage, and 100% leakage (according to Figure 2-7B). We further estimate the number of peptides that are required to line a pore that permits passage of a 40 kD dextran through the bilayer. In particular, we reason that the pore must have a radius that is at least equal to the hydrodynamic radius of 40 kDa dextran, 4.5 nm. If we assume that the peptides are in contact with each other and that the diameter of the pHD helix, with side chains included, is 1.2 nm, we calculate that 20-30 peptides are required to line the perimeter of such a pore. This is called a barrel-stave pore[59]. Thus, little macromolecule leakage can be expected when fewer than 20 peptides are bound per vesicle, consistent with the experiment. At least partial leakage becomes possible once the 20-30 peptide cut-off is exceeded. It is also possible that the peptides

form toroidal pores, lined by both peptides and lipid headgroups[59]. In this case, fewer peptides would be required to line the pore. On the other hand, some peptides could line non-productive pores with diameters that are too small to allow the passage the 40 kDa dextran. Overall, the partial leakage that is observed experimentally at <100 peptides per vesicle is consistent with most of the vesicle-bound peptides participating in one or a few pores.

Dynamics of peptide association with membranes

Since a small fraction of bound peptides can cause substantial leakage, it is possible that the pHD peptides can exchange between vesicles and induce pores on multiple vesicles while the overall fraction of bound peptide remains low. We tested this possibility by evaluating if membrane-bound pHD15 can transfer to new vesicles composed of the brominated lipid, diBrPSPC. The bromines, located on the 9,10 positions on the acyl chains of the lipids, will quench tryptophan when the peptide is bound to membranes[46] (Figure 2-8A). Therefore, exchange from POPC to diBrPSPC will lead to quenching. To test for this possibility, pHD15 was incubated with 1 mM POPC vesicles at pH 4.5, where ≥95% of the peptides are bound (Figure 2-3C). After 0.2 mM of POPC or diBrPC vesicles were added, the tryptophan fluorescence intensity decreased (Figure 2-8B). The decrease caused by PC vesicles can be explained by dilution, however the rapid and much larger decrease into diBrPC vesicles suggests that peptides, initially bound to POPC vesicles, are rapidly quenched by diBRPC lipids with a halftime of a few seconds. Quenching is greater when more diBrPSPC is added (Figure 2-8C). Most likely, the observed quenching is due to rapid transfer of peptides between vesicles. However, it is also possible that the peptides mediate the fusion of diBrPC and POPC vesicles.

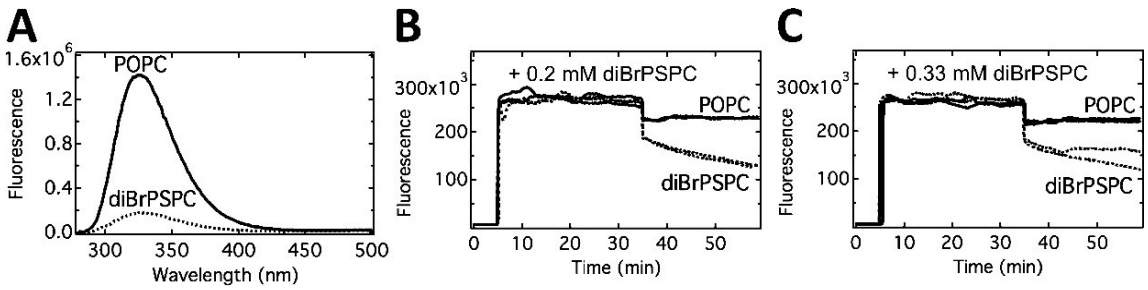

Figure 2-8: Quenching of tryptophan fluorescence by the redistribution of pHD peptides.

(A) pHD15 bound to vesicles composed of diBrPSPC displays quenched fluorescence. Peptide at 20 μM was incubated with 1 mM vesicles at pH 4.5 for 1 h before the emission spectra of tryptophan was measured (ex = 270, em = 280–500 nm). Peptides in the presence of vesicles composed of POPC or diBrPSPC show blue-shifted fluorescence, indicating that the peptide is bound. However, the tryptophan peak, in the presence of brominated lipids, is 87% lower in intensity. (B) Tryptophan fluorescence as a function of time upon the addition of a second batch of vesicles. Original samples are prepared with 1 mM vesicles. At t = 500 s, 20 μM pHD15 is added. After about 30 min, 0.2 mM POPC or diBrPSPC vesicles are added to the cuvette. (C) Same time course as in panel B, but 0.33 mM new vesicles are added after 30 min.

Discussion

Here we have studied membrane interactions, secondary structure, and function of the pHD peptides across a range of peptide concentrations and pH values to better understand their sequence-structure-function relationships. Overall, the observed dependencies of binding, structure and membrane permeabilization on pH are sigmoidal with sharp transitions that occur, in most cases, over ~1 pH unit. In comparison, an unaltered protonation equilibrium will be much shallower; e.g. protonation as described by the Henderson-Hasselbalch equation occurs over about 2.6 pH units, for a 5% to 95% transition. This suggests that the protonation/deprotonation of the acidic residues occurs synergistically. The free energy of membrane binding likely contributes to the observed cooperativity. The pH50 values, ranging from 5.0 to 6.4 for the various measurements reported here, are significantly higher than the inherent pKa values of isolated Asp and Glu side chains, (~3.5), further implying that there are significant interactions between these side chains and that they are not acting independently. Indeed, the charges engineered into the pHD library are positioned with helical spacings so that they will repel one another maximally when the peptide has α-helical structure. The very fact that the screen selected only for peptides with five or six acidic residues suggests that the synergistic interactions between the charges is critical for pHD function.

Cooperativity in binding

For peptide binding, positive cooperativity with peptide concentration will arise if there are strong attractive interactions between peptides in the membranes that are at least as energetic as the peptide-membrane interactions. This can occur if peptides self-assemble tightly into higher order oligomeric structures in the membrane. While this effect has been reported at least once[110], it is not frequently observed, probably because membrane partitioning is inherently stronger than

the likely magnitude of peptide-peptide interactions in membranes. Alternately, if the presence of peptides in the membrane changes the membrane structure in a way that improves the binding of additional peptides, positive cooperativity could be observed. This scenario could occur, for example, if the expansion of a membrane pore is more energetically favorable (or less costly) than its initial formation of the pore.

For the pHD peptides, positive cooperativity will result in a rightward shift of the pH-binding curves for higher total peptide concentration. With pHD24 and pHD108, we indeed observed small upward shifts in pH50 for binding at the highest peptide concentrations, suggesting positive cooperativity (Figure 2-3). However, given that the peptide concentrations varied by 100-fold, the cooperativity is small. The binding of one peptide to the bilayer is not strongly influenced by the presence of other peptides already bound to the membrane. Peptide-membrane interactions are dominant over peptide-peptide interactions. Thus, we can describe pHD peptide binding and folding in classical thermodynamic terms of membrane partitioning[81,82,111].

Coupling of binding and folding

The actions of peptides that bind to membranes are usually considered within the framework of a canonical thermodynamic model that includes coupled partitioning of the peptide into the membrane and acquisition of secondary structure[111,112]. This well-supported concept of binding-folding coupling is a consequence of the high energetic penalty of partitioning open peptide bonds into the membrane, relative to a peptide bond that is involved in hydrogen bonded secondary structure[112]. For the pHD peptides the observable properties are intentionally coupled to the protonation states of the 5 or 6 acidic residues that were identified in the high-throughput screen[22]. Potential acidic residues in the library were placed with helical spacing patterns to

maximize their influence on binding and structure propensity. Here, we show that binding and folding have very similar dependencies on peptide concentrations and pH, at least for the conditions under which both could be measured. We observe a small positive cooperativity in binding that is not apparent in secondary structure measurements, but the latter is a less sensitive measurement overall and can only be measured for the highest few peptide concentrations. In any event, the pH50 values for binding and folding are not significantly different from one another (Figure 2-5). They are coupled; binding does not occur without folding and folding does not occur without binding. The steepness of the pH curves and the upward shift in pH50 compared to free carboxylate groups shows that there is also coupling of protonation to binding and secondary structure. The fully deprotonated peptides do not interact with membranes or fold into α-helices, while protonation of at least some acidic sidechains enables membrane interaction and folding.

The pH- and concentration dependence of permeabilization

We also measured the dependence of *function*, membrane permeabilization to macromolecules, on pH and peptide concentration. The behavior of function is very different from binding and structure. In this case, the pH50 values and slopes vary significantly with total peptide concentration. At the highest peptide concentrations, the pH50 values for leakage are highest, and the pH curves are steepest. As peptide concentration is decreased, pH50 and slope both decrease. However, slopes, when measurable, are never as shallow as predicted for simple protonation equilibrium, and pH50 values are never as low as expected for a water-exposed carboxyl sidechain.

For comparison, we also measured the pH50 values for leakage of the small molecule ANTS at several peptide concentrations. The pH50 values for ANTS leakage and for dextran

leakage are statistically indistinguishable from one another. This demonstrates that pore formation for small molecules and for macromolecules are not distinct processes.

Coupling of binding and poration

Interestingly, the functional data show that efficient poration can occur at pH values significantly higher than those that enable efficient binding, an effect that becomes greater for higher peptide concentrations (Figure 2-6). Indeed, there are pH values at which substantial macromolecule leakage occurs despite the fact that fractional binding and folding are very small. There are also conditions where there is no leakage despite 100% binding (Figure 2-6, bottom row). It might seem paradoxical that binding/folding are not tightly coupled to function (poration). However this paradox is resolved when we consider the dependence of vesicle permeabilization on the peptide *bound* per lipid, rather than total peptide per lipid (Figure 2-7). When the functional data are plotted as a function of P_{bound}:L (i.e. the actual concentration of peptide acting on the membranes), the curves, slopes and pH50 values for the various concentrations become similar for all three peptides under all conditions. Leakage depends primarily on how many peptides are bound per vesicle, and thus binding and poration are in fact tightly correlated. The apparent paradox occurs because a small *fractional* binding can drive efficient permeabilization under conditions when P_{total}:L is much higher than the P_{bound}:L required for permeabilization.

It is interesting to note that the poration curves as functions of P_{bound}:L behave as single function despite data that was collected between pH 4.5 and pH 6.5. We conclude from this observation that the structure of the pore is not sensitive to pH in this range. As long as the protonation state enables some pHD peptide to bind, the pore can be formed.

Potency, or the number of peptides required to permeabilize a vesicle.

The plot of macromolecule leakage versus P_{bound}:L in Figure 2-7A shows that the concentration that drives 50% permeabilization of PC vesicles to 40 kDa dextran is around P_{bound}:L = 1:1300, under all conditions. This is equivalent to 75 peptides per vesicle. The only other membrane permeabilizing peptides known that have this degree of potency for releasing macromolecules from PC vesicles are the closely related macrolittins[24], which were selected from the same library.

Assuming random dispersal of peptides, a Poisson function will describe the distributions of the number of peptides per vesicle (Figure 2-7C). Based on the calculation that 20-30 peptides are needed to form a barrel-stave pore of ~ 4.5 nm diameter to allow for the passage of 40 kDa dextran (4.5 nm hydrodynamic radius), we can expect no leakage when fewer than 20 peptides are bound per vesicles, and indeed we observe no leakage in this case. Only partial leakage can be expected when 75 peptides are bound. Consistent with this expectation, experimentally we observe 50% leakage when 75 peptides are bound per vesicle (Figure 2-7B). We observe 100% leakage once about 200 peptides are bound to each vesicle.

Possible pore structure

The highly potent macromolecular leakage and the large pores they imply suggest a structural hypothesis for the pHD peptides. At low pH, when at least some of the acidic groups are protonated, the pHD peptides bind to membranes and fold into amphipathic α-helices. We hypothesize that these amphipathic helices stabilize exposed bilayer edges, enabling the otherwise energetically unfavorable formation of large open pores. We envision that the amphipathic helices lie at the bilayer edge, exposing charged and polar groups to the aqueous phase while exposing the hydrophobic surfaces of the helices to the bilayer. Perhaps the pore edges are further

stabilized by lateral electrostatic interactions between acidic sidechains and the two basic residues on the pHD peptides.

Our recent description of the macrolittins[24], closely related peptides that also have very potent macromolecular poration activity at pH 7, supports these conclusions. The macrolittins were selected from the same library as the pHD peptides, except that they were selected for their ability to permeabilize bilayers to macromolecules at pH 7. They are nearly identical to the pHD peptides in sequence, structure and potency, except that they have three acidic residues total, compared to five or six in the pHD peptides. In the pHD peptides, protonation of several residues in the other acidic positions enables the pore structure to form only at acidic pH, while in the macrolittins this pore structure is possible at pH 7 because of the smaller number of acidic residues.

By oriented circular dichroism, the parent peptide of the pHD library, MelP5, resides in a mostly membrane spanning, perpendicular orientation[33]. The same is true for the macrolittins[24]. Thus, it is likely that the pHD peptides are also mostly perpendicular to the membrane plane at acidic pH. However it is difficult to study the orientation of the pHD peptides because it is difficult to control or determine the effective pH in the typical oriented CD sample, a stacked multibilayer system that is hydrated through the vapor phase[35,84,113]. Further, AFM has shown that MelP5 causes membrane thinning in the vicinity of the pores, while the macrolittins and pHD peptides cause pores, but not much membrane thinning[24,114]. Thus, by progressing from MelP5 to the pHD peptides and macrolittins, we have evolved peptides that more effectively span the bilayer “edge” and enable large pores to form in the membrane.

The effect of sequence

The physical chemistry and sequence of the pHD peptides affects their potency and pH dependence. For instance, pHD15, has a lower potency and a lower pH50 compared to the other two peptides (Figure 2-1), suggesting a sequence-dependent effect that may be due to the number of acidic residues; pHD15 is the only pHD peptide with six acidic residues, instead of the usual five. On the other hand, the most potent peptide, pHD108, has 5 glutamic acids, which were significantly overrepresented in the pHD sequences, whereas pHD15 and pHD24 have 3 and 2 aspartic acids, respectively. These observations of sequence-specific effects suggest that additional changes in sequence, which can be either rationally engineered or identified via high-throughput screens from peptide libraries, can be used to fine-tune the properties of the pHD peptides for desired applications.

Conclusion

Here we study the mechanism of action of the pHD peptides, which form large pores in POPC bilayers in a pH-dependent manner. The activity of these highly potent peptides is controlled by both pH and peptide concentration, and ultimately depends on the number of peptides that are bound per vesicle. The physical chemical sequence-structure-function relationships that we described here will be useful in the future design and optimization of membrane permeabilizing peptides for specific applications. Such applications could include the release of endosomal contents for drug delivery upon acidification, as well as anti-cancer therapies that exploit the low pH of the tumor environment.

CHAPTER 3: EFFECT OF LIPID COMPOSITION ON THE ACTIVITY OF PHD15

Abstract

Peptides that self-assemble into pore-like structures in lipid bilayers could have utility in a variety of biotechnological and clinical applications due to their ability to breach the barrier imposed by lipid bilayers. To empower such discoveries, we have used synthetic molecular evolution to select for the pHD peptides, a family of membrane-active, pore-forming peptides that assemble into macromolecular pores at acidic pH. Since cell membranes are complex, with lipids of various headgroups and acyl chains, we sought to determine the effect of lipid composition on pHD activity. To understand the effect of anionic headgroups and acyl chain length on the mechanism of action of the pHD peptides, we measured the binding and activity of pHD15 on vesicles composed of 1:9 POPS:POPC, 1:9 POPG:POPC, as well as PC lipids with singly unsaturated acyl chains ranging from 14 to 22 carbons in length. We find that pHD15 retains its pH-sensitivity, and is extremely sensitive to the composition of the bilayer. The peptide partitions equally favorably to anionic and neutral membranes, and is equally potent in 1:9 POPG:POPC and POPC membranes, but less potent in 1:9 POPS:POPC membranes. The peptide binds to membranes of various thicknesses in a pH-sensitive manner that is affected by the chain lengths. Leakage is decreased for thicker membranes, which cannot be accounted for by the amount of peptide bound. Noteworthy, pHD15 is most potent in POPC membranes, the lipid composition used when screening for the peptides. Taken together, the data highlights the power of discovering peptides that are optimized for the conditions of the screen.

Introduction

pH-sensitive, pore-forming peptides can be useful for a variety of biotechnological applications, such as delivery agents for the endosomal escape of cargo to the cytoplasm or as therapeutics that target cancer cells. However, cell membranes are composed of hundreds of different lipid species that affect the physical properties of the membrane[115–119], and consequently the activity of membrane-active peptides. In particular, membrane thickness and charge have been shown to modulate the insertion, aggregation, and activity of peptides[101,120–127].

The pHD peptides are 26 amino acid peptides that bind to membranes, fold into alpha helices, and cooperatively assemble into macromolecular-sized pores under acidic conditions. My work in the previous chapters has shown that pH, peptide concentration, and sequence modulate the number of peptides bound per vesicle. When greater than 75 peptides are bound per vesicle, the peptides act cooperatively to form pores in neutrally charged, POPC membranes[25].

Here, I test the effect of anionic headgroups and acyl chain length on the activity of one of the pHD peptides, pHD15 (sequence: GIGEVLHELADDLPDLQEWIHAAQQL). When selecting anionic lipids, we chose the lipid POPS, which is found in mammalian cell membranes[128]. Furthermore, the lipid has palmitoyl (16:0) and oleyol (18:1) acyl chains, which permits comparison with POPC, the lipid used to characterize the activity of the pHD peptides in Chapter 2[25]. We also used POPG, another lipid with an anionic headgroup that is commonly used [129–131]. We selected a lipid composition of 1:9 POPS:POPC and 1:9 POPG:POPC (hereafter referred to as 10% POPS or 10% POPG) to study the effect of anionic membranes on the binding and pore-forming activity of pHD15. To measure binding and poration, we used the tryptophan fluorescence assay and the FRET-based dextran leakage assays.

We further note that cells are composed of lipids of various acyl chains which can modulate membrane thickness[109]. Hydrophobic mismatch may play a role in membrane protein segregation, activation, trafficking, and membrane protein stability[132–134]. To study the effect of membrane thickness on pHD15 binding and activity, the bilayer thickness was varied by using phosphatidylcholine headgroup lipids with acyl chain lengths ranging from 14 to 22 carbon atoms and containing *cis* double bonds. The binding and pore-formation of pHD15 to these membranes was measured by tryptophan fluorescence and dextran leakage assays.

We find that the peptides retain their pH-sensitivity and are exquisitely sensitive to lipid composition. pHD15 is most potent in POPC and 10% POPG membranes, and less effective in 10% POPS and thicker membranes. Notably, the high throughput screens used to discover the pHD peptides were performed with POPC vesicles, the lipid composition for which the peptides are most potent. Thus, my data show that high throughput screening is highly effective in selecting for peptides that have precisely the behavior we screen for.

Results

Macromolecular leakage across anionic membranes in response to pHD15

To evaluate the effect of anionic membranes on the function of pHD15, dextran leakage assays were performed to assess macromolecular poration of a bilayer by pHD15. In this FRET-based assay (Figure 3-1A), the acceptor molecule, TAMRA-Biotin-Dextran (TBD), is encapsulated inside vesicles. The dextran is 40 kDa in size. The donor molecule, streptavidin-AlexaFluor488 (SA-AF488), is outside the vesicles. If large pores form while the peptide is incubated with these vesicles, streptavidin and biotin will come into contact, placing the acceptor and donor fluorophores in close enough proximity for FRET to occur.

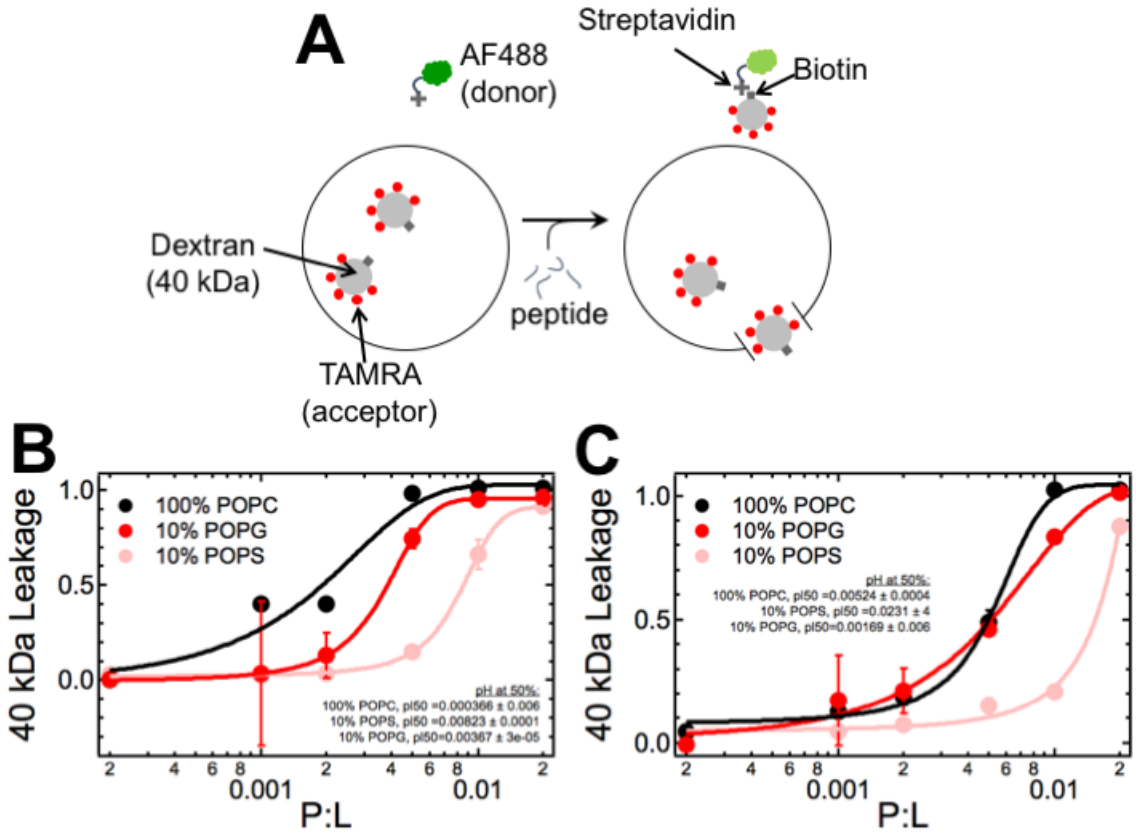

Figure 3-1: Macromolecular leakage across anionic membranes in response to pHD15.

Schematic of the FRET-based dextran leakage assay to measure the formation of large pores (A). Leakage of 40 kDa dextran from vesicles composed of 10% POPG and 10% POPS at pH 4.5 (B) and pH 5.5 (C). Peptide was incubated with 1 mM lipid for 1 hour before FRET was measured. Data shown is the average of three replicates.

In Figure 3-1B,C we show the fractional leakage of TBD, measured after 1 hour, as a function of peptide-to-lipid ratio (P:L) and pH. At the lowest peptide concentrations, little or no leakage is observed at any pH. As the peptide concentration increases, leakage increases to 100%. At pH 4.5, the peptide is most potent in POPC membranes (LIC_{50} of 1:520 P:L), less potent in 10% POPG membranes (LIC_{50} of 1:260) and least potent in 10% POPS membranes (LIC_{50} of 1:120). At pH 5.5, the peptide is similarly potent in POPC and 10% POPG membranes (LIC_{50} = 1:200), and less potent in 10% POPS membranes (LIC_{50} = 1:65).

Partitioning of pHD15 to anionic membranes

To determine if anionic headgroups affect the binding of pHD15 to membranes, we measured the extent of peptide binding to membranes composed of POPC, 10% POPS or 10% POPG by tryptophan fluorescence as a function of pH and peptide concentration on. pHD15 has one tryptophan residue, with a fluorescence that is dependent on the polarity of its environment. Tryptophan's fluorescence is higher in hydrophobic environments like that within the hydrocarbon core of the membrane, and lower in hydrophilic environments like that of the solution phase (Figure 3-2A). The peptide was incubated with LUVs for 1 hour before tryptophan fluorescence was measured. The nanomoles of peptide bound per lipid was calculated and shown in Figure 3-2B. At pH 4, the amount of peptide bound per lipid increases as the total peptide to lipid increases, with nearly all peptide bound to the membrane. As the pH increases, the number of peptides bound per lipid decreases, until there are no peptides bound at pH 7. Equivalent amounts of peptide are bound to POPC, 10% POPG, and 10% POPS membranes, suggesting that anionic headgroups neither inhibit nor promote the binding of pHD15 to membranes at any pH.

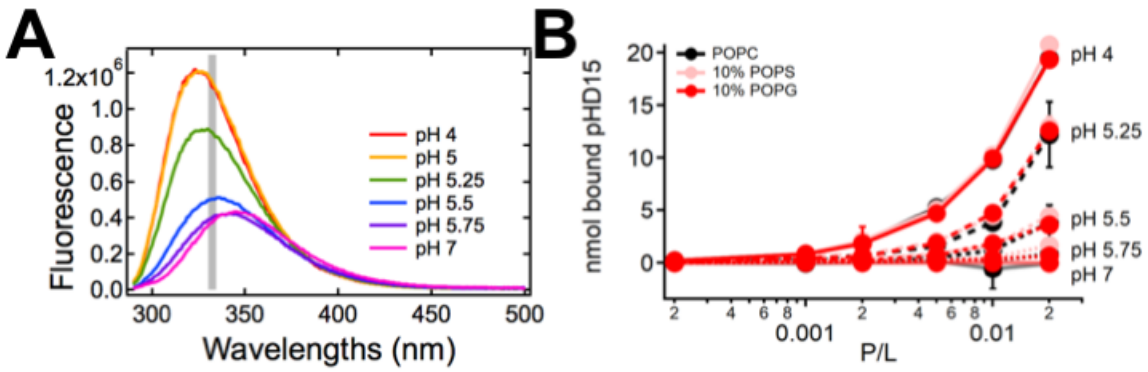

Figure 3-2: Binding of pHD15 to neutral and anionic membranes.

Binding of pHD15 to vesicles composed of POPC, 10% POPG, and 10% POPS membranes as measured by tryptophan fluorescence. (A) Tryptophan fluorescence measured after a 1 hour incubation of peptide with 10% POPG membranes at P:L = 1:50. The fluorescence from 330-335 nm, as indicated by the gray region, was averaged to calculate the percent of peptide bound. (B) The percent of peptide bound was used to calculate the nmol of peptide bound to membranes.

Folding of pHD15 in anionic membranes

To determine the folding of pHD15 in anionic membranes, circular dichroism spectra was measured as a function of pH and P:L after incubating the peptide with 10% POPS membranes for 1 hour (Figure 3-3A). The extent to which the peptide had formed a helix was calculated from the average ellipticity at 217-227 nm. The relative percent helicity is shown as a function of peptide concentration and pH in Figure 3-4B-D. For all peptide concentrations, little peptide is helical at pH 7. As the pH decreases, increasing fractions of the peptide are folded. The pHs at which 50% helix is measured, or the 'pH50', are 5.6-5.7 for POPC membranes and 5.4 for 10% POPS membranes. By ANOVA, the differences between the pH50s for POPC and 10% POPS membranes are not statistically significant at any concentration, suggesting that anionic headgroups do not promote nor inhibit the folding of pHD15 into alpha helices.

Macromolecular leakage across membranes of increasing thickness in response to pHD15

To characterize the macromolecular leakage of macromolecules through membranes of increasing thickness, we used the same dextran leakage assay described for anionic membranes. Leakage was measured as a function of pH and peptide concentration through membranes composed of lipids with singly unsaturated acyl chains of 14, 16, 18, and 20 carbons (Figure 3-4). The extent of leakage depends on pH. There is no leakage at pH 7, and leakage increases as the pH decreases. The transition from 0 to 100% leakage occurs over 0.5 to 1 pH units. The pH50 is dependent on concentration, with the pH50 decreasing as peptide concentration decreases. For the thinnest membranes, composed of lipids with 14 acyl chain carbons, the pH50 decreases from 5.96 at P:L = 1:50 to 5.41 at P:L = 1:200. Negligible leakage is detected at P:L = 1:1000 and P:L = 1:5000, even under acidic conditions. For membranes with intermediate chain lengths of 16 or 18 carbons, leakage is greatest at P:L = 1:50, with the midpoint decreasing as the membrane

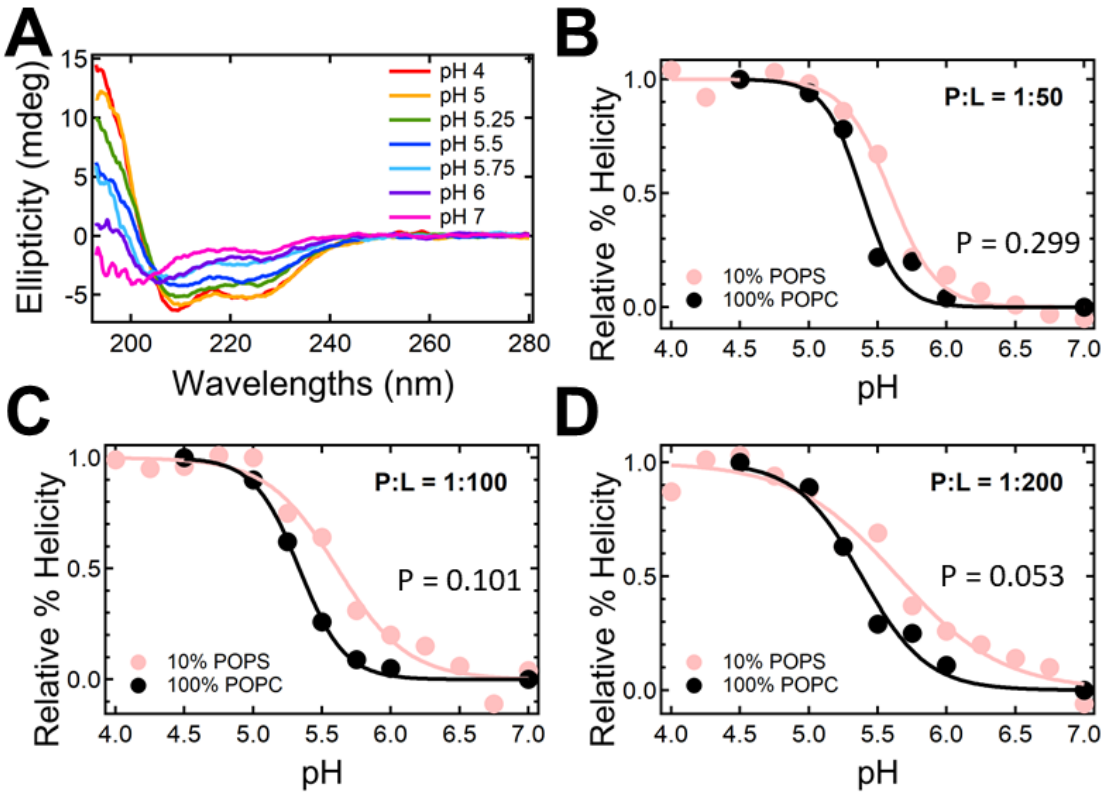

Figure 3-3: Folding of pHD15 on 10% POPS membranes.

pHD15 was incubated with 10% POPS membranes for 1 hour before the circular dichroism spectra were measured. Shown is an example set of CD spectra at P:L = 1:100 (A). The helicity was calculated with the average ellipticity from 217-227 nm, then normalized between 0 and 1 at a P:L of 1:50 (B), 1:100 (C), and 1:200 (D). The P-value of the pH50s were calculated in Prism with ordinary one-way ANOVA. Standard errors used in the calculation of the P-values were determined to be 0.05 by a simulation for P:L = 1:50 and 1:100. For P:L = 1:200, the error determined by the sigmoidal fit was used.

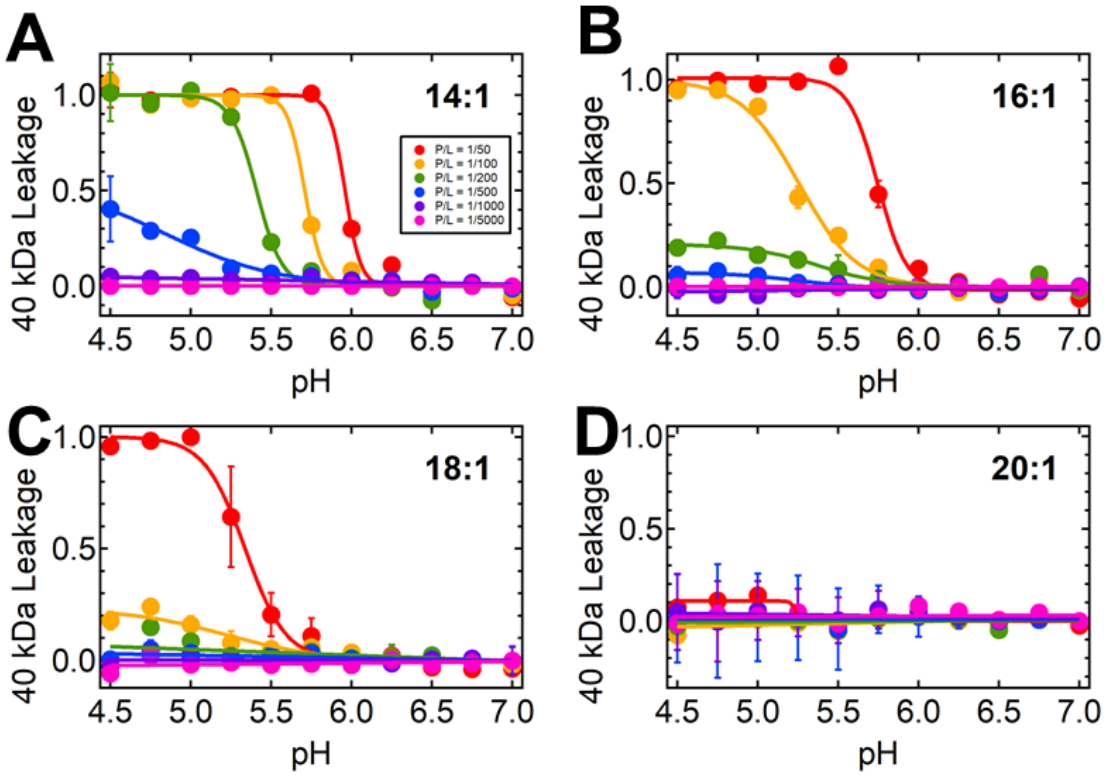

Figure 3-4: Macromolecular leakage across membranes of increasing thickness in response to pHD15.

pHD15 was incubated for 1 hour at room temperature with 1 mM lipids before leakage was measured. This experiment was performed with membranes composed of PC-headgroup lipids with singly unsaturated acyl chains with 14 (A), 16 (B), 18 (C), and 20 carbons (D).

becomes thicker.

The pH50 decreases from 5.96 for C14 membranes to 5.39 for C18 membranes. No leakage is detectable at any pH with C16 membranes at P:L = 1:1:1000, and with C18 membranes at P:L = 1:500. Very little activity is observed at any P:L or pH with C20 membranes, with only about 10% leakage at the conditions where leakage is most likely to occur at P:L = 1:50 and pH 4.5 (Figure 3-4D). These observations suggest that pore-formation is most efficient in thin membranes, less efficient at membranes of intermediate thicknesses, and inefficient in the membranes of greatest thickness.

Partitioning of pHD15 into membranes of increasing thickness

To determine the extent to which peptides bind to membranes of increasing thickness, we measured the binding of pHD15 to membranes composed of PC-headgroup lipids with singly unsaturated acyl chains of 14, 16, 18, 20, or 22 carbons using tryptophan fluorescence. In Figure 3-5, we show the normalized, average fluorescence intensities at 330-335 nm as a function of pH and lipid composition for pHD15.

For all concentrations, binding is dependent on pH, with little to no peptide bound at pH 7, and increasing amounts of peptide bound as the pH becomes more acidic. The pH50 depends on peptide concentration and the number of carbons in the acyl chains of the lipids. For the thinnest membranes, composed of lipids with 14 carbons in the acyl chains (Figure 3-5A), the peptide is most active at P:L = 1:50, the highest peptide concentration for which binding was measured, and least active at the lowest peptide concentration of P:L = 1:1000. The ΔpH50, defined as $pH50_{P:L=1:50} - pH50_{P:L = 1:1000}$ is about 0.8 pH units. The difference between the $pH50_{P:L=1:50}$ and $pH50_{P:L = 1:1000}$ is highly significant ($P < 0.0001$, calculated in Prism using ordinary one-way ANOVA). For membranes of intermediate thicknesses (Figures 3-5B, C), the pH50s are not so highly dependent on peptide concentration, with a ΔpH50 of 0.2 pH units in

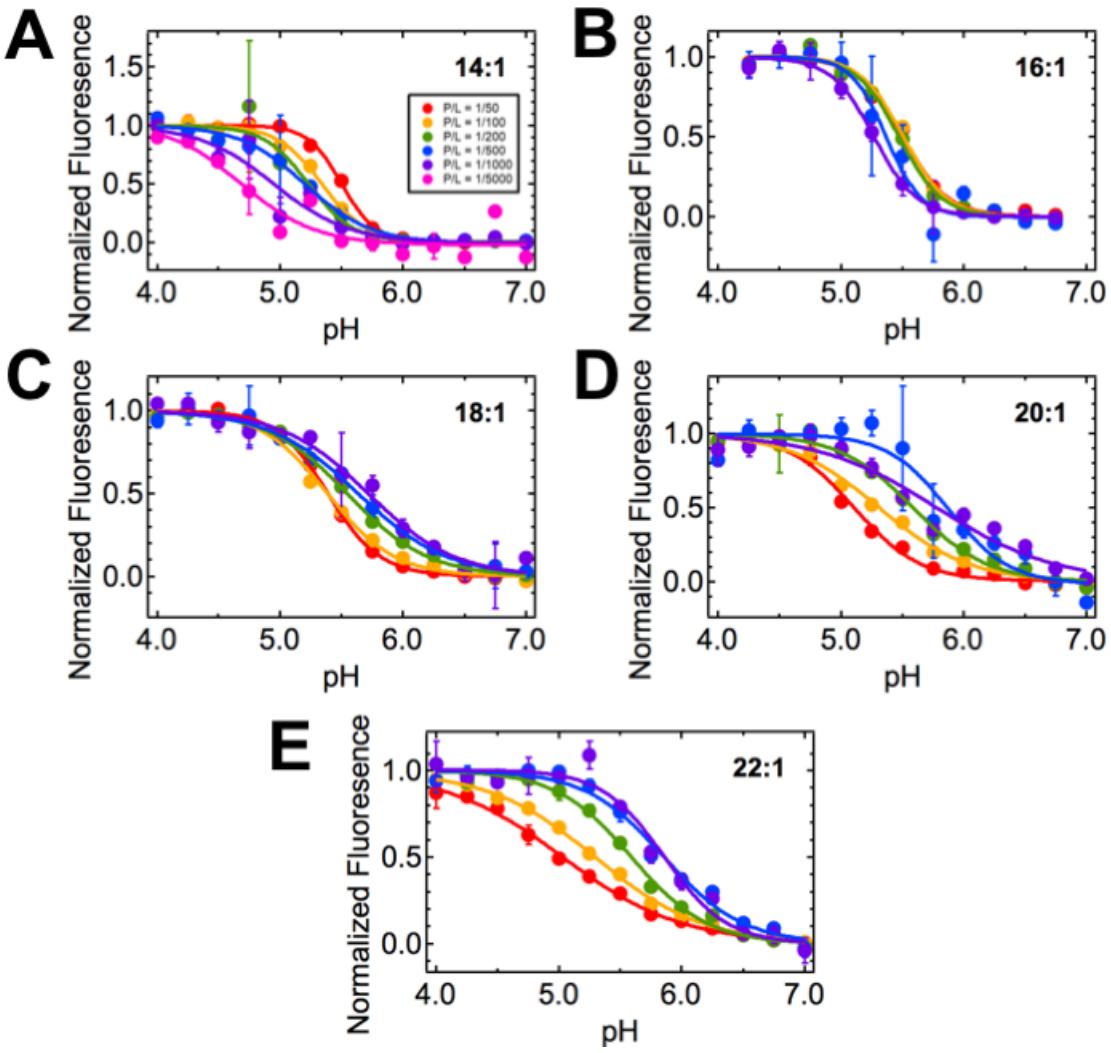

Figure 3-5: Binding of pHD15 to increasingly thicker membranes, as monitored by tryptophan fluorescence.

Binding of pHD15 to vesicles composed of singly unsaturated acyl chains of 14 (A), 16 (B), 18 (C), 20 (D), and 22 (E) carbons was measured by tryptophan fluorescence after 1 hour incubation with 1 mM lipids at a P:L of 1:50 to 1:1000. The average fluorescence at 330-335nm was averaged and normalized. Data shown is the average of three samples.

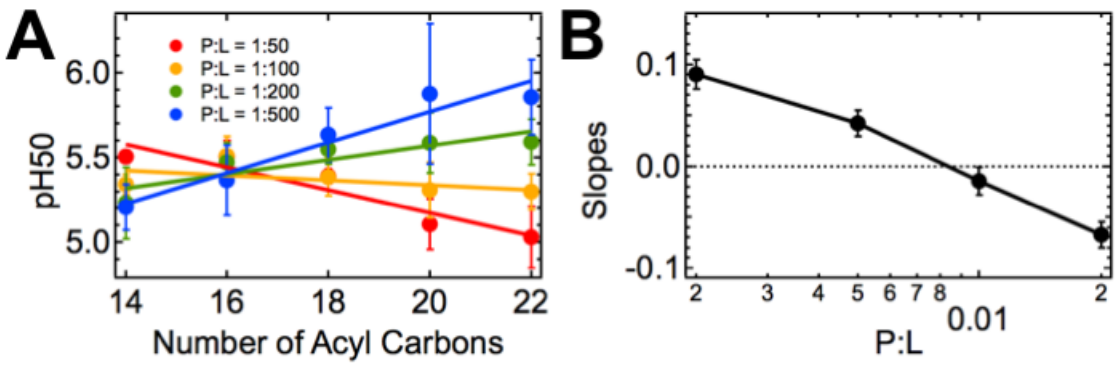

Figure 3-6: Change in pH50 of binding curves, acquired for pHD15 binding to membranes of various thicknesses.

The pH50s were calculated by a sigmoidal fit of the tryptophan fluorescence versus pH curves shown in Figure 3-5. The pH50s (A) were plotted as a function of acyl chain carbons. The slopes of the pH50s were plotted as a function of peptide to lipid ratio in (B).

C16 membranes (P = 0.046), and -0.3 pH units in C18 membranes (P = 0.0003). Notably, although the P:L dependence of pH50 is slight, in C18 membranes, there is an inversion of dependence on peptide concentration, with the peptides being most active at P:L = 1:1000 and least active at P:L = 1:50. For the thickest membranes, the inverse relationship between peptide concentration and pH50 is magnified (Figure 3-5D,E). Indeed, the ΔpH50 for C20 membranes is -0.7 pH units (P < 0.0001), and the ΔpH50 for C22 membranes is -0.8 pH units (P < 0.0001).

The change in pH50s as a function of the number of acyl chain carbons is summarized in Figure 3-6A, and the slope of these curves are plotted in Figure 3-6B as a function of peptide to lipid ratios. For the thinnest membranes, the pH50 increases as concentration increases, suggesting a cooperative process, i.e., binding becomes more efficient as the concentration of peptides increases. For the thickest membranes, the pH50 decreases as peptide concentration increases, suggesting an anti-cooperative process, i.e., binding becomes less efficient as the concentration increases. For membranes of intermediate thicknesses, there is a convergence of pH50s centered at around slightly greater than 16 carbons. Intriguingly, the pH50s for different peptide concentrations coincide at about 17 carbons, which is the average number of carbons on POPC acyl chains, for which the pH50s also coincide[25].

Orientation of pHD15 in membranes of increasing thickness

Pore-formation is likely mediated by peptides that are oriented perpendicular to the plane of the bilayer. To determine the orientation of the peptide in thin and thick membranes, the oriented circular dichroism spectra of pHD15 were measured in C14 and C22 membranes. In C14 membranes, the dry spectrum exhibits two dips with peaks at 212 and 222 nm (Figure 3-7A). This shape is generally consistent with a peptide that is parallel to the membrane[35,84]. After about 70 minutes of hydration with MilliQ water through the vapor phase, the shape of the spectrum shifts

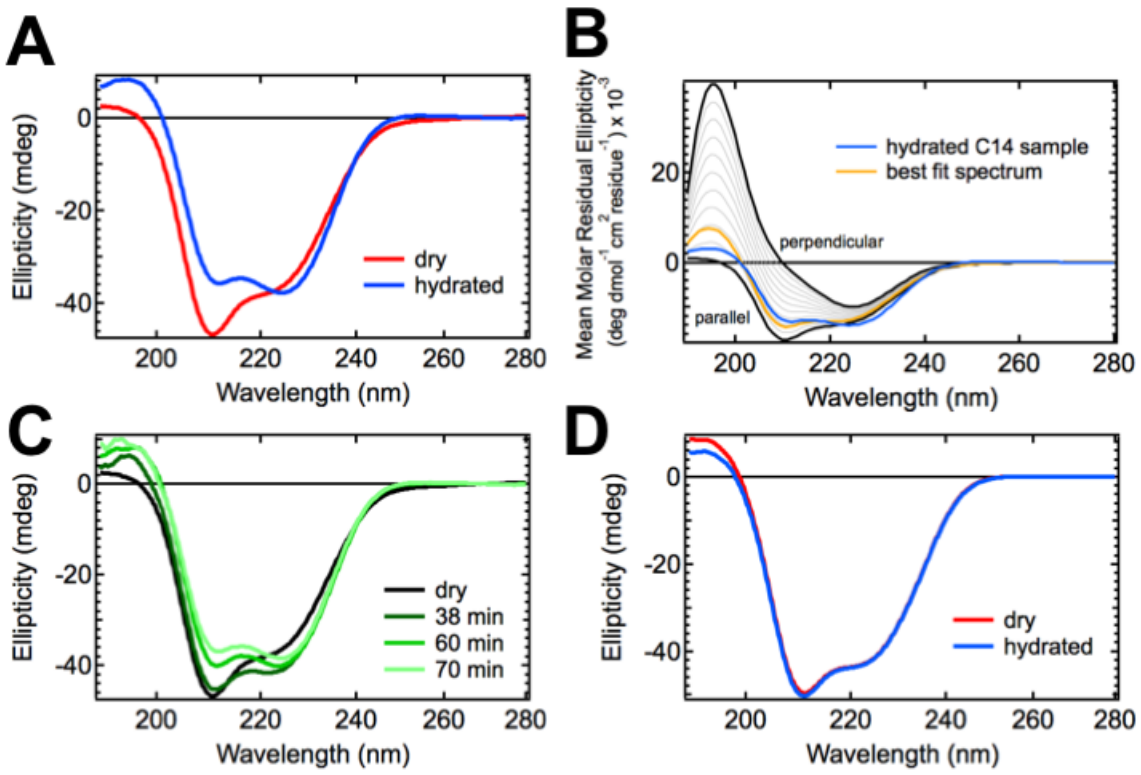

Figure 3-7: Oriented circular dichroism spectra of pHD15 in membranes of different thickness.

Comparison of the OCD spectra of pHD15 in stacked, oriented bilayers composed of C14 lipids (A) on a quartz substrate in the dry state and after 70 minutes of hydration with water through the vapor phase. The average of eight spectra measured at 45° rotations of the sample around the beam axis are shown. The lipid only spectra have been subtracted, and a correction has been made for the baseline. (B) The OCD spectrum of pHD15 on hydrated C14 membrane is shown in blue, and dry and theoretical OCD spectrum are shown in black. Linear combinations of the basis spectra, in increments of % perpendicular helix increasing by 10% per step, are shown in gray. The best fit spectrum, representing ~20% perpendicular helix, is in orange. (C). Time course of the evolution of the OCD spectrum. (D). Comparison of the OCD spectra of pHD15 in C22 membranes in the dry state and 85 minutes after hydration.

such that the intensity of the 212 nm peak decreases. This likely suggests a transition towards a transmembrane state with a theoretical spectrum with one dip shown in Figure 3-7B. The hydrated spectrum is assumed to be a linear combination of the dry spectrum and the spectrum of a helical peptide in a transmembrane orientation. Under this assumption, the spectrum corresponds to about 20% of the peptides in the transmembrane orientation, suggesting that the peptide has partially inserted into the membrane. We monitored the change in pHD15's OCD spectra in C14 membranes as a function of time after hydration (Figure 3-7C). The change in the shape of the spectrum occurs over time, with no further changes after 70 minutes. The transition suggests that the change in orientation occurs slowly, and that the peptide may have been kinetically trapped in an orientation parallel to the surface of the membrane.

In C22 membranes, the OCD spectrum also exhibits two dips at 212 and 222 nm, but the shape of the spectra does not change even after 85 minutes after hydration (Figure 3-7D), suggesting that the peptide remains oriented parallel to the membrane.

Insights from a P_{bound}:Lipid analysis

Since pore-formation must be mediated by peptides that are bound to vesicles, we show the leakage as a function of peptide bound per lipid in Figure 3-8. No leakage is observed when few peptides are bound to vesicles of any lipid composition. As the number of peptides bound per vesicle increases, leakage increases. At 500 peptides bound per vesicle, pHD15 induces 100% leakage for most lipid compositions. The peptide is most potent in POPC and 10% POPG, for which 50% leakage occurs at about 100 bound peptides per vesicle. The peptides are less potent in 10% POPS vesicles, for which 50% leakage occurs at about 460 bound peptides per vesicle. When we are varying the chain length, we find that pHD15 is most potent in C14 membranes, for which 50% leakage occurs at about 190 bound peptides per vesicle, and least potent for C20 vesicles, for which 50% leakage is estimated to occur at 2,650 bound peptides per vesicle.

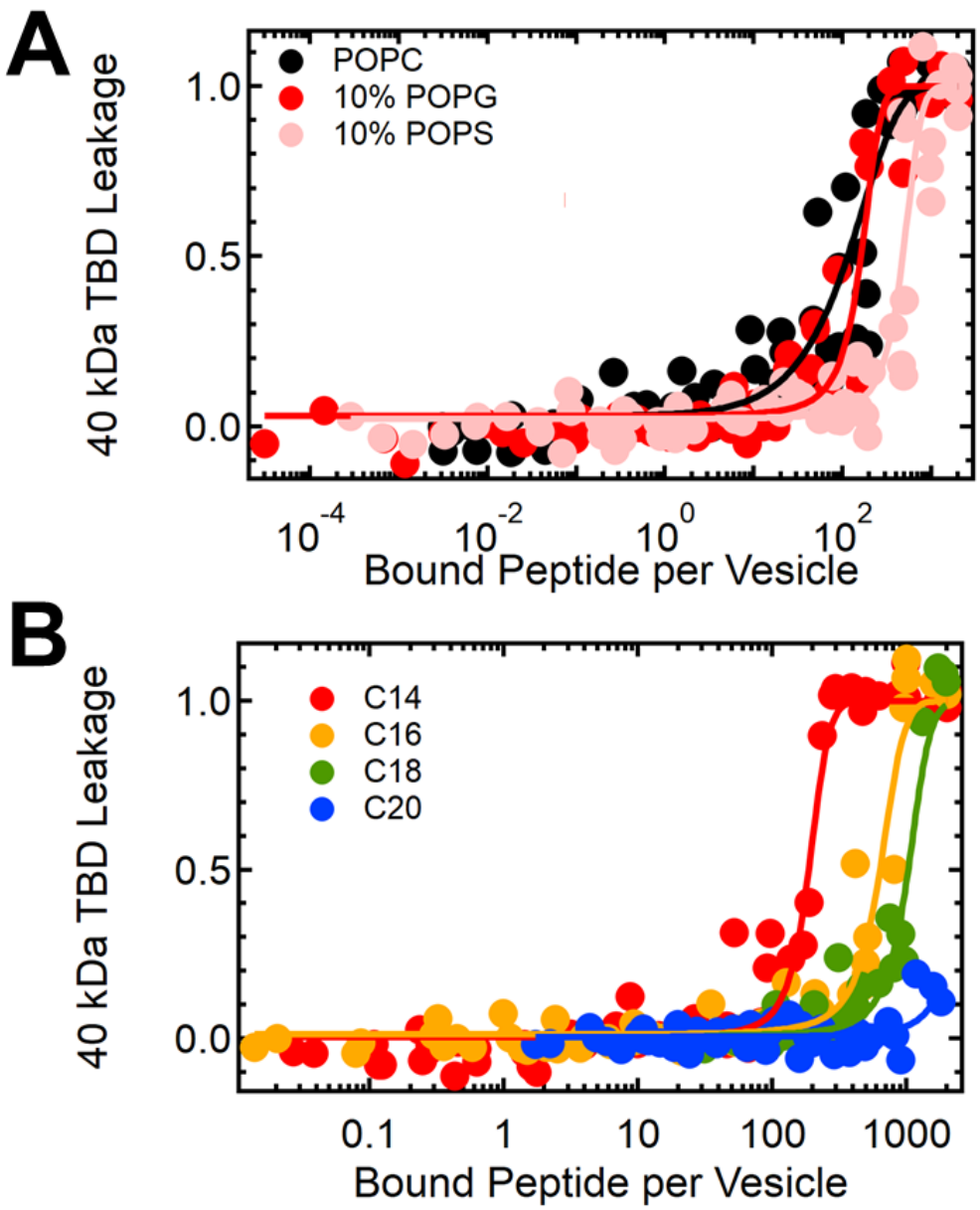

Figure 3-8: Activity versus bound peptide per lipid for various lipid compositions. The leakage as a function of the number of peptides bound per lipid in POPC, 10% POPS, and 10% POPG vesicles (A) and membranes of various thicknesses (B).

Discussion

Here we have shown that pHD15 retains its pH-sensitive binding and activity in membranes with anionic headgroups and various acyl chain lengths. We have also shown that the peptide is exquisitely sensitive to lipid composition.

pHD15 partitions equally favorably to membranes composed of neutral and anionic headgroups. Despite this, pHD15 is consistently less active in 10% POPS membranes than in 10% POPG or POPC membranes. We can understand pHD15's behavior with a model that describes the steps leading to pore-formation that was proposed by Cymer et al[135]. In this model, the peptides begin unfolded in solution, partition to membranes, fold into alpha helices, insert to be perpendicular to the plane of the bilayer, and associate to form pores. For pHD15, we have seen that binding and folding are equally favorable in neutral and anionic membranes, as expected, due to the partitioning-folding coupling. The finding that the early steps of pore-formation are not hindered by anionic headgroups suggests that the latter steps in pore-formation, such as insertion or association, are inhibited. PS is known to form interheadgroup hydrogen bonds[136], so it is possible that PS sequesters the peptide in a surface bound orientation, limiting the peptide's ability to insert into PS membranes when PS is present[137]. Furthermore, the peptide may favor peptide-lipid interactions versus peptide-peptide interactions, limiting peptide association. In either case, the result is that less pores will form in membranes with PS headgroups.

Both pHD15's binding and leakage are decreased in thicker membranes. Leakage and insertion of the peptide into membranes is nearly obliterated in thick membranes. Taken together, the binding, OCD, and leakage data suggest that binding to thin and thick membranes are fundamentally different processes. For the thinnest membranes, binding is a cooperative process in which peptides insert into the membrane and form pores. For the thickest membranes,

however, binding is an anticooperative process in which peptides orient parallel to the surface of the membrane, and do not form pores. Intriguingly, this is the first observed instance in which the pHD peptides work anticooperatively, or are inhibited from forming pores. Anticooperativity could be a consequence of peptide that is accumulating on the surface of thick membranes. Since pHD15 has four basic side chains, it is likely that the peptide is charged upon binding under acidic conditions. The accumulation of charged peptide could result in the electrostatic repulsion of peptide away from the membrane. Furthermore, as the peptides bind and accumulate, oriented parallel to the surface of the membrane, the interface may experience packing stress. The binding of additional peptide would be less favorable.

Conclusion

These studies have uncovered intriguing effects with no precedent in the literature, to the best of our knowledge. Due to the complexity of the interactions between peptide and lipids, and effects of pH, they warrant further investigation by molecular dynamic simulations.

We have found that pHD15 is most potent in POPC membranes, the lipid composition used when screening for the peptides. This work highlights the power of synthetic molecular evolution in discovering peptides that are optimized for the conditions of the screen.

BIBLIOGRAPHY

1. Cornell, C. E. *et al.* Prebiotic amino acids bind to and stabilize prebiotic fatty acid membranes. *Proc. Natl. Acad. Sci.* **116**, 17239–17244 (2019).

2. Canton, I. & Battaglia, G. Endocytosis at the nanoscale. *Chem. Soc. Rev.* **41**, 2718–2739 (2012).

3. Lodish, H. *et al. Molecular Cell Biology*. (W. H. Freeman, 2000).

4. Milanetti, E., Raimondo, D. & Tramontano, A. Prediction of the permeability of neutral drugs inferred from their solvation properties. *Bioinformatics* **32**, 1–7 (2016).

5. Lipinski, C. A., Lombardo, F., Dominy, B. W. & Feeney, P. J. Experimental and computational approaches to estimate solubility and permeability in drug discovery and development settings. *Adv. Drug Deliv. Rev.* **23**, 3–25 (1997).

6. Nikaido, H. Molecular Basis for Bacterial Outer Membrane Permeability Revisited. *Microbiol. Mol. Biol. Rev.* **67**, 593–656 (2003).

7. Khalili-Araghi, F. *et al.* Molecular dynamics simulations of membrane channels and transporters. *Curr. Opin. Struct. Biol.* **19**, 128–137 (2009).

8. Kim, M. K. *et al.* Oncolytic and immunotherapeutic vaccinia induces antibody-mediated complement-dependent cancer cell lysis in humans. *Sci. Transl. Med.* **5**, (2013).

9. Schweizer, F. Cationic amphiphilic peptides with cancer-selective toxicity. *Eur. J. Pharmacol.* **625**, 190–194 (2009).

10. Leuschner, C. & Hansel, W. Membrane Disrupting Lytic Peptides for Cancer Treatments. *Curr. Pharm. Des.* **10**, 2299–2310 (2004).

11. Papo, N. & Shai, Y. Host defense peptides as new weapons in cancer treatment. *Cell. Mol. Life Sci.* **62**, 784–790 (2005).

12. Billingsley, M. L. Druggable targets and targeted drugs: Enhancing the development of new therapeutics. *Pharmacology* **82**, 239–244 (2008).

13. Torchilin, V. Intracellular delivery of protein and peptide therapeutics. *Drug Discov. Today Technol.* **5**, (2008).

14. Amir K. Varkouhi, Marije Scholte, Gert Storm, H. J. H. Endosomal Escape Pathways for Delivery of Biologicals. *J. Control. Release* **151**, 220–228 (2011).

15. Zhang, X., Lin, Y. & Gillies, R. J. Tumor pH and its measurement. *J Nucl Med.* **51**, 1167–1170 (2010).

16. Liberti, M. V. & Locasale, J. W. The Warburg Effect: How Does it Benefit Cancer Cells? *Trends Biochem. Sci.* **41**, 211–218 (2016).

17. Hanahan, D. & Weinberg, R. A. Hallmarks of cancer: the next generation. *Cell* **144**, 646–674 (2011).

18. Deacon, J. C., Engelman, D. M. & Barrera, F. N. Targeting acidity in diseased tissues: Mechanism and applications of the membrane-inserting peptide, pHLIP. *Arch. Biochem. Biophys.* **565**, 40–48 (2015).

19. Danhier, F., Feron, O. & Préat, V. To exploit the tumor microenvironment: Passive and active tumor targeting of nanocarriers for anti-cancer drug delivery. *J. Control. Release* **148**, 135–146 (2010).

20. Huotari, J. & Helenius, A. Endosome maturation. *EMBO J.* **30**, 3481–3500 (2011).

21. Doherty, G. J. & McMahon, H. T. Mechanisms of Endocytosis. *Annu. Rev. Biochem.* **78**, 857–902 (2009).

22. Wiedman, G., Kim, S. Y., Zapata-Mercado, E., Wimley, W. C. & Hristova, K. pH-triggered, macromolecule-sized poration of lipid bilayers by synthetically evolved peptides. *J. Am. Chem. Soc.* **139**, 937–945 (2017).

23. Wiedman, G., Wimley, W. C. & Hristova, K. Testing the limits of rational design by engineering pH sensitivity into membrane-active peptides. *Biochim. Biophys. Acta - Biomembr.* **1848**, 951–957 (2015).

24. Li, S. *et al.* Potent Macromolecule-Sized Poration of Lipid Bilayers by the Macrolittins, A Synthetically Evolved Family of Pore-Forming Peptides. *J. Am. Chem. Soc.* **140**, 6441–6447 (2018).

25. Kim, S. Y. *et al.* Mechanism of Action of Peptides That Cause the pH-Triggered Macromolecular Poration of Lipid Bilayers. *J. Am. Chem. Soc.* **141**, 6706–6718 (2019).

26. Behr, J. P. The proton sponge: A trick to enter cells the viruses did not exploit. *Chimia (Aarau).* **51**, 34–36 (1997).

27. Torchilin, V. P. Recent advances with liposomes as pharmaceutical carriers. *Nat. Rev. Drug Discov.* **4**, 145–160 (2005).

28. Karanth, H. & Murthy, R. S. R. pH-Sensitive liposomes-principle and application in cancer therapy. *J. Pharm. Pharmacol.* **59**, 469–483 (2007).

29. Martens, T. F., Remaut, K., Demeester, J., De Smedt, S. C. & Braeckmans, K. Intracellular delivery of nanomaterials: How to catch endosomal escape in the act. *Nano Today* **9**, 344–364 (2014).

30. Zasloff, M. Antimicrobial peptides of multicellular organisms. *Nature* **415**, 389–395 (2002).

31. Pukala, T. L., Bowie, J. H., Maselli, V. M., Musgrave, F. & Tyler, M. J. Host-defence peptides from the glandular secretions of amphibians: Structure and activity. *Nat. Prod. Rep.* **23**, 368–393 (2006).

32. Sato, A. K., Viswanathan, M., Kent, R. B. & Wood, C. R. Therapeutic peptides: technological advances driving peptides into development. *Curr. Opin. Biotechnol.* **17**, 638–642 (2006).

33. Krauson, A. J., He, J. & Wimley, W. C. Gain-of-function analogues of the pore-forming peptide melittin selected by orthogonal high-throughput screening. *J. Am. Chem. Soc.* **134**, 12732–12741 (2012).

34. Ladokhin, A. S. & White, S. H. Folding of amphipathic α-helices on membranes: Energetics of helix formation by melittin. *J. Mol. Biol.* **285**, 1363–1369 (1999).

35. Hristova, K., Dempsey, C. E. & White, S. H. Structure, location, and lipid perturbations of melittin at the membrane interface. *Biophys. J.* **80**, 801–811 (2001).

36. Wiedman, G., Herman, K., Searson, P., Wimley, W. C. & Hristova, K. The electrical response of bilayers to the bee venom toxin melittin: Evidence for transient bilayer permeabilization. *Biochim. Biophys. Acta - Biomembr.* **1828**, 1357–1364 (2013).

37. Uggerhøj, L. E. *et al.* Rational design of alpha-helical antimicrobial peptides: Do's and don'ts. *ChemBioChem* **16**, 242–253 (2015).

38. Marks, J. R., Placone, J., Hristova, K. & Wimley, W. C. Spontaneous membrane-translocating peptides by orthogonal high-throughput screening. *J. Am. Chem. Soc.* **133**,

8995–9004 (2011).

39. Rausch, J. M., Marks, J. R. & Wimley, W. C. Rational Combinatorial Design of Pore-Forming β-Sheet Peptides. *Proc. Natl. Acad. Sci. U. S. A.* **102**, 10511–10515 (2005).

40. Rathinakumar, R. & Wimley, W. C. Biomolecular engineering by combinatorial design and high-throughput screening: Small, soluble peptides that permeabilize membranes. *J. Am. Chem. Soc.* **130**, 9849–9858 (2008).

41. Kauffman, W. B., Guha, S. & Wimley, W. C. Synthetic molecular evolution of hybrid cell penetrating peptides. *Nat. Commun.* **9**, 2568 (2018).

42. Wiedman, G. *et al.* Highly efficient macromolecule-sized poration of lipid bilayers by a synthetically evolved peptide. *J. Am. Chem. Soc.* **136**, 4724–4731 (2014).

43. Li, W., Nicol, F. & Szoka, F. C. GALA: A designed synthetic pH-responsive amphipathic peptide with applications in drug and gene delivery. *Adv. Drug Deliv. Rev.* **56**, 967–985 (2004).

44. Stewart, J. C. M. Colorimetric Determination of Phospholipids Ferrothiocyanate. *Anal. Biochem.* **104**, 10–14 (1980).

45. Ladokhin, A. S., Jayasinghe, S. & White, S. H. How to measure and analyze tryptophan fluorescence in membranes properly, and why bother? *Anal. Biochem.* **285**, 235–245 (2000).

46. Ladokhin, A. S. Distribution analysis of depth-dependent fluorescence quenching in membranes: A practical guide. *Methods Enzymol.* **278**, 462–473 (1997).

47. Rathinakumar, R., Walkenhorst, W. F. & Wimley, W. C. Broad-spectrum antimicrobial peptides by rational combinatorial design and high-throughput screening: The importance

of interfacial activity. *J. Am. Chem. Soc.* **131**, 7609–7617 (2009).

48. Krauson, A. J., He, J., Wimley, A. W., Hoffmann, A. R. & Wimley, W. C. Synthetic molecular evolution of pore-forming peptides by iterative combinatorial library screening. *ACS Chem. Biol.* **8**, 823–831 (2013).

49. Atherton, E. & Sheppard, R. C. *Solid phase peptide synthesis*. (IRL Press, 1989).

50. Kakudo, T. *et al.* Transferrin-Modified Liposomes Equipped with a pH-Sensitive Fusogenic Peptide: An Artificial Viral-like Delivery System. *Biochemistry* **43**, 5618–5628 (2004).

51. Oliveira, S., van Rooy, I., Kranenburg, O., Storm, G. & Schiffelers, R. M. Fusogenic peptides enhance endosomal escape improving siRNA-induced silencing of oncogenes. *Int. J. Pharm.* **331**, 211–214 (2007).

52. Kullberg, M., Owens, J. L. & Mann, K. Listeriolysin O enhances cytoplasmic delivery by Her-2 targeting liposomes. *J. Drug Target.* **18**, 313–320 (2010).

53. Lam, J. K. W. *et al.* Effective endogenous gene silencing mediated by pH responsive peptides proceeds via multiple pathways. *J. Control. Release* **158**, 293–303 (2012).

54. Shai, Y. & Oren, Z. From 'carpet' mechanism to de-novo designed diastereomeric cell-selective antimicrobial peptides. *Peptides* **22**, 1629–1641 (2001).

55. Kauffman, W. B., Fuselier, T., He, J. & Wimley, W. C. Mechanism Matters: A Taxonomy of Cell Penetrating Peptides. *Trends Biochem. Sci.* **40**, 749–764 (2015).

56. Komin, A., Russell, L. M., Hristova, K. A. & Searson, P. C. Peptide-based strategies for enhanced cell uptake, transcellular transport, and circulation: Mechanisms and challenges. *Adv. Drug Deliv. Rev.* **110**–**111**, 52–64 (2017).

57. Wimley, W. C. & Hristova, K. Antimicrobial peptides: Successes, challenges and unanswered questions. *J. Membr. Biol.* **239**, 27–34 (2011).

58. Soman, N. R. *et al.* Molecularly targeted nanocarriers deliver the cytolytic peptide melittin specifically to tumor cells in mice, reducing tumor growth. *J. Clin. Invest.* (2009). doi:10.1172/JCI38842

59. Sani, M. A. & Separovic, F. How Membrane-Active Peptides Get into Lipid Membranes. *Acc. Chem. Res.* **49**, 1130–1138 (2016).

60. Andreev, O. A., Engelman, D. M. & Reshetnyak, Y. K. PH-sensitive membrane peptides (pHLIPs) as a novel class of delivery agents. *Mol. Membr. Biol.* **27**, 341–352 (2010).

61. Pantaleo, M. A. *et al.* Molecular imaging and targeted therapies in oncology: New concepts in treatment response assessment. A collection of cases. *Int. J. Oncol.* **33**, 443–452 (2008).

62. Gillies, R. J., Robey, I. & Gatenby, R. A. Causes and consequences of increased glucose metabolism of cancers. *J. Nucl. Med.* **49**, 24S (2008).

63. Duncan, R. The dawning era of polymer therapeutics. *Nat. Rev. Drug Discov.* **2**, 347 (2003).

64. Heitz, F., Morris, M. C. & Divita, G. Twenty years of cell - penetrating peptides : from molecular mechanisms to therapeutics Introduction:challengesindrugdelivery. *Br. J. Pharmacol.* **157**, 195–206 (2009).

65. Bechinger, B. Peptide-nucleic acid nanostructures for transfection. *Biomol. Concepts* **3**, 283–293 (2012).

66. Räägel, H., Säälik, P. & Pooga, M. Peptide-mediated protein delivery-Which pathways are

penetrable? *Biochim. Biophys. Acta - Biomembr.* **1798**, 2240–2248 (2010).

67. Majdoul, S. *et al.* Molecular determinants of vectofusin-1 and its derivatives for the enhancement of lentivirally mediated gene transfer into hematopoietic stem/progenitor cells. *J. Biol. Chem.* **291**, 2161–2169 (2016).

68. Hällbrink, M. *et al.* Cargo delivery kinetics of cell-penetrating peptides. *Biochim. Biophys. Acta - Biomembr.* (2001). doi:10.1016/S0005-2736(01)00398-4

69. Muro, S. Challenges in design and characterization of ligand-targeted drug delivery systems. *J. Control. Release* (2012). doi:10.1016/j.jconrel.2012.05.052

70. Maiolo, J. R., Ottinger, E. A. & Ferrer, M. Specific redistribution of cell-penetrating peptides from endosomes to the cytoplasm and nucleus upon laser illumination. *J. Am. Chem. Soc.* (2004). doi:10.1021/ja044867z

71. Yu, H. *et al.* Overcoming endosomal barrier by amphotericin B-loaded dual pH-responsive PDMA- b-PDPA micelleplexes for siRNA delivery. *ACS Nano* (2011). doi:10.1021/nn203503h

72. Yao, L., Daniels, J., Wijesinghe, D., Andreev, O. A. & Reshetnyak, Y. K. PHLIP®-mediated delivery of PEGylated liposomes to cancer cells. *J. Control. Release* **167**, 228–237 (2013).

73. Subbarao, N. K., Parente, R. A., Szoka, F. C., Nadasdi, L. & Poneracz, K. pH-Dependent Bilayer Destabilization by an Amphipathic Peptide. *Biochemistry* **26**, 2964–2972 (1987).

74. Parente, R. A., Nadasdi, L., Subbarao, N. K. & Szoka, F. C. Association of a pH-Sensitive Peptide with Membrane Vesicles: Role of Amino Acid Sequence. *Biochemistry* **29**, 8713–8719 (1990).

75. Fendos, J., Barrera, F. N. & Engelman, D. M. Aspartate embedding depth affects pHLIP's insertion pKa. *Biochemistry* **52**, 4595–4604 (2013).

76. Parente, R. A., Nir, S. & Szoka, F. C. Mechanism of Leakage of Phospholipid Vesicle Contents Induced by the Peptide GALA. *Biochemistry* **29**, 8720–8728 (1990).

77. An, M., Wijesinghe, D., Andreev, O. A., Reshetnyak, Y. K. & Engelman, D. M. PH-(low)-insertion-peptide (pHLIP) translocation of membrane impermeable phalloidin toxin inhibits cancer cell proliferation. *Proc. Natl. Acad. Sci. U. S. A.* **107**, 20246–20250 (2010).

78. Nishimura, Y. *et al.* A display of pH-sensitive fusogenic GALA peptide facilitates endosomal escape from a Bio-nanocapsule via an endocytic uptake pathway. *J. Nanobiotechnology* (2014). doi:10.1186/1477-3155-12-11

79. Endoh, T. & Ohtsuki, T. Cellular siRNA delivery using cell-penetrating peptides modified for endosomal escape. *Advanced Drug Delivery Reviews* (2009). doi:10.1016/j.addr.2009.04.005

80. Mularski, A., Wilksch, J. J., Hanssen, E., Strugnell, R. A. & Separovic, F. Atomic force microscopy of bacteria reveals the mechanobiology of pore forming peptide action. *Biochim. Biophys. Acta - Biomembr.* **1858**, 1091–1098 (2016).

81. Wimley, W. C. Describing the mechanism of antimicrobial peptide action with the interfacial activity model. *ACS Chem. Biol.* **5**, 905–917 (2010).

82. White, S. H., Wimley, W. C., Ladokhin, A. S. & Hristova, K. Protein Folding in Membranes: Determining Energetics of Peptide-Bilayer Interactions. *Methonds Enzymol.* **295**, 62–87 (1998).

83. Terwilliger, T. C., Weissman, L. & Eisenberg, D. The structure of melittin in the form I

crystals and its implication for melittin's lytic and surface activities. *Biophys. J.* **37**, 353–361 (1982).

84. Wu, Y., Huang, H. W. & Olah, G. A. Method of oriented circular dichroism. *Biophys. J.* **57**, 797–806 (1990).

85. Ganz, T. *et al.* Defensins. *Eur. J. Haematol.* **44**, 1–8 (1990).

86. Brown, K. L. & Hancock, R. E. W. Cationic host defense (antimicrobial) peptides. *Current Opinion in Immunology* (2006). doi:10.1016/j.coi.2005.11.004

87. Bechinger, B. Structure and function of membrane-lytic peptides. *Critical Reviews in Plant Sciences* (2004). doi:10.1080/07352680490452825

88. Dempsey, C. E. The actions of melittin on membranes. *BBA - Reviews on Biomembranes* (1990). doi:10.1016/0304-4157(90)90006-X

89. Snider, C., Jayasinghe, S., Hristova, K. & White, S. H. MPEx: A tool for exploring membrane proteins. *Protein Sci.* (2009). doi:10.1002/pro.256

90. Akinc, A., Thomas, M., Klibanov, A. M. & Langer, R. Exploring polyethylenimine-mediated DNA transfection and the proton sponge hypothesis. *J. Gene Med.* (2005). doi:10.1002/jgm.696

91. Erazo-Oliveras, A., Muthukrishnan, N., Baker, R., Wang, T. Y. & Pellois, J. P. Improving the endosomal escape of cell-penetrating peptides and their cargos: Strategies and challenges. *Pharmaceuticals* (2012). doi:10.3390/ph5111177

92. Bechinger, B. Structure and functions of channel-forming peptides: Magainins, cecropins, melittin and alamethicin. *J. Membr. Biol.* **156**, 197–211 (1997).

93. Krauson, A. J., He, J. & Wimley, W. C. Determining the mechanism of membrane permeabilizing peptides: Identification of potent, equilibrium pore-formers. *Biochim. Biophys. Acta - Biomembr.* **1818**, 1625–1632 (2012).

94. Wimley, W. C. How Does Melittin Permeabilize Membranes? *Biophys. J.* **114**, 251–253 (2018).

95. Frey, S. & Tamm, L. K. Orientation of melittin in phospholipid bilayers. A polarized attenuated total reflection infrared study. *Biophys. J.* **60**, 922–930 (1991).

96. Vargas, C., Arenas, R. C., Frotscher, E. & Keller, S. Nanoparticle self-assembly in mixtures of phospholipids with styrene/maleic acid copolymers or fluorinated surfactants. *Nanoscale* **7**, 20685–20696 (2015).

97. Epand, R. M., Shai, Y., Segrest, J. P. & Anantharamiah, G. M. Mechanisms for the modulation of membrane bilayer properties by amphipathic helical peptides. *Biopolymers* **37**, 319–338 (1995).

98. De Angelis, A. A. & Opella, S. J. Bicelle samples for solid-state NMR of membrane proteins. *Nat. Protoc.* **2**, 2332–2338 (2007).

99. Gazzara, J. A. *et al.* Effect of vesicle size on their interaction with class A amphipathic helical peptides. *J. Lipid Res.* **38**, 2147–2154 (1997).

100. Sengupta, D., Leontiadou, H., Mark, A. E. & Marrink, S. J. Toroidal pores formed by antimicrobial peptides show significant disorder. *Biochim. Biophys. Acta - Biomembr.* **1778**, 2308–2317 (2008).

101. Allende, D., Simon, S. A. & McIntosh, T. J. Melittin-induced bilayer leakage depends on lipid material properties: Evidence for toroidal pores. *Biophys. J.* **88**, 1828–1837 (2005).

102. Yang, L., Harroun, T. A., Weiss, T. M., Ding, L. & Huang, H. W. Barrel-stave model or toroidal model? A case study on melittin pores. *Biophys. J.* **81**, 1475–1485 (2001).

103. Bechinger, B. Towards membrane protein design: PH-sensitive topology of histidine-containing polypeptides. *J. Mol. Biol.* **263**, 768–775 (1996).

104. Moulay, G. *et al.* Histidine-rich designer peptides of the LAH4 family promote cell delivery of a multitude of cargo. *J. Pept. Sci.* **23**, 320–328 (2017).

105. Bohrer, M. P., Deen, W. M., Robertson, C. R., Troy, J. L. & Brenner, B. M. Influence of molecular configuration on the passage of macromolecules across the glomerular capillary wall. *J. Gen. Physiol.* **74**, 583–593 (1979).

106. Hunt, J. F., Rath, P., Rothschild, K. J. & Engelman, D. M. Spontaneous, pH-dependent membrane insertion of a transbilayer α-helix. *Biochemistry* **36**, 15177–15192 (1997).

107. Ladokhin, A. S., Wimley, W. C., Hristova, K. & White, S. H. Mechanism of Leakage of Contents of Membrane Vesicles Determined by Fluorescence Requenching. *Methods Enzymol.* **278**, 474–486 (1997).

108. Kaiser, E. T. & Kezdy, F. J. Secondary structures of proteins and peptides in amphiphilic environments (A Review) Pro-Lys-Leu-Glu-Glu-Leu-Lys-Glu-Lys-Leu-Lys-. *Rev. Lit. Arts Am.* **80**, 1137–1143 (1983).

109. Cornell, B. A. & Separovic, F. Membrane thickness and acyl chain length. *BBA - Biomembr.* **733**, 189–193 (1983).

110. Wimley, W. C. *et al.* Folding of β-sheet membrane proteins: A hydrophobic hexapeptide model. *J. Mol. Biol.* **277**, 1091–1110 (1998).

111. White, S. H. & Wimley, W. C. Membrane protein folding and stability: Physical

Principles. *Annu. Rev. Biophys. Biomol. Struct.* **28**, 319–365 (1999).

112. Wimley W C & White S H. Experimentally determined hydrophobicity scale for proteins at membrane interfaces. *Nat. Struct. Biol.* **3**, 842–848 (1996).

113. Hristova, K. *et al.* An amphipathic α-helix at a membrane interface: A structural study using a novel X-ray diffraction method. *J. Mol. Biol.* **290**, 99–117 (1999).

114. Pittman, A. E., Marsh, B. P. & King, G. M. Conformations and Dynamic Transitions of a Melittin Derivative That Forms Macromolecule-Sized Pores in Lipid Bilayers. *Langmuir* **34**, 8393–8399 (2018).

115. Dowhan, W. Molecular Basis for Membrane Phospholipid Diversity:Why Are There So Many Lipids? *Annu. Rev. Biochem.* **66**, 199–232 (1997).

116. Papahadjopoulos, D. & Miller, N. Phospholipid model membranes. I. Structural characteristics of hydrated liquid crystals. *Biochim. Biophys. Acta (BBA)-Biomembranes* **135**, 624–638 (1967).

117. Shevchenko, A. & Simons, K. Lipidomics: Coming to grips with lipid diversity. *Nat. Rev. Mol. Cell Biol.* **11**, 593–598 (2010).

118. Levental, I. & Veatch, S. L. The Continuing Mystery of Lipid Rafts. *J. Mol. Biol.* **428**, 4749–4764 (2016).

119. Needham, D. & Hochmuth, R. M. Electro-mechanical permeabilization of lipid vesicles. Role of membrane tension and compressibility. *Biophys. J.* **55**, 1001–1009 (1989).

120. Barrera, F. N., Fendos, J. & Engelman, D. M. Membrane physical properties influence transmembrane helix formation. *Proc. Natl. Acad. Sci. U. S. A.* **109**, 14422–14427 (2012).

121. Andersen, O. S. & Koeppe, R. E. Bilayer thickness and membrane protein function: An energetic perspective. *Annu. Rev. Biophys. Biomol. Struct.* **36**, 107–130 (2007).

122. Karabadzhak, A. G. *et al.* Bilayer Thickness and Curvature Influence Binding and Insertion of a pHLIP Peptide. *Biophys. J.* **114**, 2107–2115 (2018).

123. Yu, X. & Zheng, J. Cholesterol promotes the interaction of alzheimer β-amyloid monomer with lipid bilayer. *J. Mol. Biol.* **421**, 561–571 (2012).

124. Lee, D. K., Bhunia, A., Kotler, S. A. & Ramamoorthy, A. Detergent-Type Membrane Fragmentation by MSI-78, MSI-367, MSI-594, and MSI-843 Antimicrobial Peptides and Inhibition by Cholesterol: A Solid-State Nuclear Magnetic Resonance Study. *Biochemistry* **54**, 1897–1907 (2015).

125. Teixeira, V., Feio, M. J. & Bastos, M. Role of lipids in the interaction of antimicrobial peptides with membranes. *Prog. Lipid Res.* **51**, 149–177 (2012).

126. Dowhan, W. & Bogdanov, M. Lipid-Dependent Membrane Protein Topogenesis. *Annu. Rev. Biochem.* **78**, 515–540 (2009).

127. Babakhani, A., Gorfe, A. A., Kim, J. E. & McCammon, J. A. Thermodynamics of peptide insertion and aggregation in a lipid bilayer. *J. Phys. Chem. B* **112**, 10528–10534 (2008).

128. Van Meer, G., Voelker, D. R. & Feigenson, G. W. Membrane lipids: Where they are and how they behave. *Nat. Rev. Mol. Cell Biol.* **9**, 112–124 (2008).

129. Ziegler, A. Thermodynamic studies and binding mechanisms of cell-penetrating peptides with lipids and glycosaminoglycans. *Adv. Drug Deliv. Rev.* **60**, 580–597 (2008).

130. Lee, D. K. *et al.* Lipid composition-dependent membrane fragmentation and pore-forming mechanisms of membrane disruption by pexiganan (MSI-78). *Biochemistry* **52**, 3254–

3263 (2013).

131. Elmore, D. E. Molecular dynamics simulation of a phosphatidylglycerol membrane. *FEBS Lett.* **580**, 144–148 (2006).

132. Lewis, B. A. & Engelman, D. M. Bacteriorhodopsin remains dispersed in fluid phospholipid bilayers over a wide range of bilayer thicknesses. *J. Mol. Biol.* **166**, 203–210 (1983).

133. Lee, T. H., Sani, M. A., Overall, S., Separovic, F. & Aguilar, M. I. Effect of phosphatidylcholine bilayer thickness and molecular order on the binding of the antimicrobial peptide maculatin 1.1. *Biochim. Biophys. Acta - Biomembr.* **1860**, 300–309 (2018).

134. Phillips, R., Ursell, T., Wiggins, P. & Sens, P. Emerging roles for lipids in shaping membrane-protein function. *Nature* **459**, 379–385 (2009).

135. Cymer, F., Von Heijne, G. & White, S. H. Mechanisms of integral membrane protein insertion and folding. *J. Mol. Biol.* **427**, 999–1022 (2015).

136. Boggs, J. M. Lipid intermolecular hydrogen bonding: influence on structural organization and membrane function. *Biochim. Biophys. Acta - Biomembr.* **906**, 353–404 (1987).

137. Huang, H. W. Action of antimicrobial peptides: Two-state model. *Biochemistry* **39**, 8347–8352 (2000).

CURRICULUM VITAE

SARAH YEON-KYOUNG KIM

Program of Molecular Biophysics 204H Shaffer Hall
Johns Hopkins University 3400 N. Charles Street
Email: skim321@jhu.edu Baltimore, MD 21218
Phone: 623-695-4726

EDUCATION

Ph.D. Candidate in Molecular Biophysics, Johns Hopkins University expected Summer 2019
B.A. in Chemistry and Biology (*Magna Cum Laude)*, Cornell University May 2013

RESEARCH EXPERIENCE

Graduate Student Researcher Mar 2014-Present
Program of Molecular Biophysics, Johns Hopkins University *Advisor*: Kalina Hristova, Ph. D.
Discovered and characterized pH sensitive membrane permeabilizing peptides for the endocytotic release of macromolecules by high-throughput screening of a combinatorial library of 18,300+ unique peptide sequences.

Undergraduate Researcher Sep 2011-Aug 2013
Department of Molecular Biology & Genetics, Cornell University *Advisor*: Gerald Feigenson, Ph.D.
Measured the partition coefficient of fluorescently labeled dyes and gramicidin between the liquid ordered and liquid disordered phases as a function of membrane domain size in the model system DSPC/DOPC/POPC/Chol.

Undergraduate Researcher Jun 2011-Jul 2011
Center for Innovations in Medicine, Arizona State University *Advisor*: Kathryn Sykes, Ph.D.
Aided in developing a protocol to determine if membrane proteins synthesized for crystallization were in their native fold with reporter GFP. Assisted in investigating how proteins expressed in a cell-free human *in vitro* system bound to tosylactivated magnetic beads.

Undergraduate Researcher Jun 2010-Jul 2010
Center for Innovations in Medicine, Arizona State University *Advisor*: Kathryn Sykes, Ph.D.
Learned basic molecular biology techniques such as PCR, gel electrophoresis, miniprepping, and bacterial transformation.

PUBLICATIONS

Wiedman, G., **Kim, S.Y.**, Zapata-Mercado, E., Wimley, W.C. and Hristova, K., 2017. pH-triggered, macromolecule-sized poration of lipid bilayers by synthetically evolved peptides. *J. Am. Chem. Soc*., 139(2), pp.937-945.

Li, S., **Kim, S.Y.**, Pittman, A.E., King, G.M., Wimley, W.C. and Hristova, K., 2018. Potent Macromolecule-sized poration of lipid bilayers by the macrolittins, a synthetically evolved family of pore-forming peptides. *J. Am. Chem. Soc*., 140(20), pp.6441-6447.

Kim, S.Y., Pittman, A.E., Zapata-Mercado, E., King, G.M., Hristova, K., and Wimley, W.C., 2019. Mechanism of action of peptides that cause pH-triggered macromolecular poration of lipid bilayers. *Accepted at J. Am. Chem. Soc.*, 141 (16), pp 6706–6718.

CONFERENCE PARTICIPATION

Biophysical Society Annual Meeting, Baltimore, MD March 2019
Poster: *Mechanism of Action of pH-Triggered, Membrane Active Peptides*

Biophysical Society Annual Meeting, San Francisco, CA Feb 2018
Presentation: *Mechanism of Action of pH-triggered, Membrane Active Peptides: Effect of Lipid Composition*

Membrane Protein Folding Gordon Research Conference, Easton, MA June 2017
Poster: *Mechanism of Action of pH-triggered, macromolecular pore-forming peptides for endosomal escape.*

Delaware Membrane Protein Symposium, Newark, DE May 2017
Poster: *Mechanism of Action of pH-triggered, macromolecular pore-forming peptides for endosomal escape.*

Biophysical Society Annual Meeting, New Orleans, LA Feb 2017
Poster: *Mechanism of Action of pH-triggered, macromolecular pore-forming peptides for endosomal escape.*

Delaware Membrane Protein Symposium, Newark, DE April 2016
Poster: *Design of pH-triggered, macromolecular pore-forming peptides for endosomal escape.*

Biophysical Society Annual Meeting, Los Angeles, CA Feb 2016
Poster: *Design of pH-triggered, macromolecular pore-forming peptides for endosomal escape.*

Northeast Conference for Undergraduate Women in Physics, Ithaca, NY Jan 2013
Presentation: *Measuring the partitioning of lissamine rhodamine-DOPE in the four component model membrane system DSPC/DOPC/POPC/Chol.*

CAMPUS OR DEPARTMENTAL TALKS

2019 JHU Nano-Bio Symposium: Translation of Nano & Bio Research, Baltimore, MD May 2019
Poster: *Mechanism of Action of pH-Triggered, Membrane Active Peptides*

Women in STEM Symposium, Baltimore, MD April 2019
Poster: *Mechanism of Action of pH-Triggered, Membrane Active Peptides*

Institute for Biophysical Research Annual Retreat, Baltimore, MD Sep 2018
Presentation: *Mechanism of Action of pH-Triggered, Membrane Active Peptides*

2018 JHU Nano-Bio Symposium: Advanced Biomanufacturing, Baltimore, MD May 2018
Poster: *Mechanism of Action of pH-triggered, macromolecular pore-forming peptides for endosomal escape.*

Institute for Nanobiotechnology Graduate Mini Symposium, Baltimore, MD Feb 2018
Presentation: *Mechanism of Action of pH-Triggered, Membrane Active Peptides: Effect of Negative Charge.*

Institute for Biophysical Research Annual Retreat, Baltimore, MD Sep 2017
Poster: *Mechanism of Action of pH-triggered, macromolecular pore-forming peptides for endosomal escape.*

2017 JHU Nano-Bio Symposium: Engineering Vascularization May 2017
Poster: *Mechanism of Action of pH-triggered, macromolecular pore-forming peptides for endosomal escape.*

Program of Molecular Biophysics, Student Evening Series, Baltimore, MD Nov 2016
Presentation: *Mechanism of Action of pH Triggered, Membrane Active Peptides*

Institute for Biophysical Research Annual Retreat, Baltimore, MD Sep 2016
Poster: *Design of pH-triggered, macromolecular pore-forming peptides for endosomal escape.*

Institute for Nanobiotechnology Graduate Mini Symposium, Baltimore, MD Mar 2016
Presentation: *Design of pH-triggered, macromolecular pore-forming peptides for endosomal escape.*

Institute for Biophysical Research Annual Retreat, Baltimore, MD Sep 2015
Poster: *Designing pH-sensitive membrane pore forming peptides for endosomal escape.*

PATENT

Wimley, W.C., Wiedman, G., Hristova, K., **Kim, S.Y.** "pH-Triggered, Macromolecule-Sized Poration of Lipid Bilayers by Synthetically Evolved Peptides." Patent Application No. 62433109, December 12, 2016.

TEACHING EXPERIENCE

Johns Hopkins University, Maryland, MD

Guest Instructor, Biomaterials Lab. Instructor: K. Hristova Spring 2015, 2016, 2017, 2018, 2019
Guest Instructor, Introduction to Biophysical Methods, Instructor: Elmer A. Zapata-Mercado Fall 2018
Participant, Preparing Future Faculty Certificate Program 2016-2018
Instructor, Life-A Matter of Fat. Hopkins Engineering Applications & Research Tutorials Fall 2017
Fellow, Collaborative Teaching Fellows Program 2016
Guest Lecturer, Biomolecular Materials I. Instructor: K. Hristova Fall 2015 and 2016
Teaching Assistant, Proteins and Nucleic Acids. Instructors: G. Bowman and S. Woodson Fall 2014

Baltimore Under Ground Science Space (BUGSS)

Instructor, Molecular Biology Bootcamp: Building a Kill-Switch in Bacteria. Nov 2016

HONORS AND AWARDS

3 Minute Thesis Competition, Finalist April 2019
Women in STEM Symposium, 1st Place Graduate Student Poster Award April 2019
2018 JHU Nano-Bio Symposium: Advanced Manufacturing, 3rd in People's Choice Poster Presentation Award May 2018
2017 JHU Nano-Bio Symposium: Engineering Vascularization, 2nd in Poster Competition May 2017
Biophysical Society Student Research Achievement Award, Poster Competition Feb 2017
Biophysical Society Student Research Achievement Award, Poster Competition Feb 2016
Carlson Fellowship, Thomas C. Jenkins Department of Biophysics 2013-2015

COMMUNITY INVOLVEMENT AND OUTREACH

Dyslexia Tutoring Program Nov 2016-May 2019
STEM Achievement in Baltimore Elementary Schools Sep 2014-June 2017
Q?rius, Smithsonian National Museum of Natural History Mar 2015-Aug 2016
Women in Science and Engineering Program Dec. 2014-May 2015

PROFESSIONAL MEMBERSHIPS

Biophysical Society 2014-Present

MISCELANEOUS

Birthday: January 29, 1991 in Suwon, South Korea